



# Galactic transient sources of ultra-high energy cosmic rays on the example of the magnetar SGR1900+14

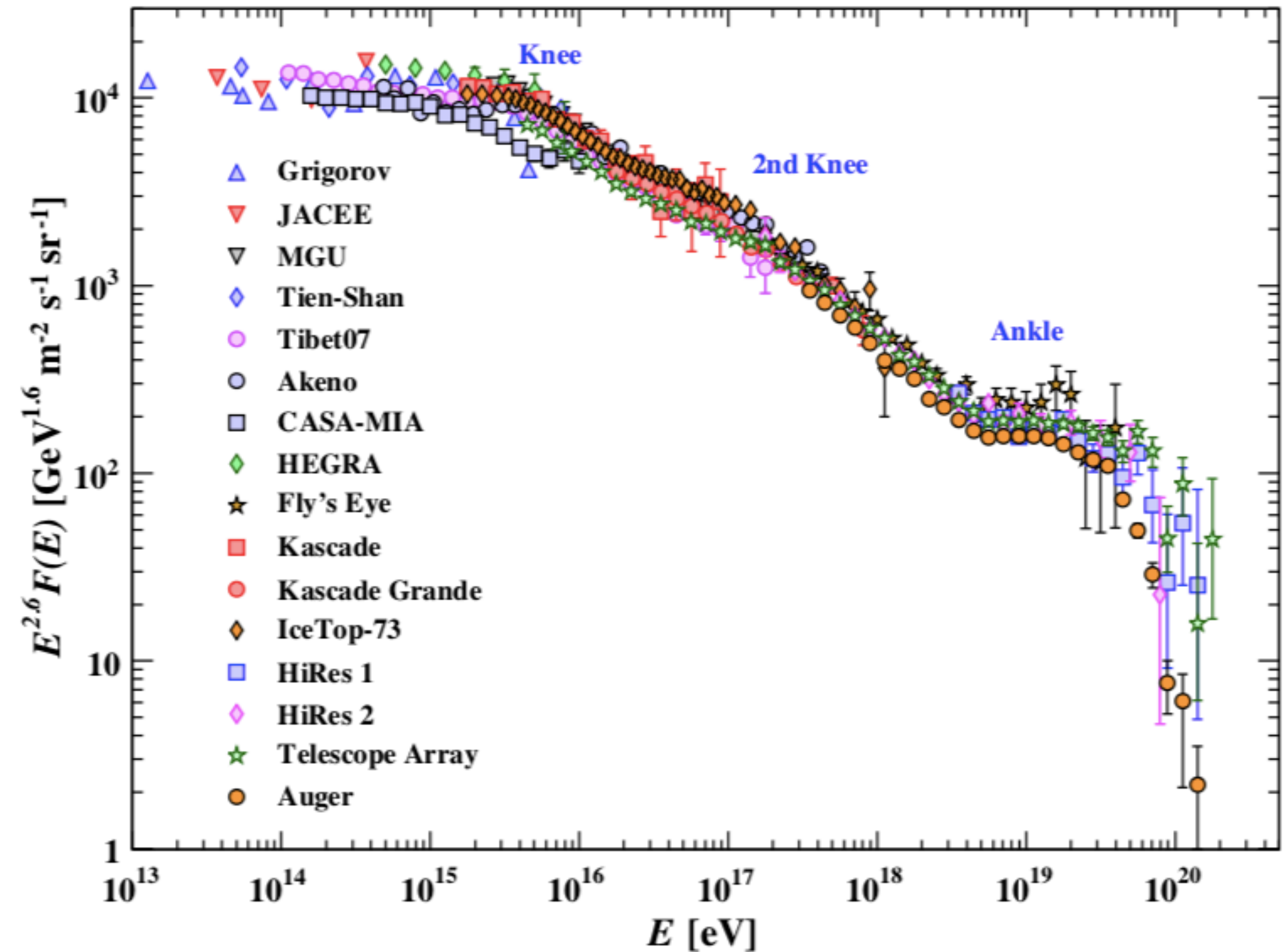
Vadym Voitsekhovskiy

*Institute of Astronomy and Astrophysics, Tuebingen University*

*Astronomical Observatory of Taras Shevchenko National University of Kyiv*

# Cosmic rays

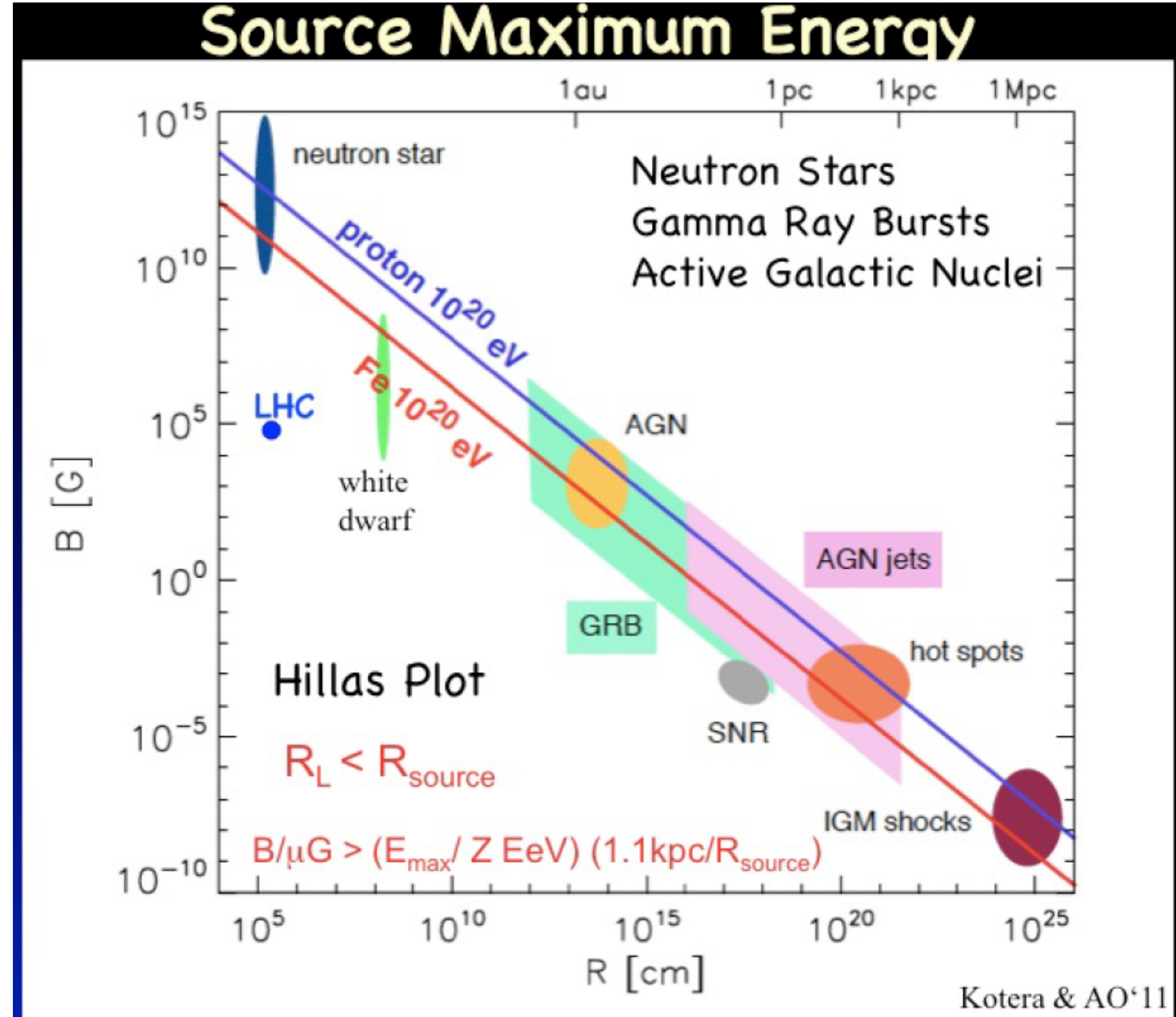
- Maximum registered cosmic ray energy:  
 $E_{max} = 3 \cdot 10^{20} eV$
- Ultra high energy cosmic rays (UHECR):  
 $E \geq 10^{18} eV$
- Extreme high energy cosmic rays (EHECR):  
 $E \geq 10^{20} eV$
- Exact sources of high energy cosmic rays remains unknown



[Patrignani et al. 2016]

# Cosmic rays: acceleration problems

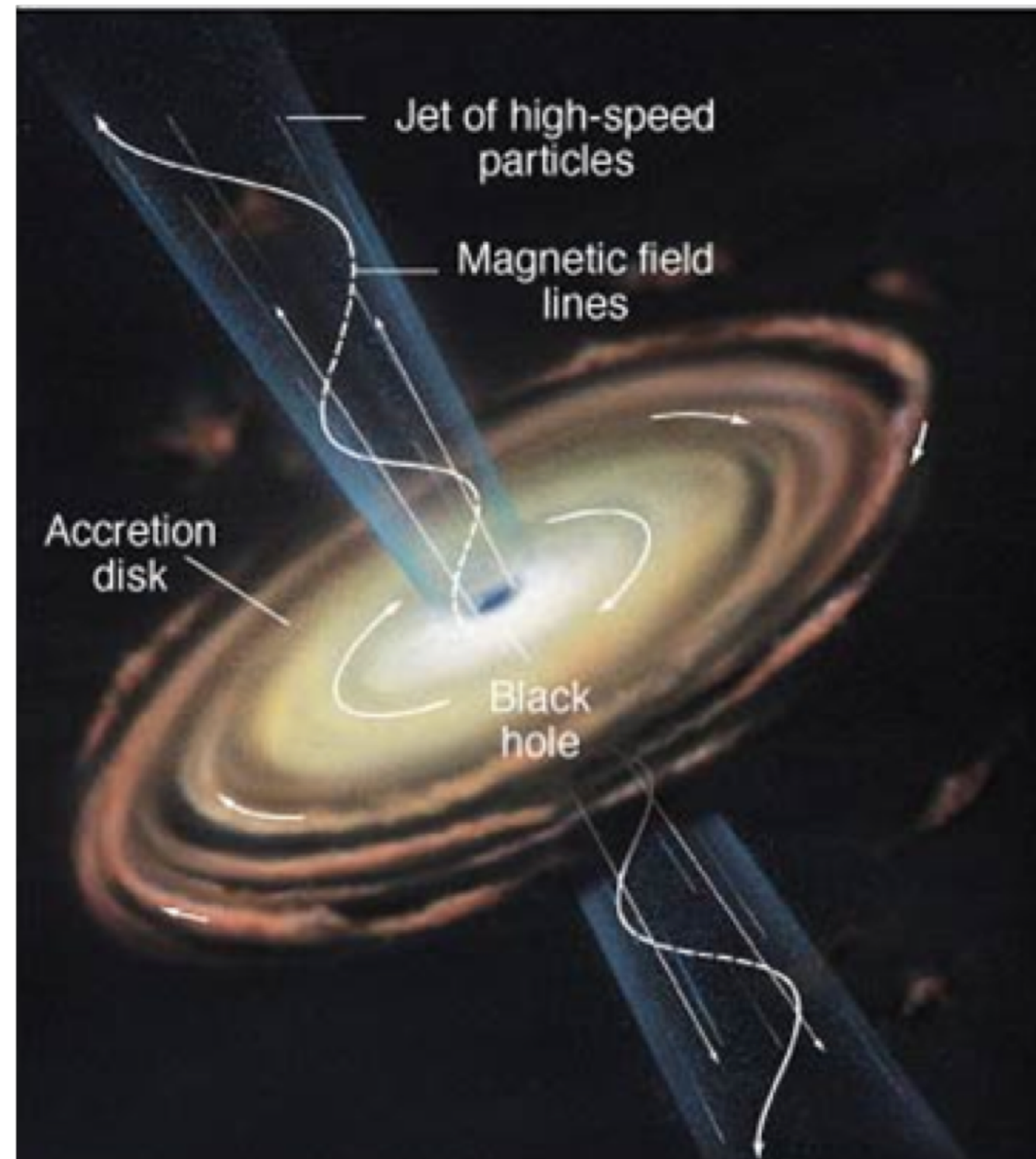
Strong magnetic fields  
and/or big sizes of  
accelerators are needed to  
achieve high energies of  
particles



# Acceleration sites for high energy cosmic rays

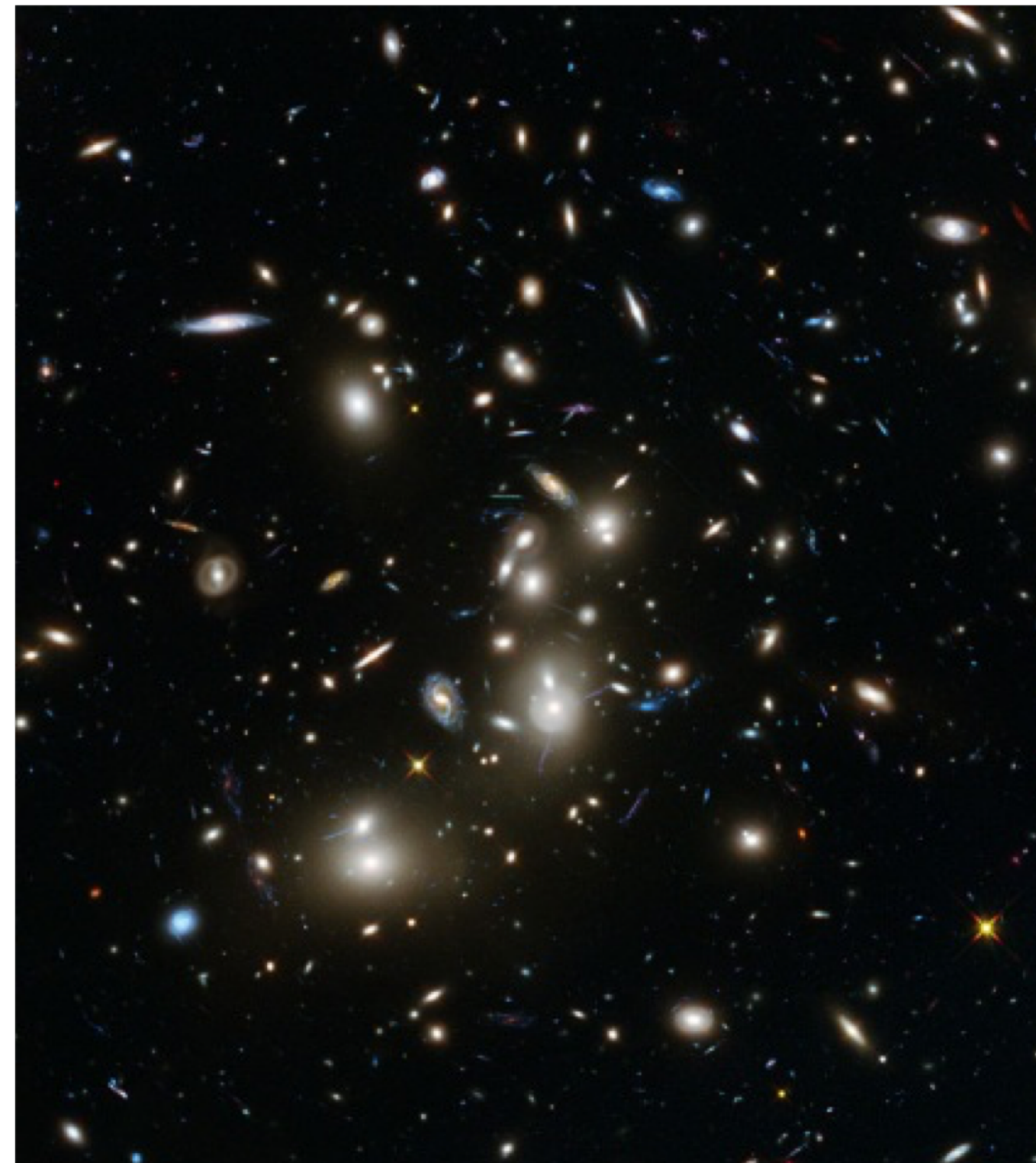
## AGN:

acceleration at shock waves  
in jets



## Galaxy clusters:

acceleration at shock waves  
in the intracluster medium



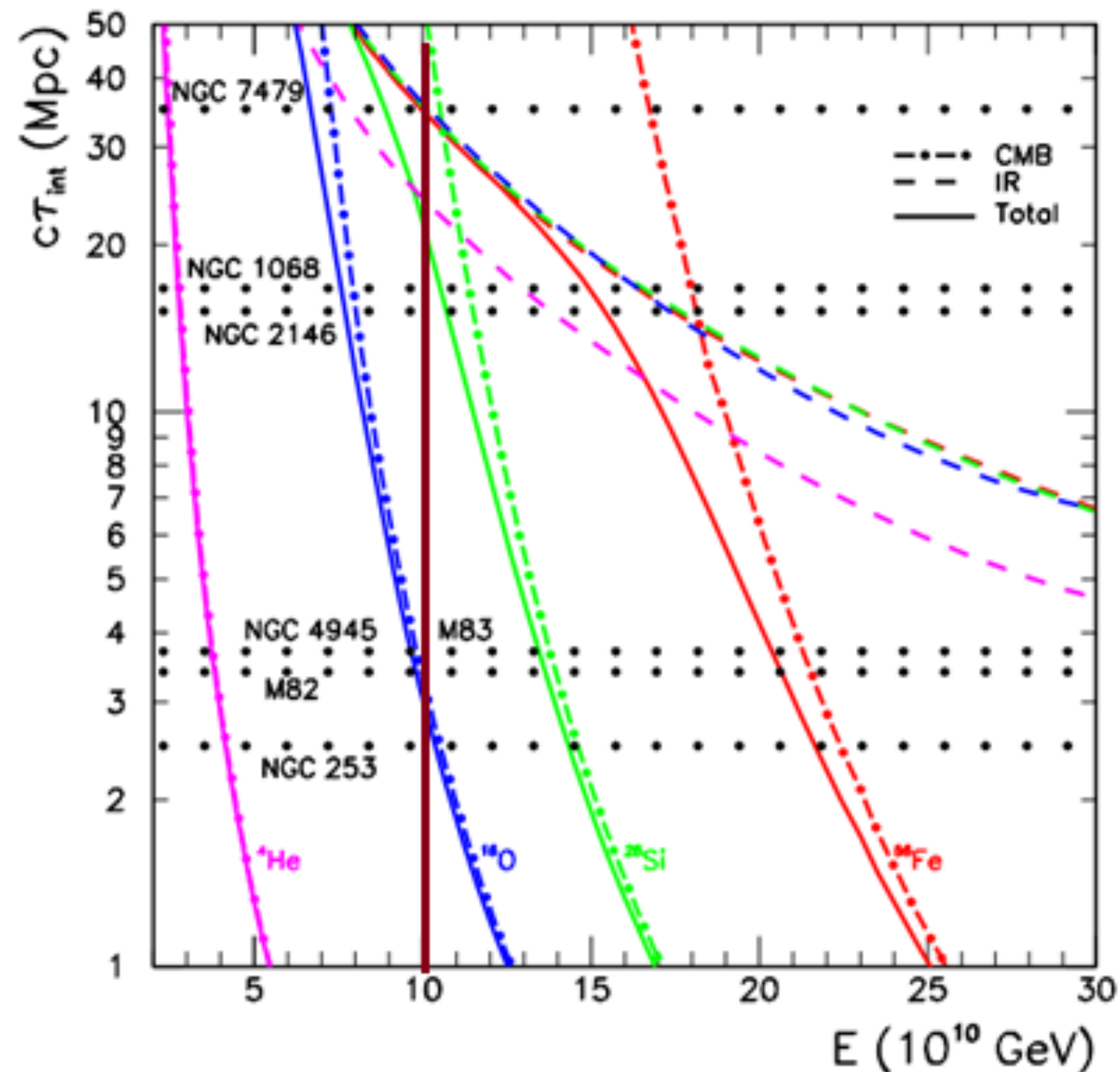
## Compact objects:

pulsars, magnetars, gamma-ray  
bursts



# Restriction on UHECR sources: the energy-loss horizon $\lambda$ of UHECR protons and nuclei as function of energy

Cosmic Mass Spectrometer Luis A. Anchordoqui<sup>1,2,3</sup> Vernon Barger<sup>4</sup> and Thomas Weiler<sup>5</sup> arXiv:1707.05408v3



For  $E > 10^{20}$  eV UHECR:

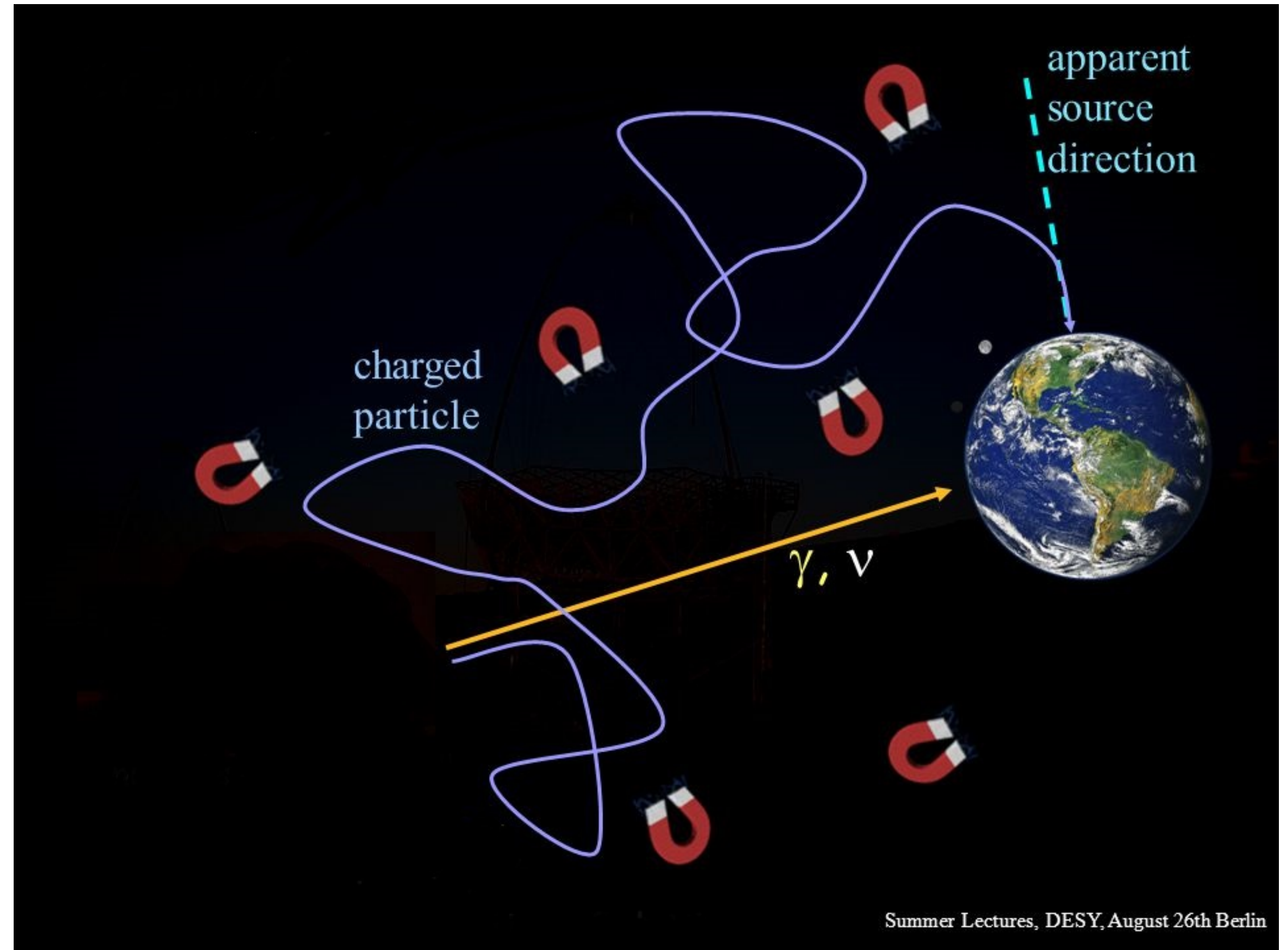
- sources of protons and Fe-nuclei should be inside 30-50 Mpc
- sources of He and C-N-O nuclei should be inside 10-30 Mpc

Inside 50 Mpc UHECR can be accelerated in (mildly) relativistic transient jets in GRB, TDE and, most frequently, in giant flares of magnetars and in magnetar wind nebulae, created by newborn millisecond magnetars

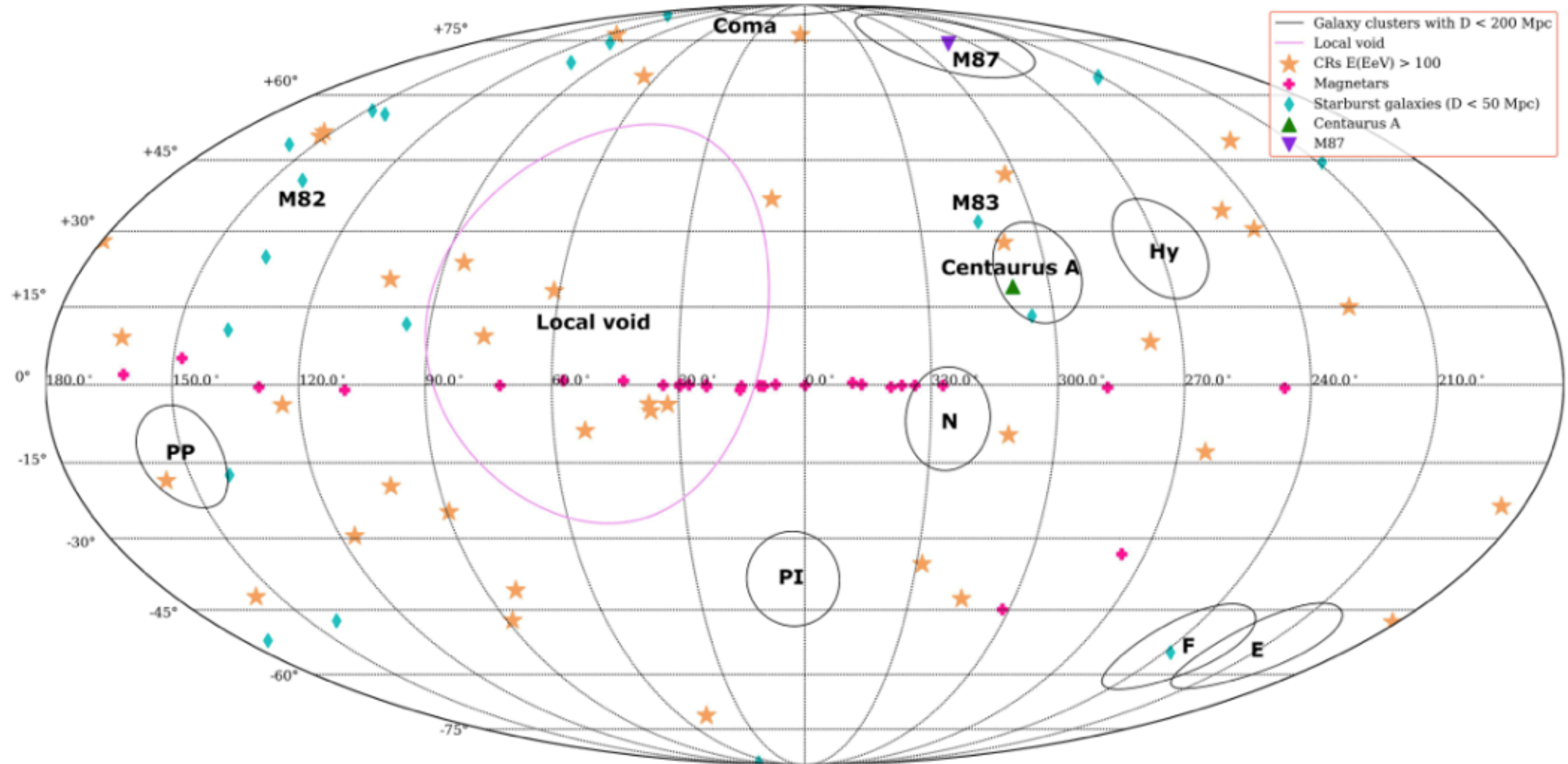
# Problem of source identification

To reduce such problems:

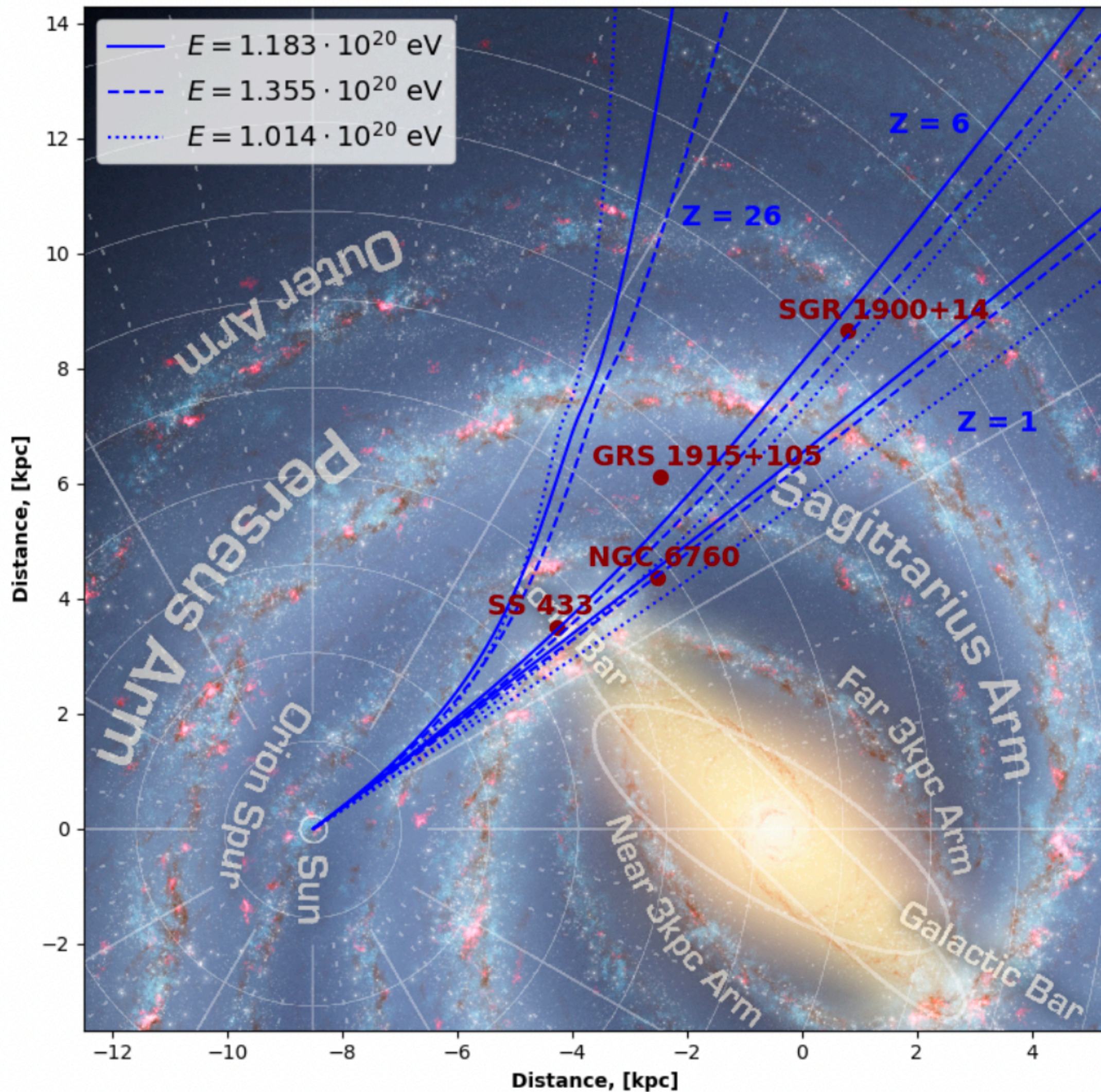
- considering events with high energies  
 $E > 10^{20} eV$
- taking into account modern magnetic field models



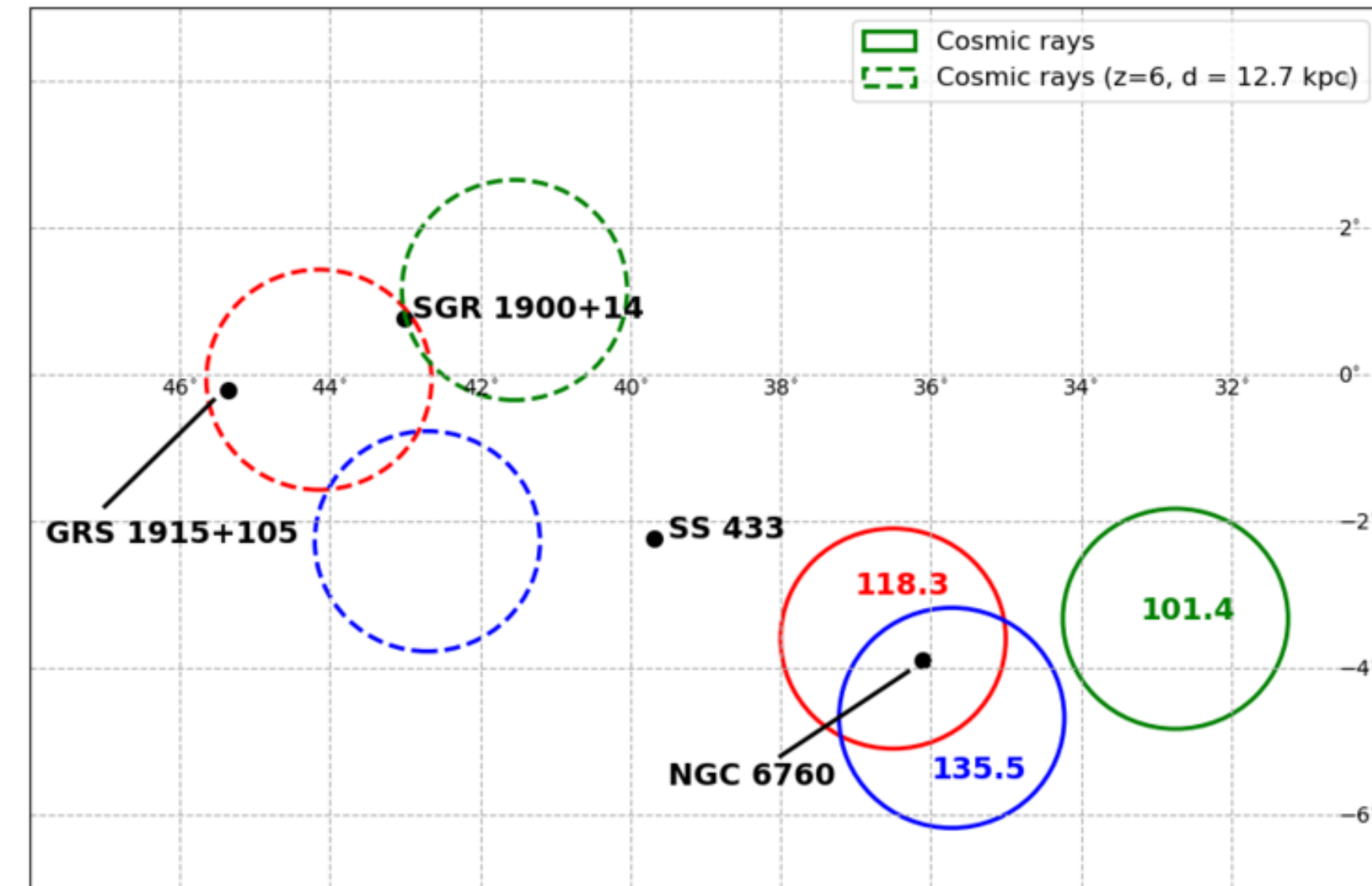
# Map of EHECR events



# Backtracking trajectories of the EHECR triplet of events



Calculated backward trajectories of EHECR triplet based on JF12 Galactic magnetic field

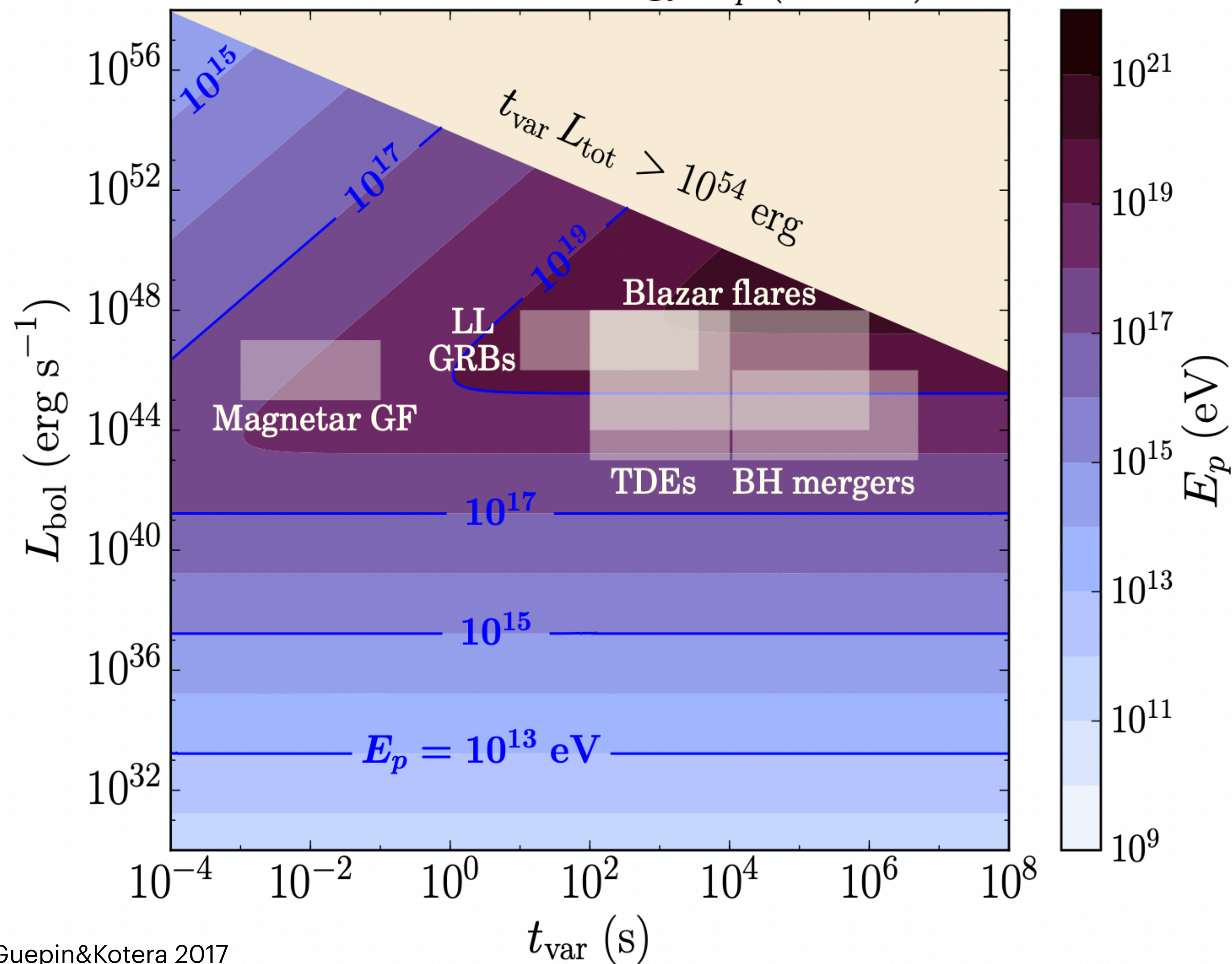


No	Name	Type	$l$ , deg	$b$ , deg	$d$ , kpc
1	GRS 1915+105	Microquasar	45.37	-0.22	$8.6 \pm 2.0$
2	SS 433	Microquasar	39.69	-2.24	$5.5 \pm 0.2$
3	NGC 6760	Globular cluster	36.11	-3.9	$7.4 \pm 0.4$
4	SGR 1900+14	Magnetar	43.02	0.77	$12.5 \pm 1.7$



# Maximum accessible proton energy $E_{p,max}$ in a flaring source, with bulk Lorentz factor $\Gamma = 10$

Proton maximal energy  $E_p$  ( $\Gamma = 10$ )



Giant magnetar flare  
on the SGR1900+14 in 1998 year

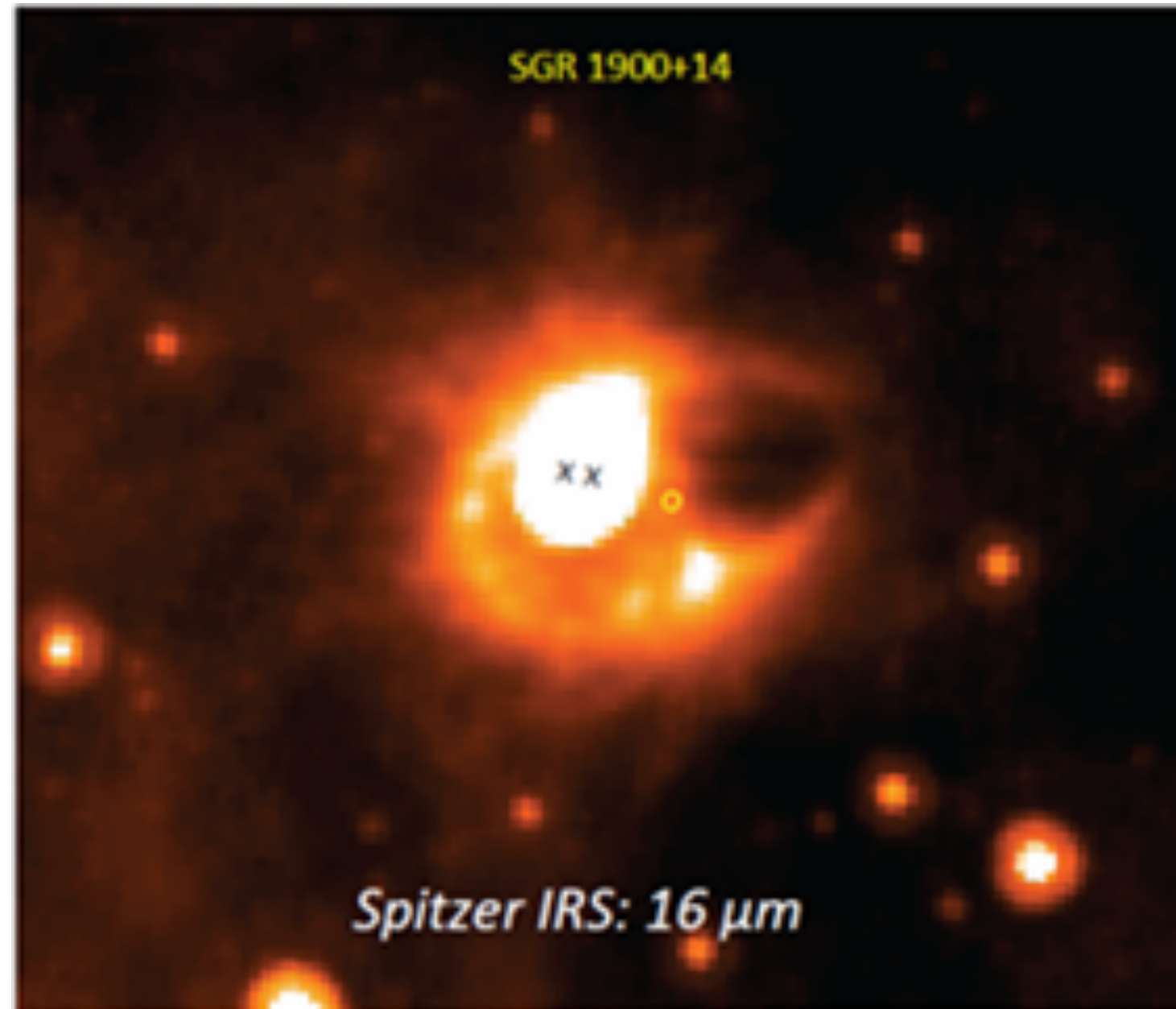
In case of SGR1900+14,  
max acceleration energy

$$E_{max} = Z \times E_{p,max} > 10^{20} \text{ eV}$$

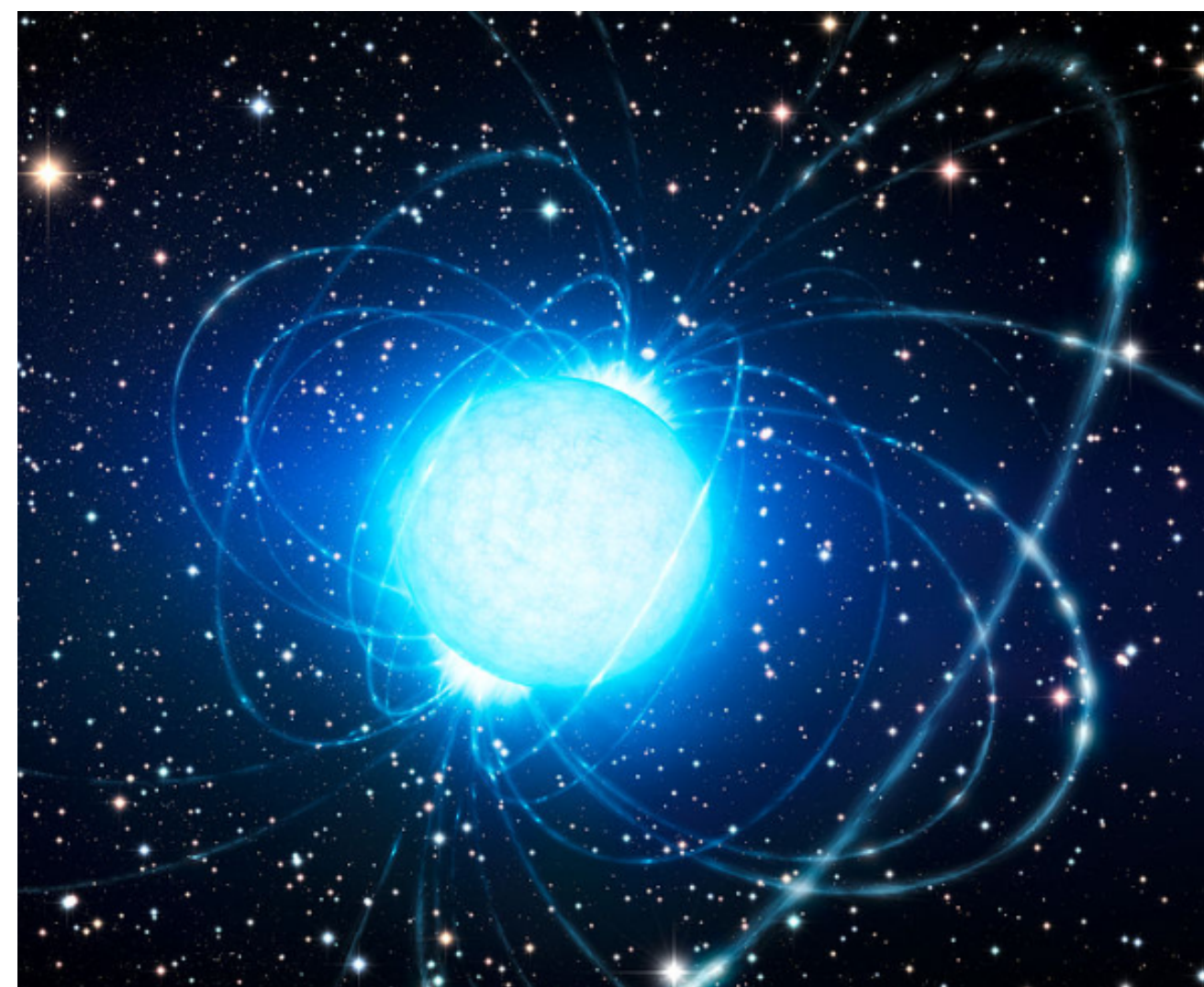
for nuclei with  $Z > 10$

# Magnetar SGR 1900+14

SGR1900+14 in IR band



Artists picture of the magnetar



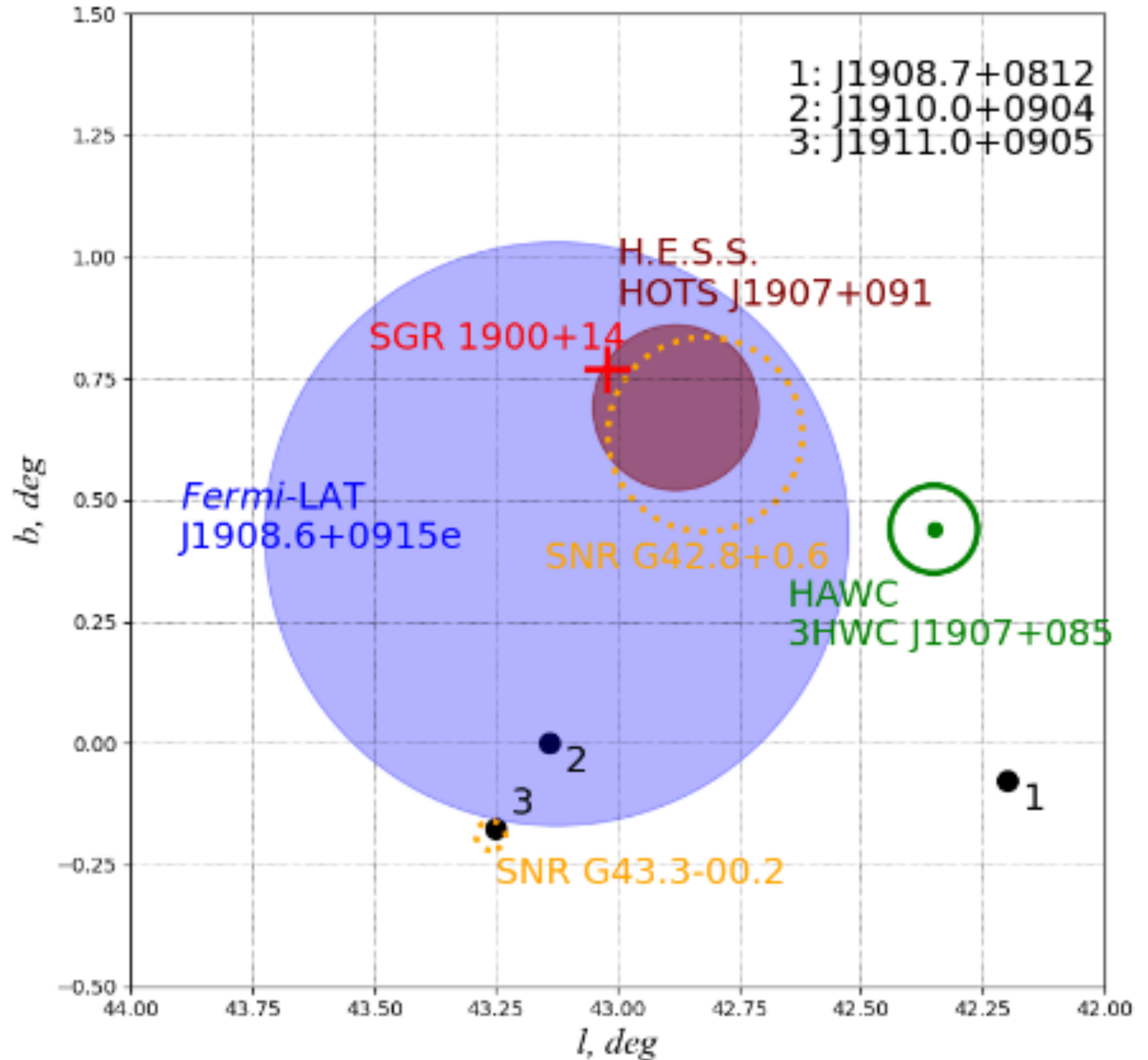
- Magnetars - neutron stars with
- relatively large rotational periods 2 ... 8 s
  - large magnetic fields of the order of  $10^{14} \dots 10^{15}$  G.

## Magnetar SGR1900+14:

- Period = 5.2 s,
- Magnetic field =  $4 \times 10^{14}$  G,
- distance = 12.5 kpc

# SGR1900+14 region

- 4FGL J1908.6+0915e
- H.E.S.S HOTS J1907+091
- HAWC 3HWC J1907+085
- SNR G42.8+0.6
- SNR G43.3-00.2



# Our model of SGR1900+14 evolution

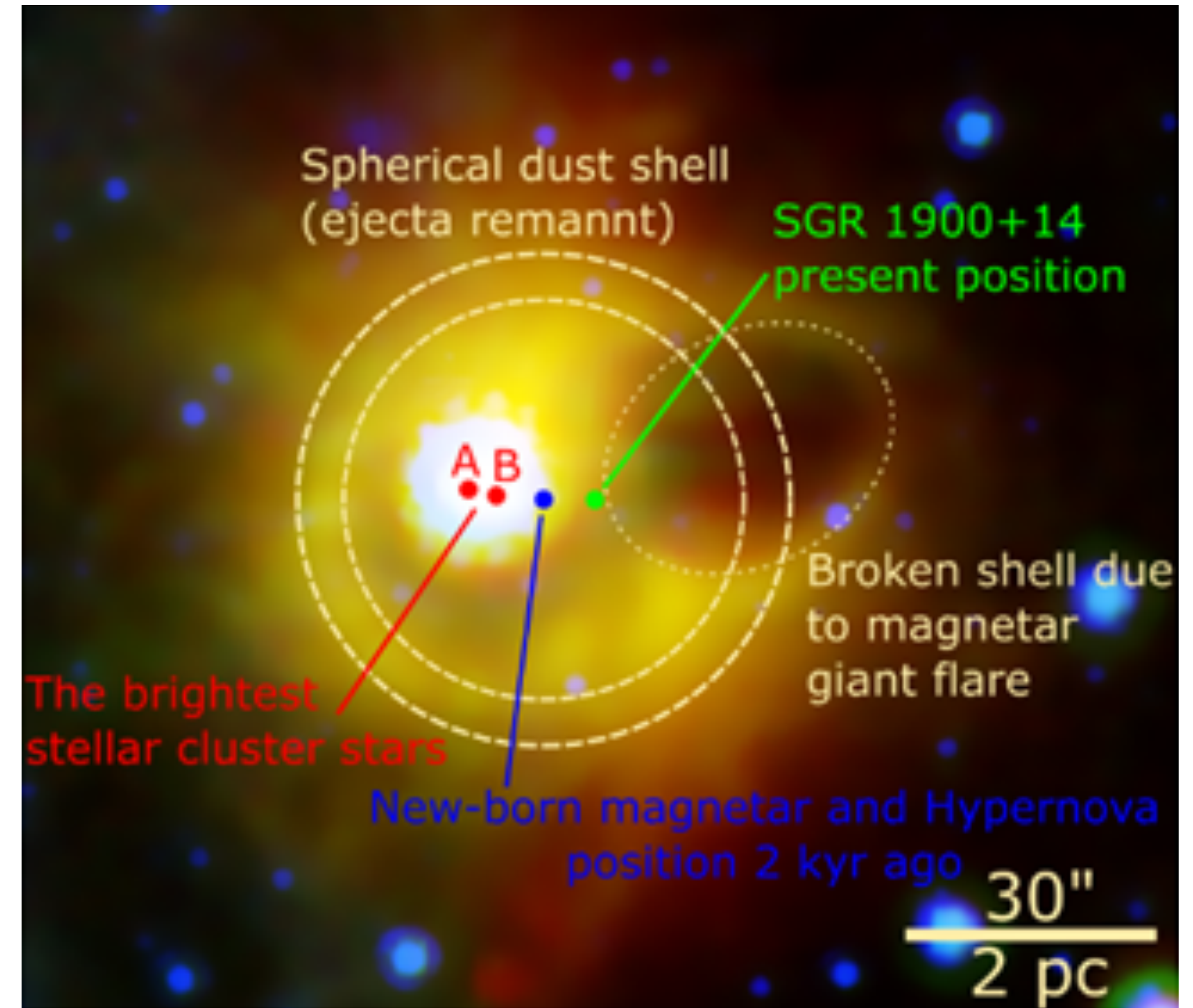
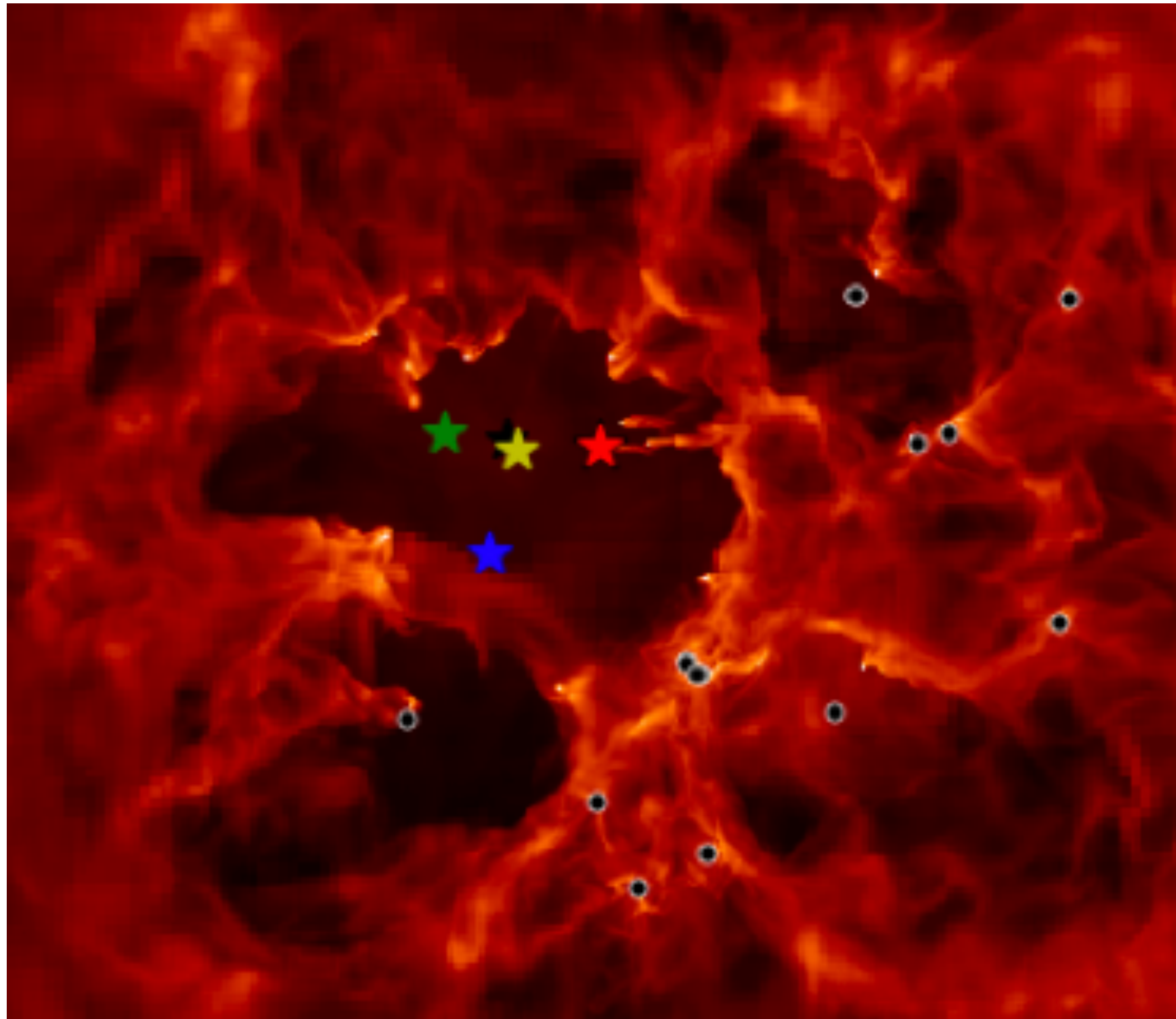
Explosion as SN Ic in stellar wind cavity

Newborn pulsar with  $P=1\text{ms}$  and  $B=4 \times 10^{14}\text{G}$

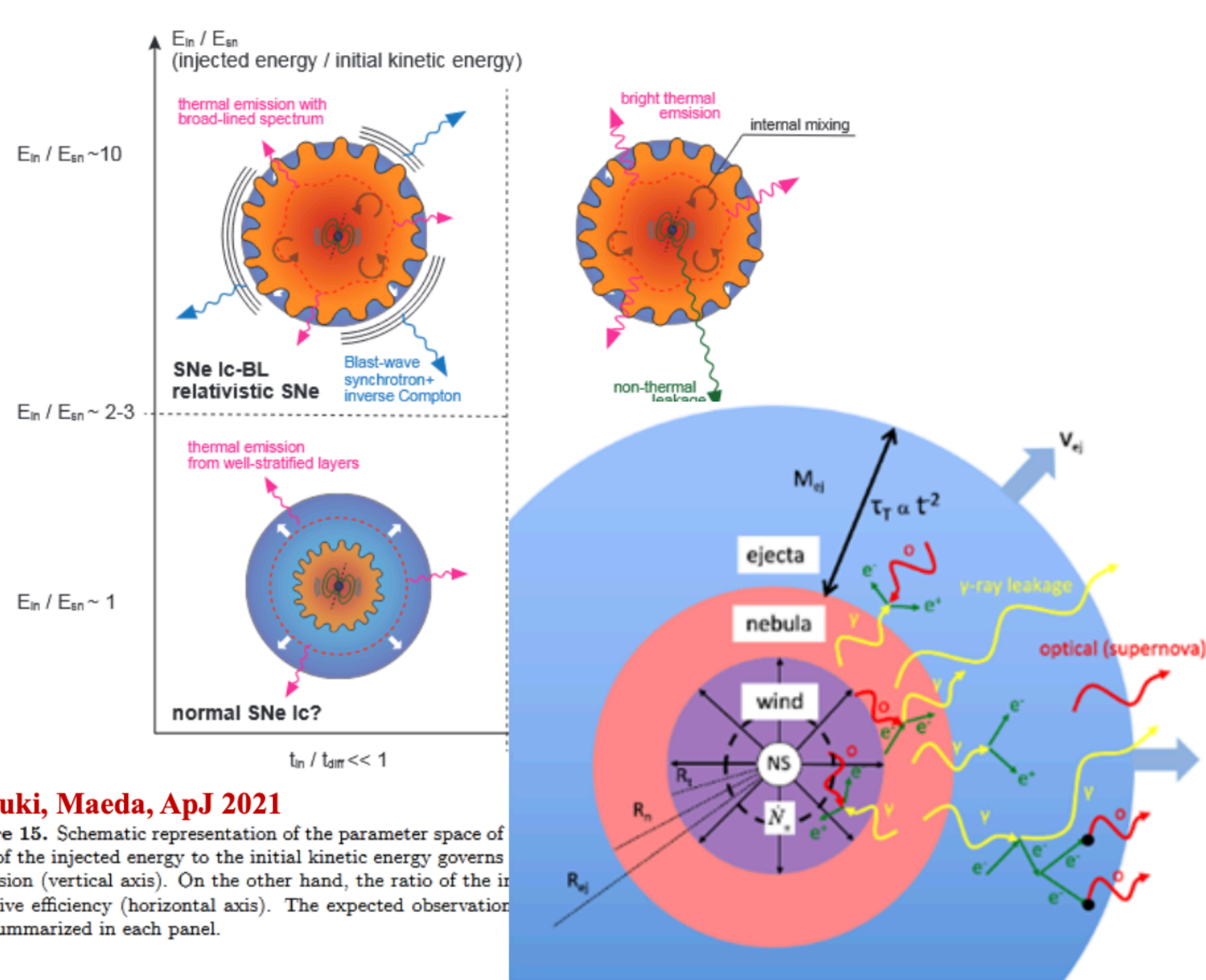
Magnetar with  $E_{rot} \approx 10^{52}\text{erg}$

$2 M_{sun}$  spherical dust shell-relic of SN shell

Broken shell is evaporated by collimated giant flare



# Evolution of the magnetar driven Hypernova/ Jet-like magnetar wind



Suzuki, Maeda, ApJ 2021

Figure 15. Schematic representation of the parameter space of ratio of the injected energy to the initial kinetic energy governs expansion (vertical axis). On the other hand, the ratio of the irradiative efficiency (horizontal axis). The expected observation also summarized in each panel.

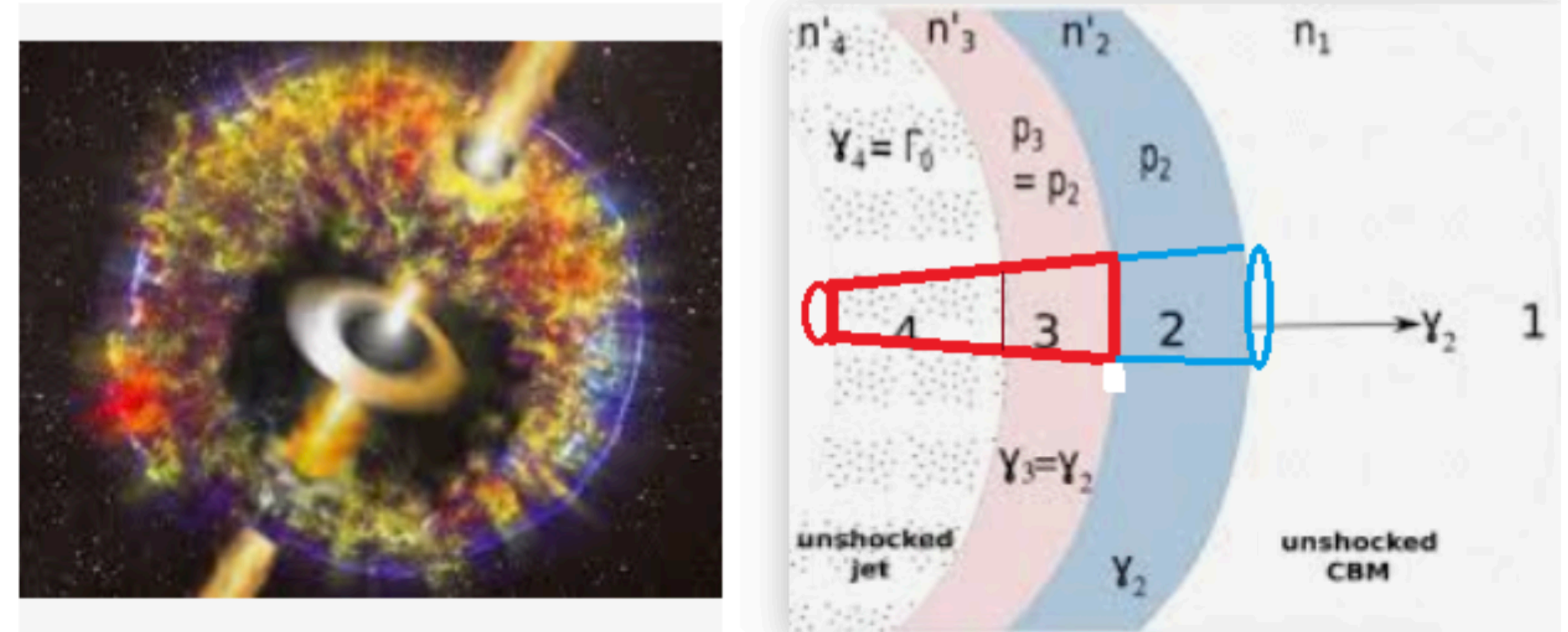
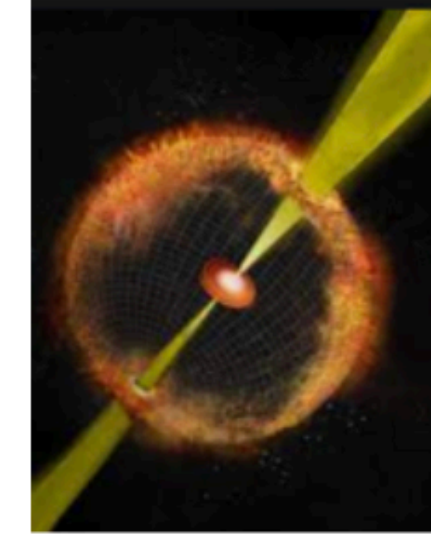
## HNR:

Magnetar Wind Nebula (MWN) pressure protrudes dense internal part of ejecta and accelerates its external layers up to  $E_{ejecta} = 10^{52}$  erg

Diffusive Shock Acceleration at HNR shock:

$$E_{cr,p} = (3-5) \cdot 10^{50} \text{ erg}, E_{cr,e} = K_{ep} \times E_{cr,p} \sim 10^{48} \text{ erg}$$

Classical long GRB

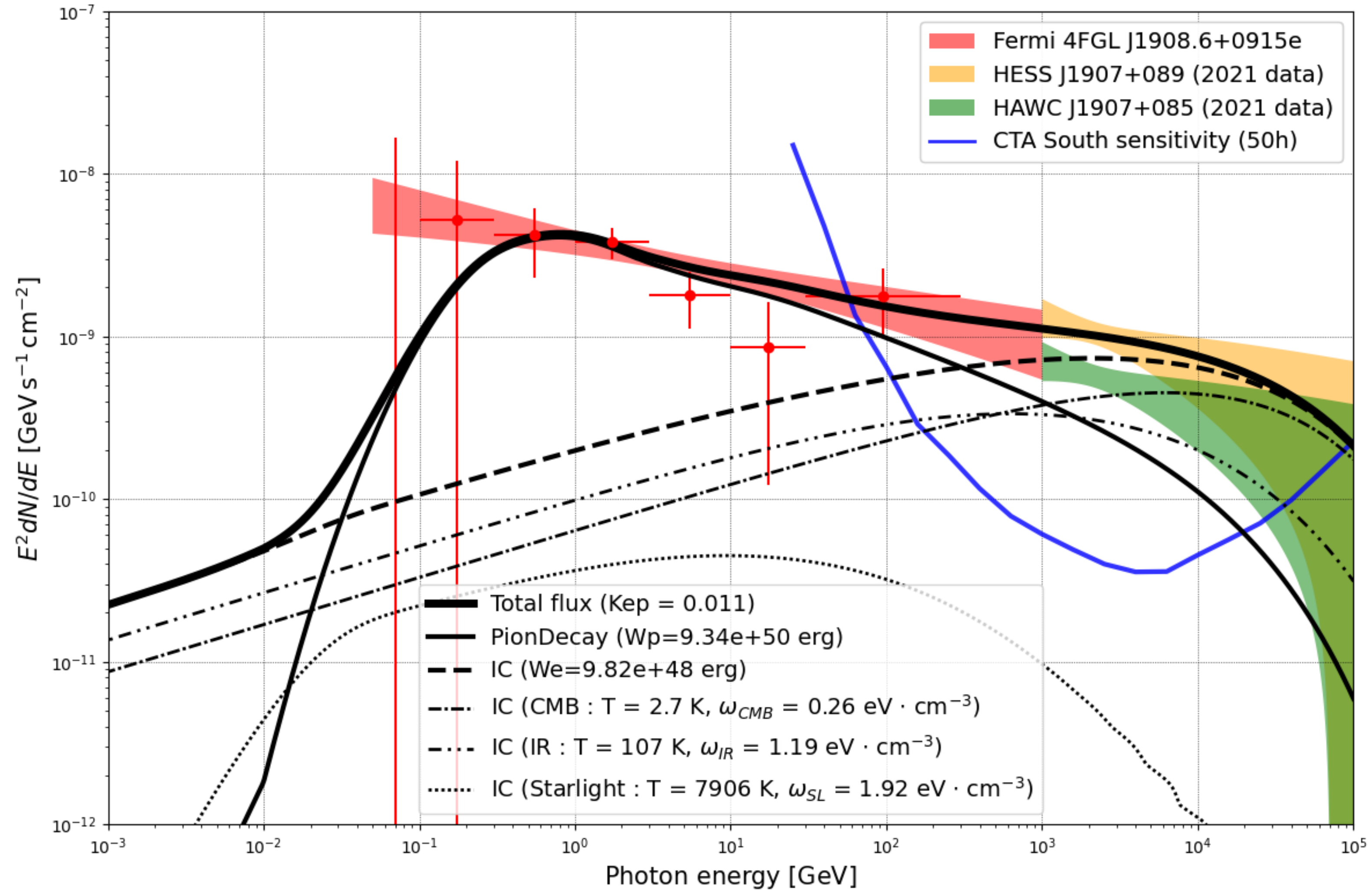


## Jet-like magnetar wind:

Relativistic outflow from a magnetar in the form of a collimated jet can drill the expanding ejecta and produce a long gamma-ray burst

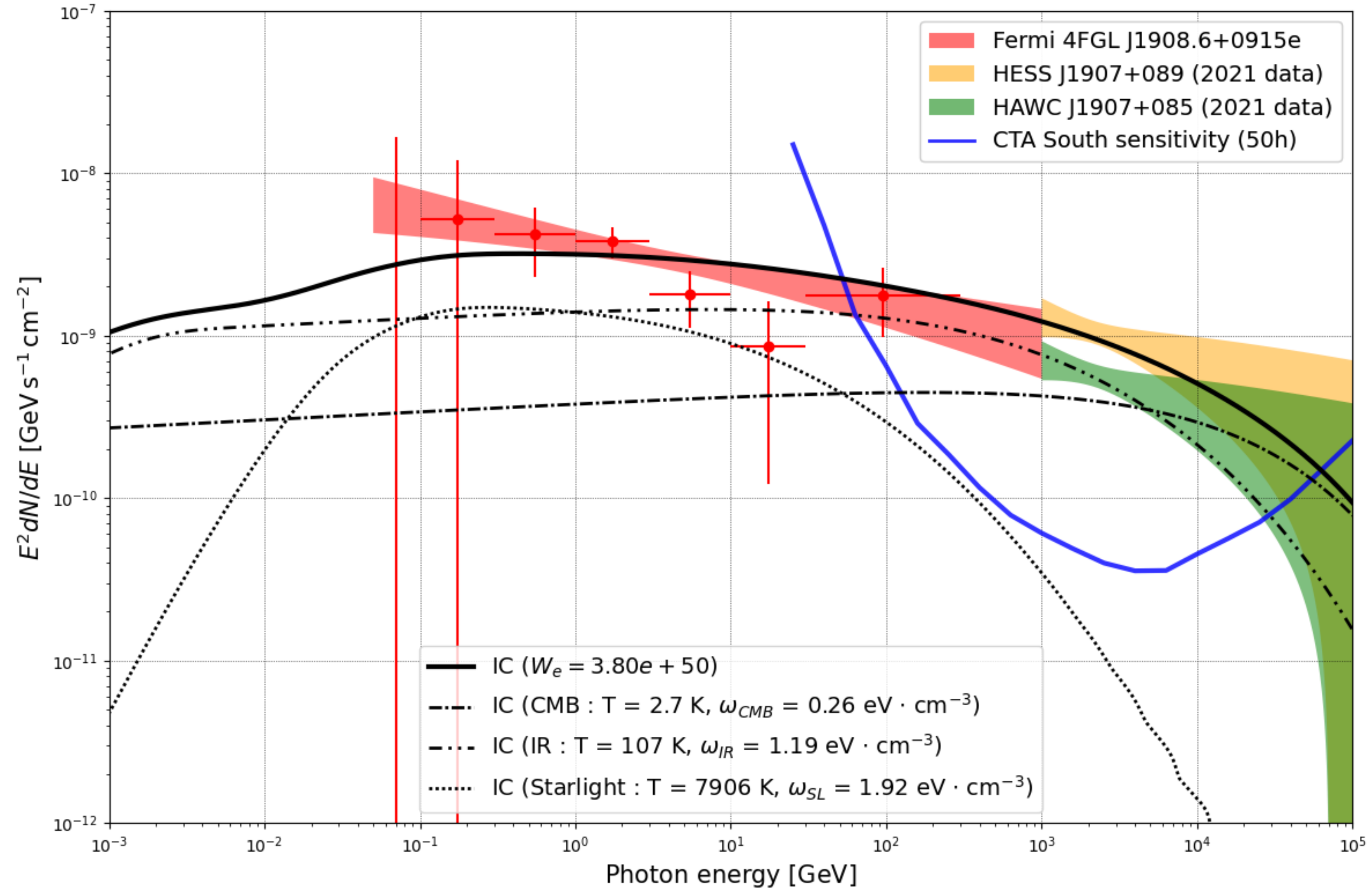
$$E_{MW} \leq 10^{52} \text{ erg and } E_{cr,e+e-} \sim 10^{50} \text{ erg}$$

# Spectral energy distribution modeling in case of HNR model



**Best-fit spectrum corresponds to  $W_p = 5 \times 10^{50} \text{ erg}$ ,  $K_{ep} = 0.004$**

# Spectral energy distribution modelling in case of MWN model with ECBPL lepton spectrum



**Best-fit spectrum corresponds to  $W_e = 3.6 \times 10^{50}$  erg**

# PARAMETERS OF HNR AND MWN MODELS OF GAMMA-RAY EMISSION FROM SGR1900+14 OUTSKIRTS

**Table 1:** HNR and MWN NAIMA-fitted models of SED from SGR 1900+14 neighbourhood

2*Parameter	HNR: PL and ECPL spectra (i=p)		MWN: ECBPL(i=e)	MWN:Two electron population spectra (i=e)	
	PL	ECPL	ECBPL	ECPL #1	ECPL #2
$E_{\min}$ [GeV](fixed)	1	1	1	1	1
$E_{\max}$ [GeV](fixed)	1e6	1e6	1e6	1e6	1e6
$N_{0,i}$ [1/ eV]	(1.18±0.04)e35	(1.42±0.05)e37	(1.90±0.12)e40	(4.41±0.51)e38	(8.81±0.44)e34
$E_{0,i}$ [TeV]	3.93±0.1	0.78±0.01	0.19±0.01	1.91±0.19	1.81±0.19
$E_{br,i}$ [TeV]	-	-	0.0047±0.0003	-	-
$E_{cut,i}$ [TeV]	-	185.2±9.5	396.7±41.7	0.0096±0.0008	9.99±1.06
$\gamma_{1,i}$	2.55±0.01	2.41±0.03	1.49±0.07	1.65±0.11	-
$\gamma_{2,i}$	-	-	3.04±0.06	-	2.58±0.17
$W_p$ [erg]	5.03e50	5.12e50	-	-	-
$W_e$ [erg]	1.04e49	2.16e48	3.60e50	5.20e50	6.08e49
$n_H$ [cm <sup>-3</sup> ]	11.42±0.66	9.81±0.35	-	-	-
$K_{ep}$	0.02 (fixed)	0.0041±0.0002	-	-	-

**In both HNR and MWN cases the TeV gamma-ray emission corresponds to CR energy  $E_{CR} \approx 5 \cdot 10^{50}$  erg in both hadronic (HNR) and leptonic (MWN) scenarios Such CR energies are expected in Hypernova model of magnetar-related Supernova**



# Summary

The most promising Galactic candidates for UHECR accelerators are Hypernovae with millisecond pulsar/magnetar, giant flares of magnetars, Kilonovae (NS-NS mergers), tidal disruption events etc. accompanied by (mildly) relativistic jets with close to the Earth directions.

Galactic magnetar SGR1900+14 may be responsible for the observed EHECR triplet

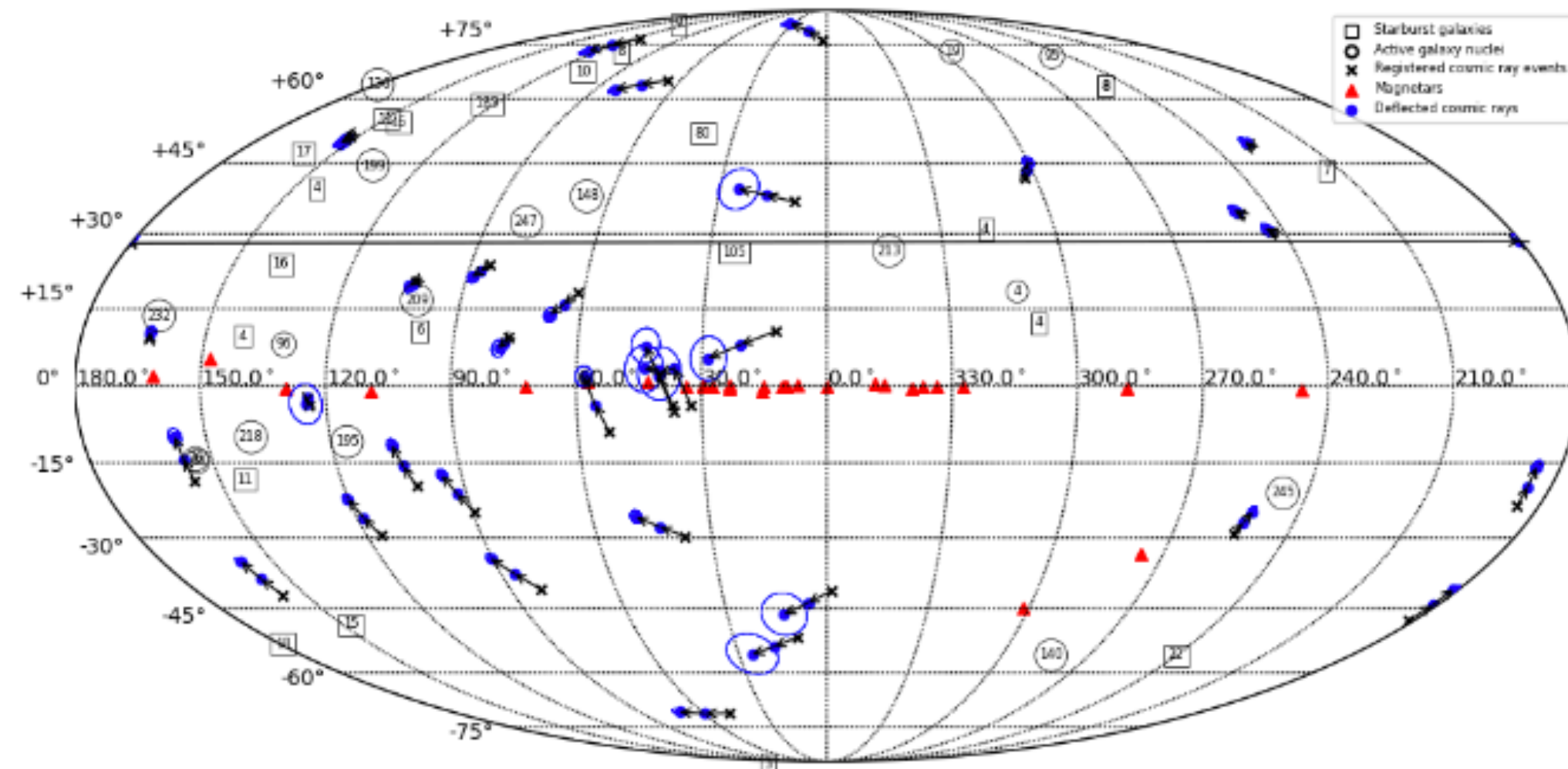
Promising signature of effective acceleration processes in magnetars' neighbourhoods should be nonthermal high-energy and very high-energy gamma-ray emission

We have explained the observed gamma-ray emission from the magnetar SGR 1900+14 neighbourhood in a model of magnetar-connected HNR and MWN created by an energy supply to a SN ejecta from a fast-rotating newborn magnetar with initial rotational energy  $E_{rot} \sim 10^{52}$  erg

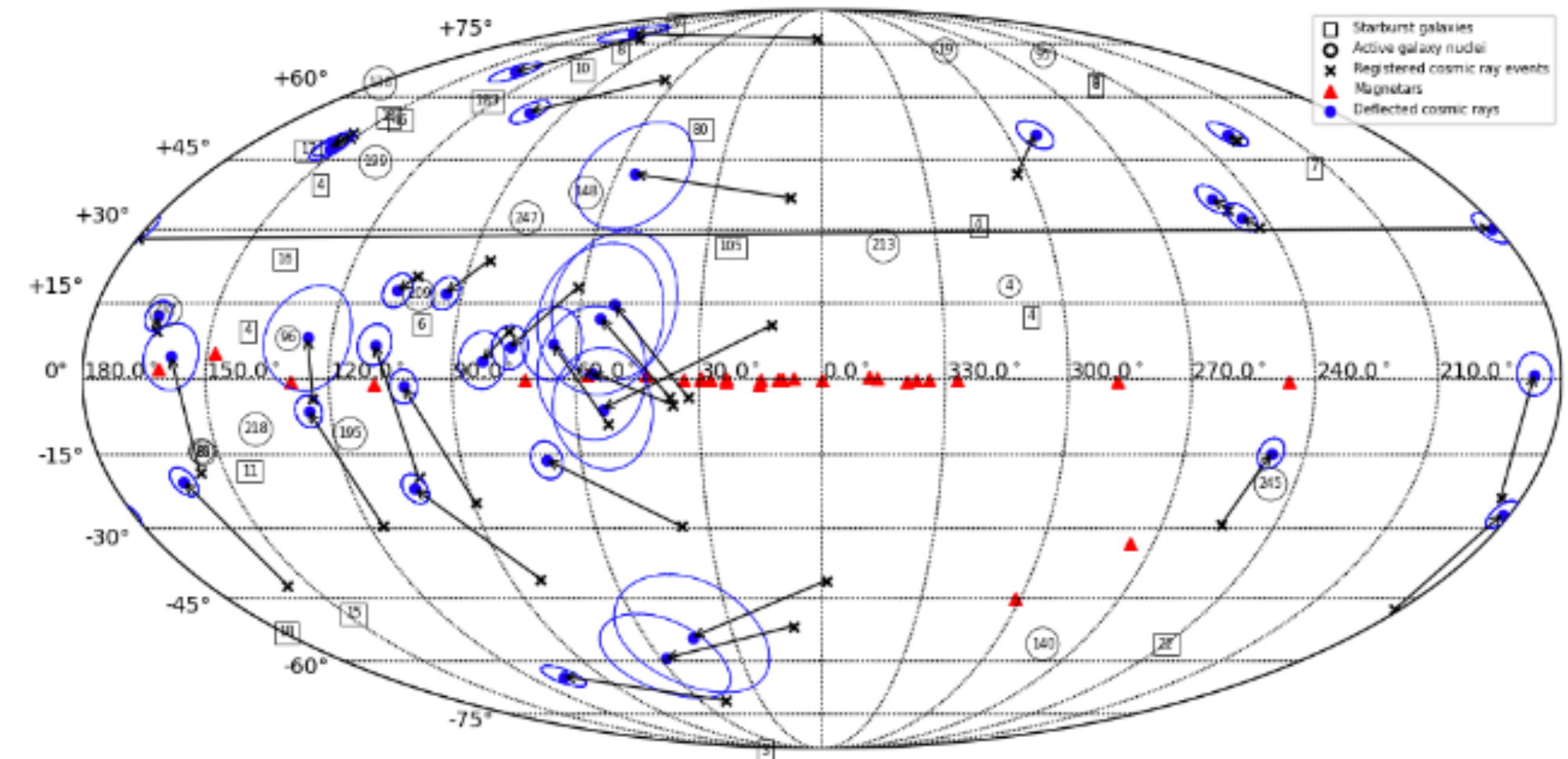
**THANK YOU!**

**back up**

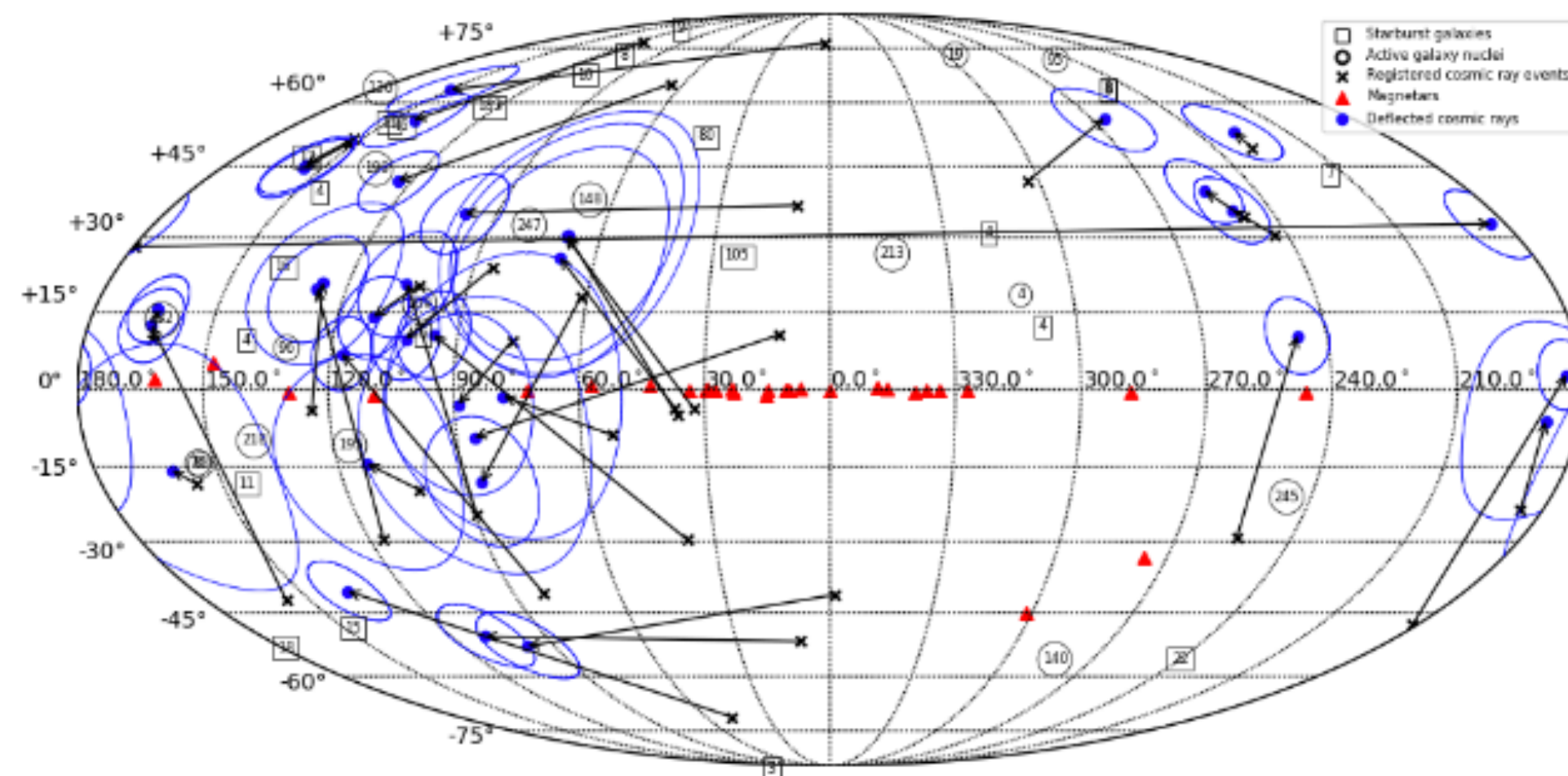
# Backtracking trajectories of EHECR events



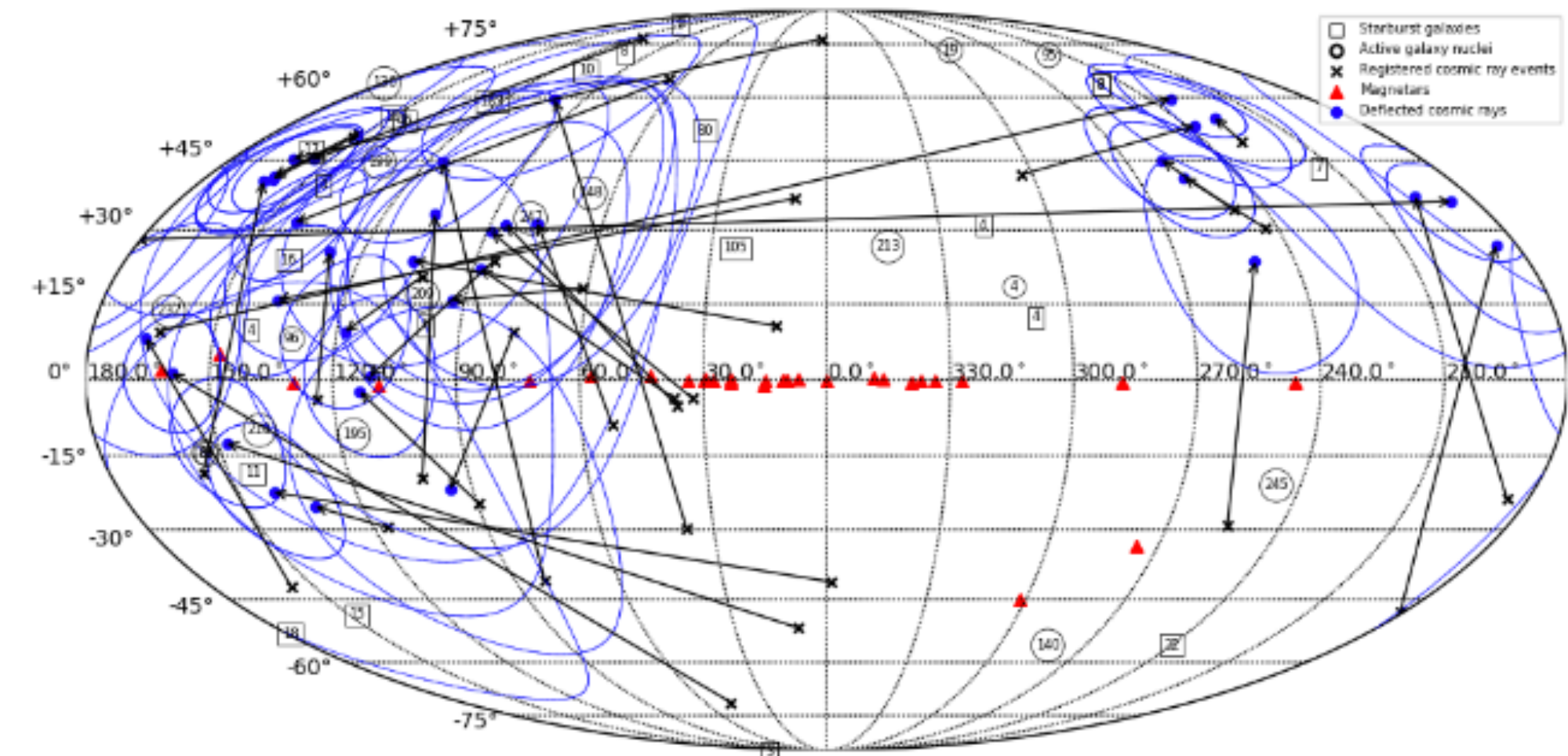
(a)  $Z=1, 2$



(b)  $Z=6$



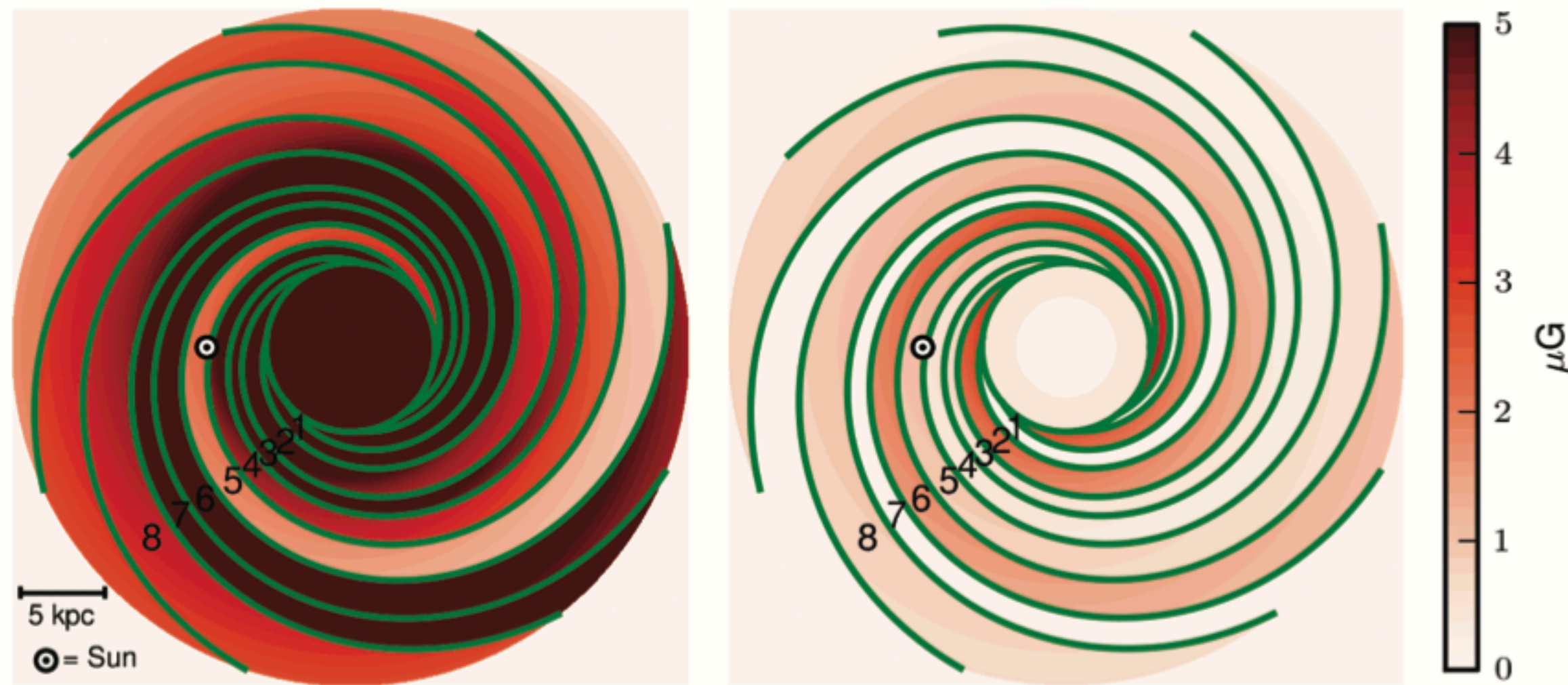
(c)  $Z=14$



(d)  $Z=26$

# Magnetic field model

## Galactic magnetic field model JF12



Jansson&Farrar, arXiv:1204.3662, arXiv:1210.7820

Field	Best fit Parameters	Description
Disk component	$b_1 = 10.81 \pm 2.33 \mu\text{G}$	field strengths at $r = 5 \text{ kpc}$
	$b_2 = 6.96 \pm 1.58 \mu\text{G}$	
	$b_3 = 9.59 \pm 1.10 \mu\text{G}$	
	$b_4 = 6.96 \pm 0.87 \mu\text{G}$	
	$b_5 = 1.96 \pm 1.32 \mu\text{G}$	
	$b_6 = 16.34 \pm 2.53 \mu\text{G}$	
	$b_7 = 37.29 \pm 2.39 \mu\text{G}$	
	$b_8 = 10.35 \pm 4.43 \mu\text{G}$	
Halo component	$b_{\text{int}} = 7.63 \pm 1.39 \mu\text{G}$	field strength at $r < 5 \text{ kpc}$
	$z_0^{\text{disk}} = 0.61 \pm 0.04 \text{ kpc}$	Gaussian scale height of disk
	$B_0 = 4.68 \pm 1.39 \mu\text{G}$	field strength
Striation	$r_0 = 10.97 \pm 3.80 \text{ kpc}$	exponential scale length
	$z_0 = 2.84 \pm 1.30 \text{ kpc}$	Gaussian scale height
Striation	$\beta = 1.36 \pm 0.36$	striated field $B_{\text{stri}}^2 \equiv \beta B_{\text{reg}}^2$

## Random extragalactic magnetic field

$$\theta(E, d) \simeq 0.8^0 Z \left( \frac{E}{10^{20} \text{eV}} \right)^{-1} \left( \frac{d}{10 \text{Mpc}} \right)^{1/2} \left( \frac{l_c}{1 \text{Mpc}} \right)^{1/2} \left( \frac{B_{\text{rms}}}{10^{-9} \text{G}} \right)$$

Waxman&Miralda-Escude, astro-ph/9607059



# Giant magnetar flares

Some magnetars, including the magnetar SGR 1900+14, can produce giant flares of gamma-ray emission (SGR 1900+14 flared on 27th August, 1998).

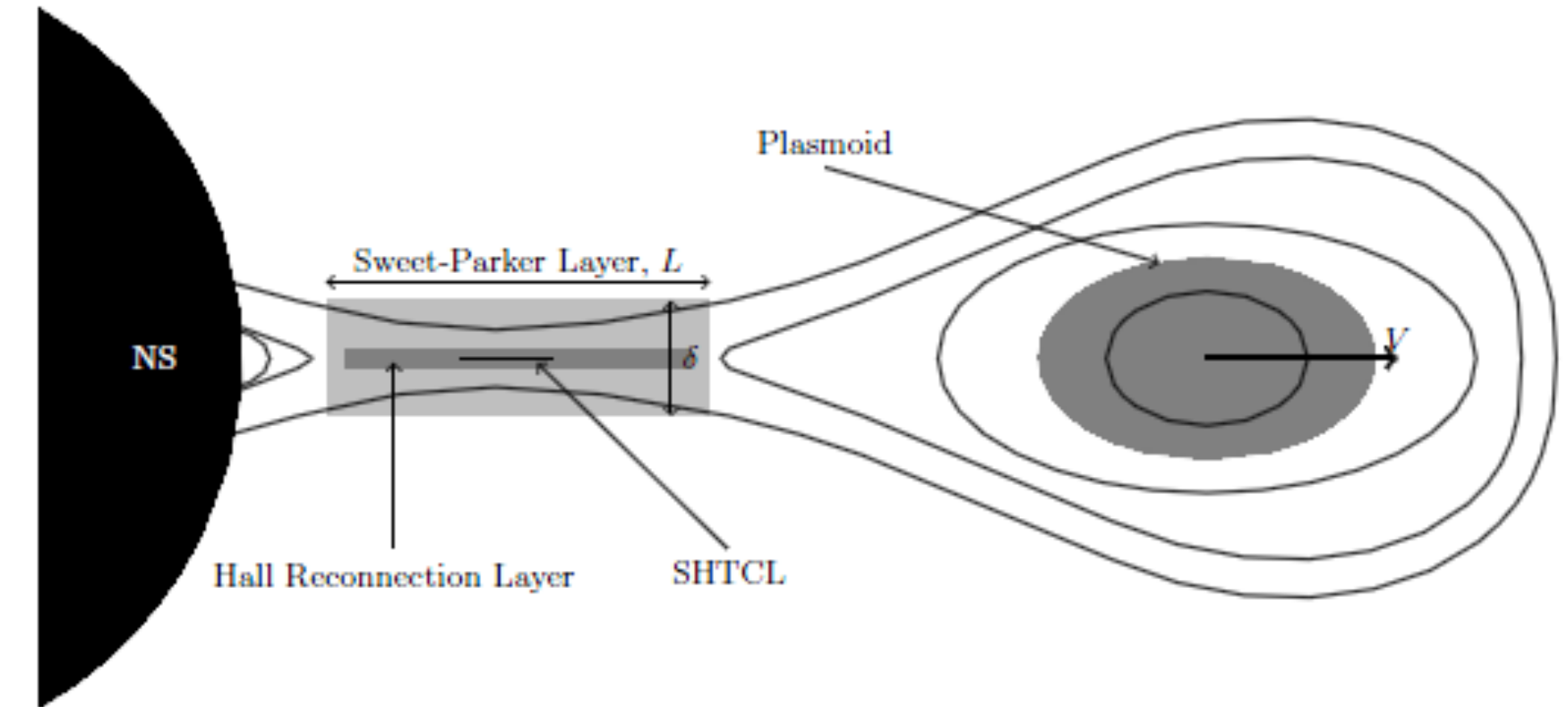
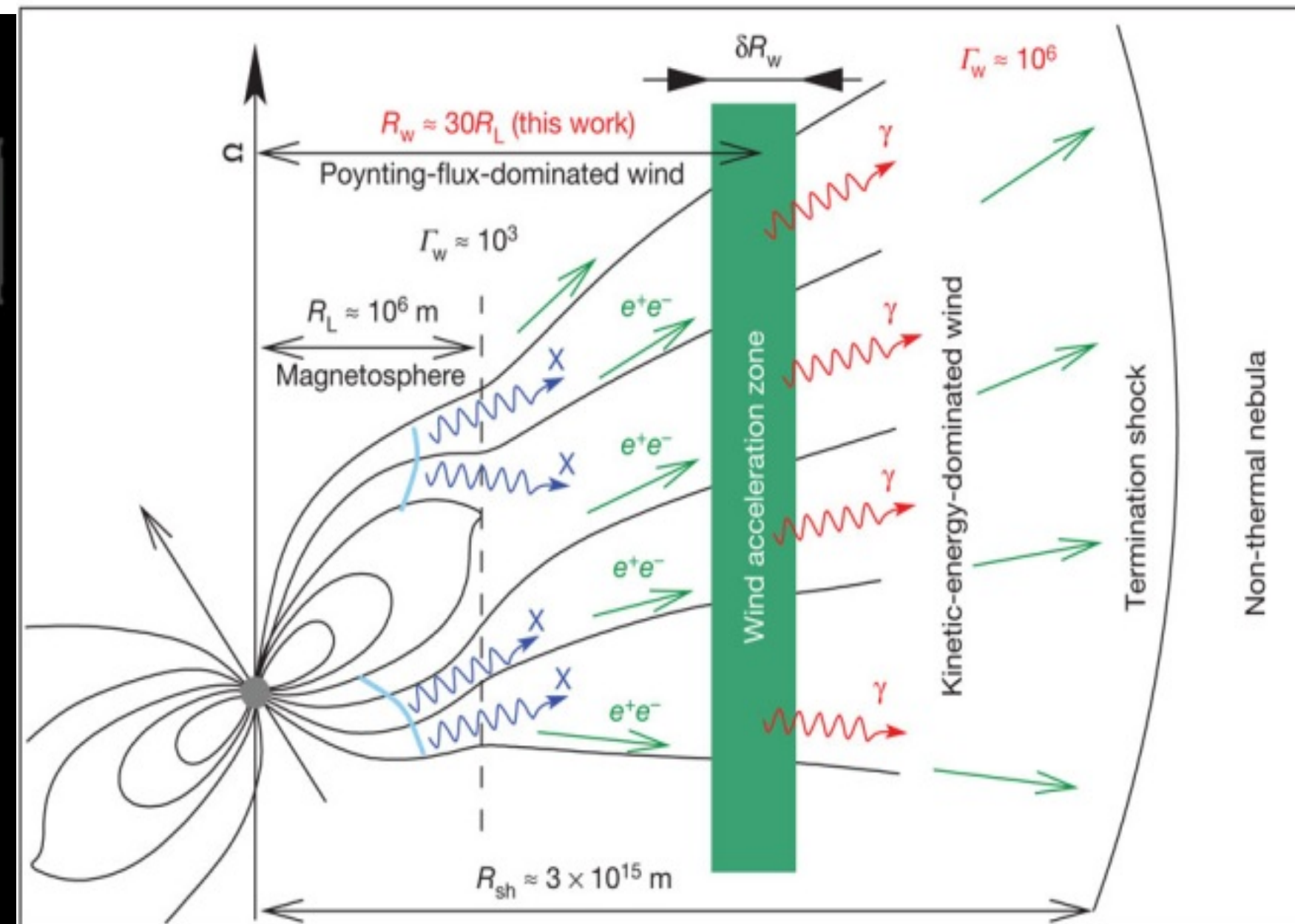
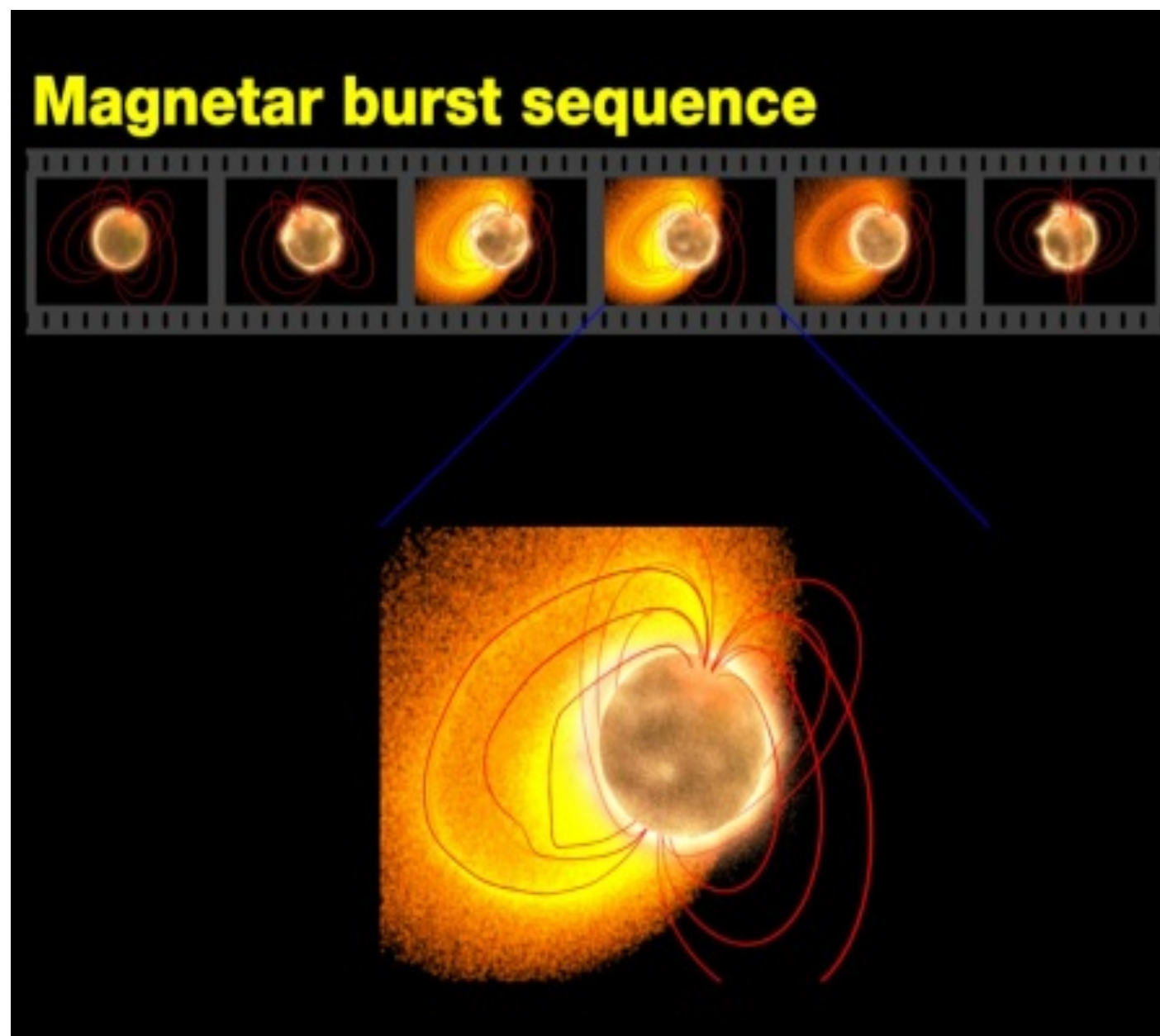


Figure 1. This figure displays the setup of the different reconnecting current layers. The macroscopic Sweet-Parker layer with length  $L \sim 10^5$  cm and width  $\delta \sim 0.01$  cm is the largest of the three. This layer is then thinned down vertically as strong magnetic flux is convected into the dissipation region. The Hall reconnection layer, represented by the dark gray region, develops when  $\delta$  becomes

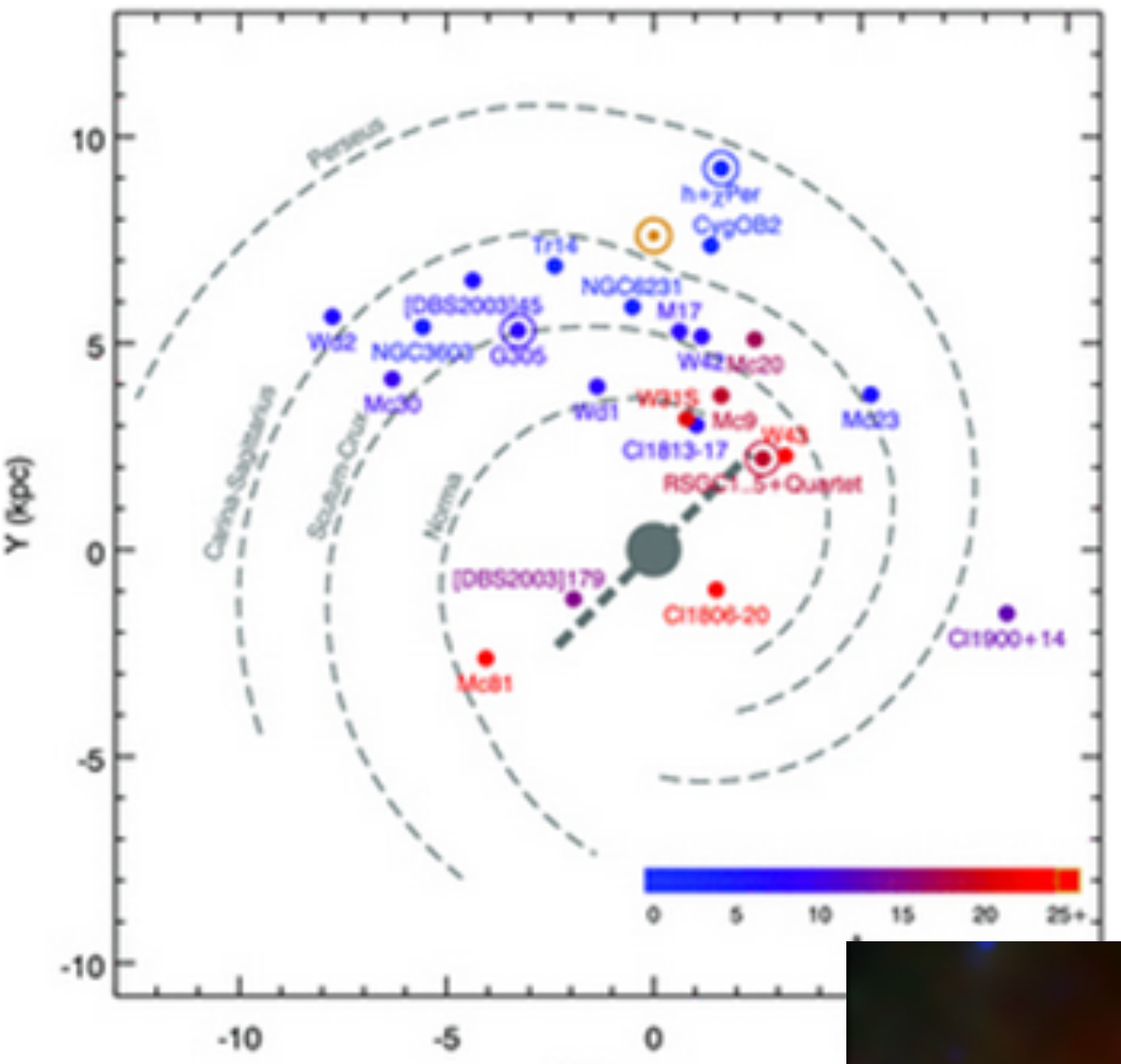
Aharonian et al. 2012



Credit & Copyright: Robert Mallozzi

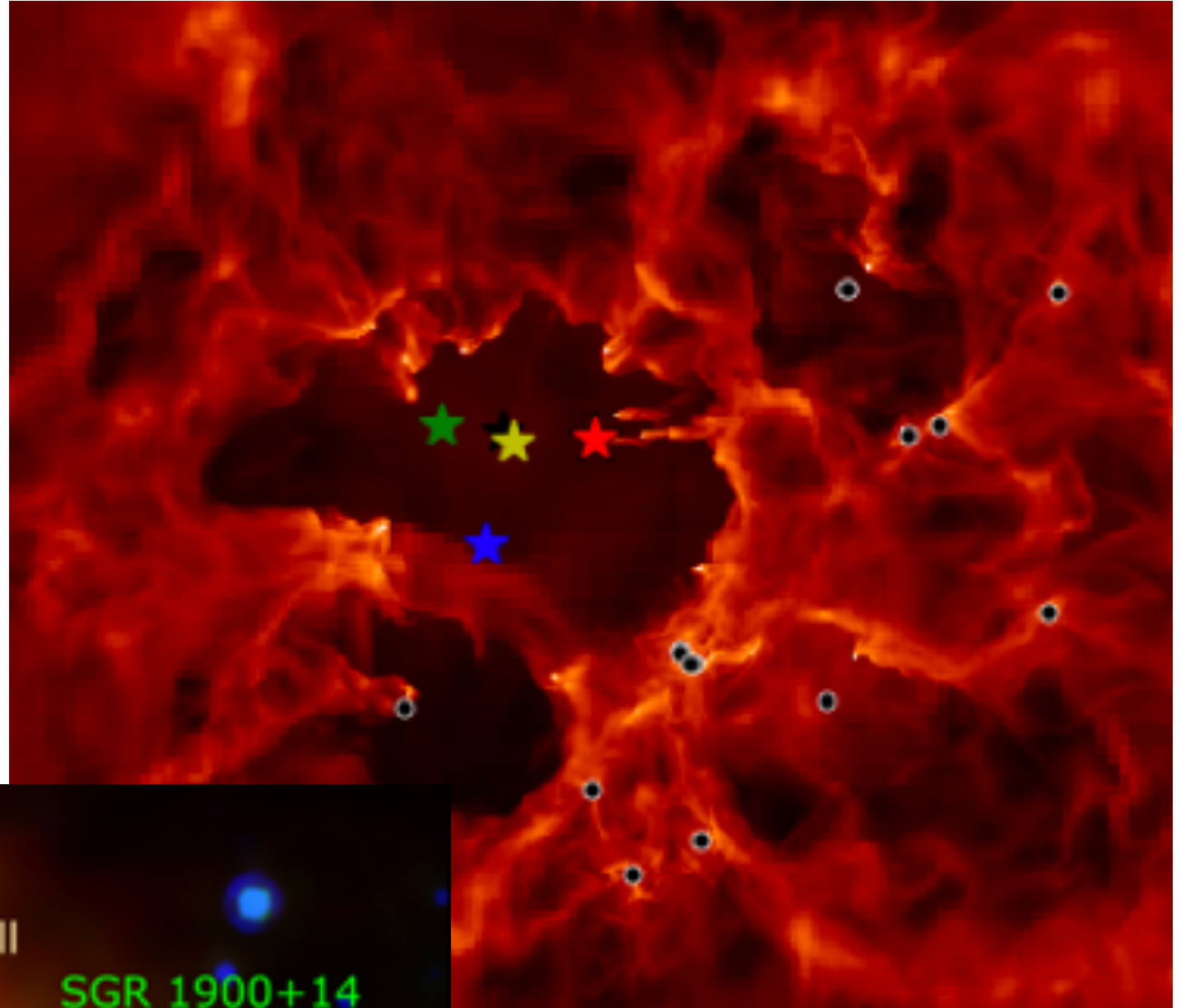
# Our model of SGR1900+14 evolution

1. Birthplace: 17 Myr ago in young stellar cluster Cl1900+14 d=12.5 kpc



2. Explosion as SN Ic in stellar wind cavity  
Newborn pulsar with  $P=1\text{ms}$  and  $B=4 \times 10^{14}\text{G}$

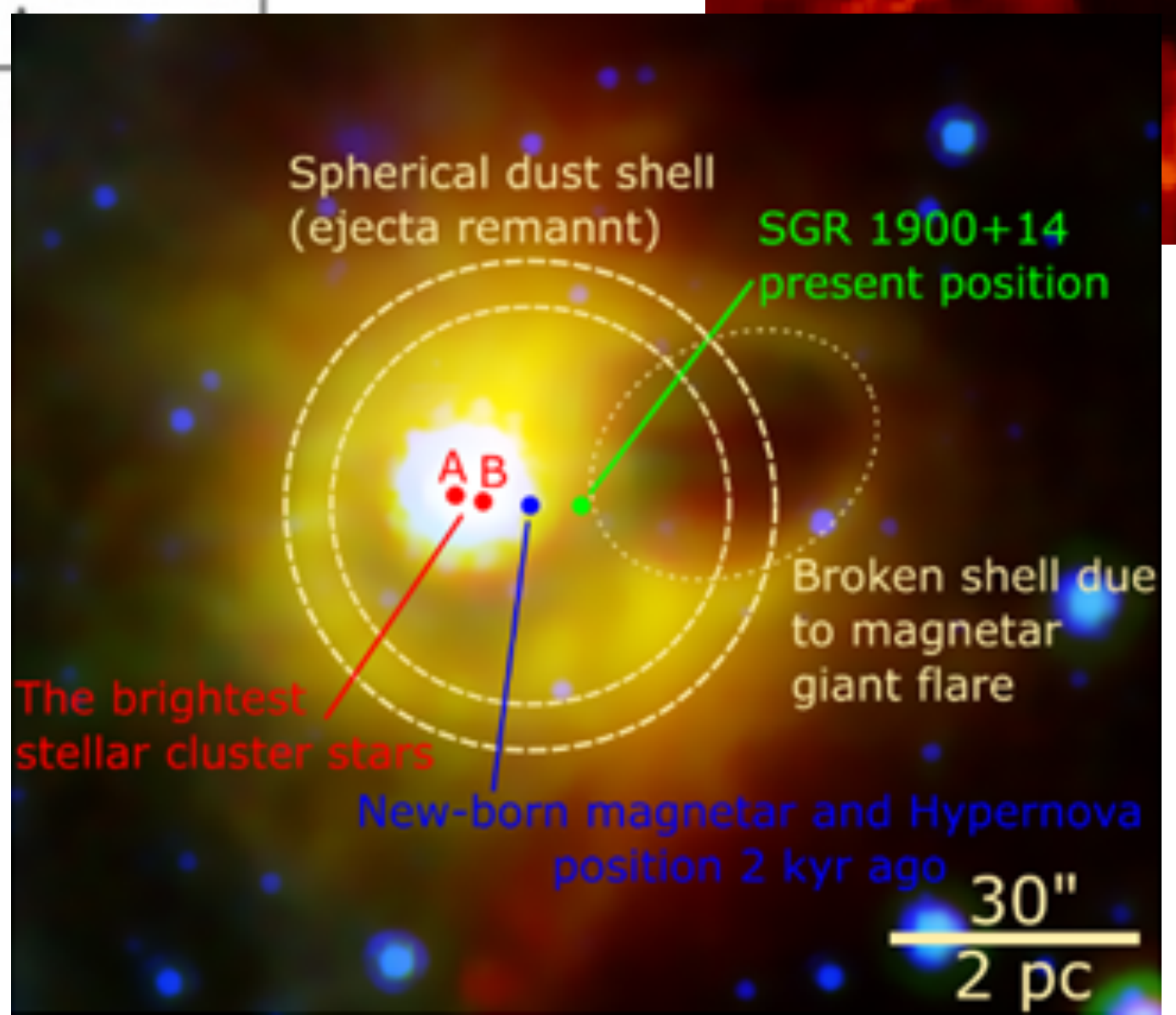
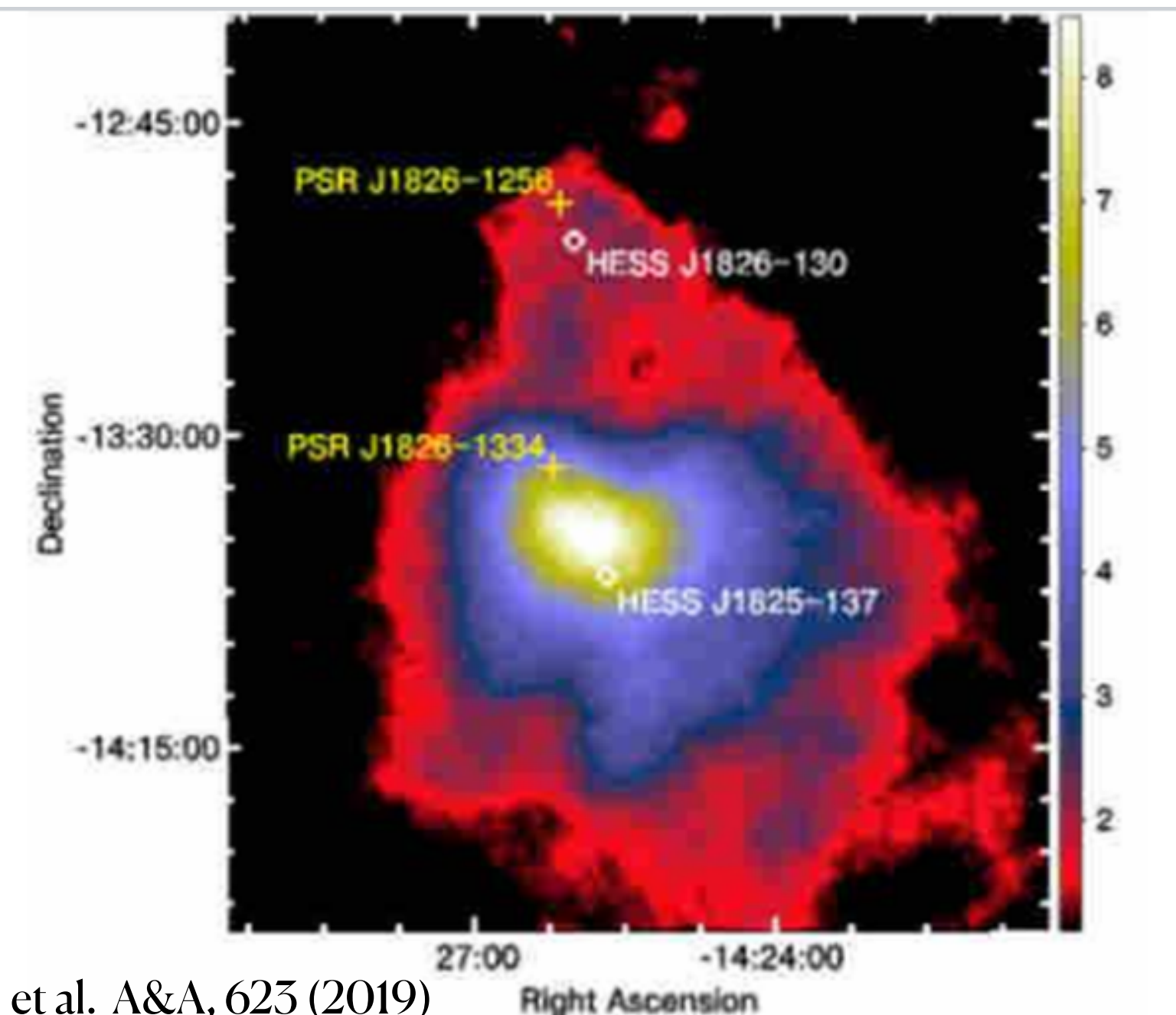
Magnetar with  $E_{rot} \approx 10^{52}\text{erg}$



$E_{rot}$  was transformed into:

- $E_{ejecta} \leq 10^{52}\text{erg}$  (Hypernova model)
- $E_{MWN} \leq 10^{52}\text{erg}$  (magnetar wind nebula model)

PWN HESS J1825-137 at 4 kps  
(SGR1900+14- twin)



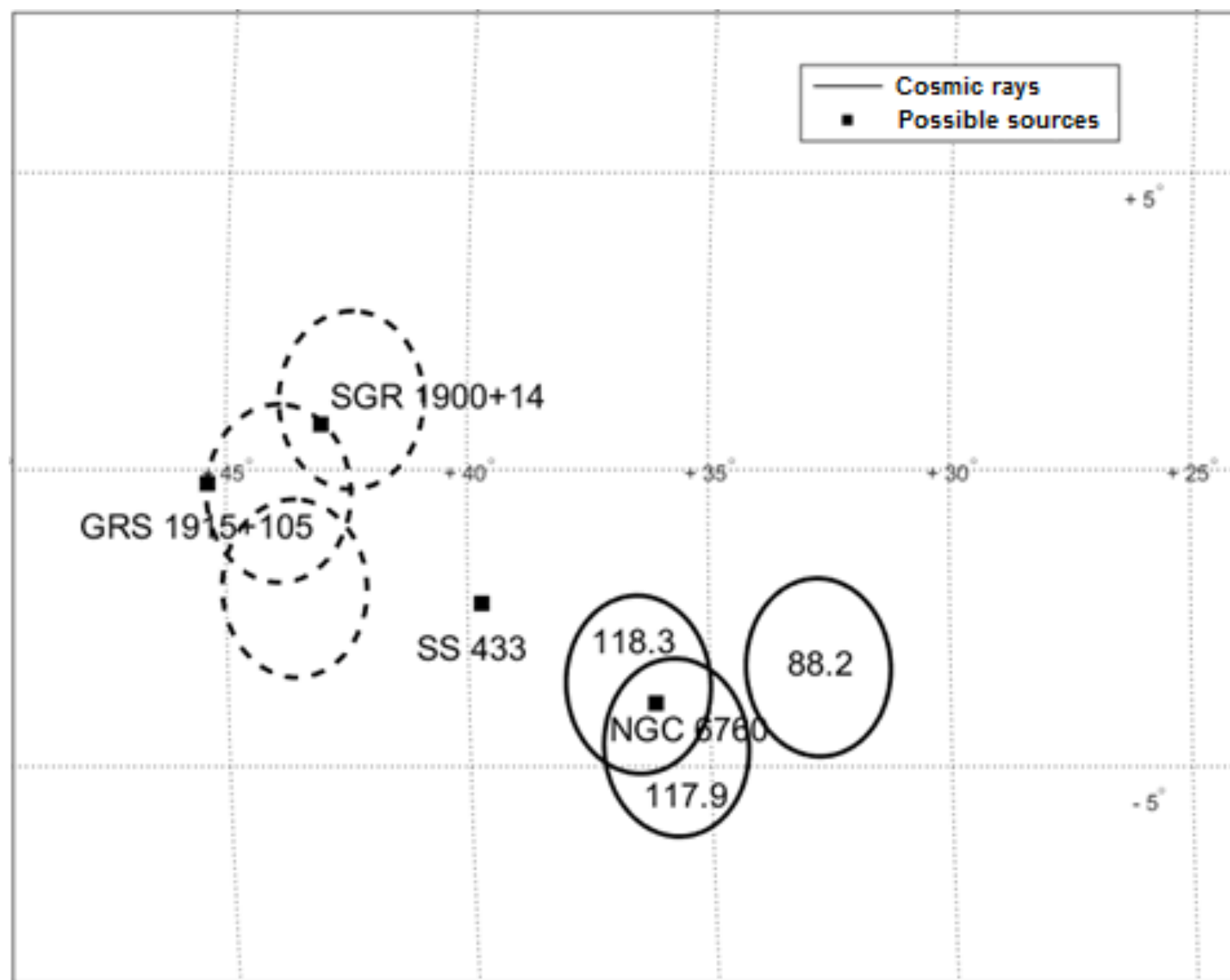
$2 M_{sun}$  spherical dust shell-relic of SN shell

Broken shell is evaporated by collimated giant flare

arXiv:1907.04316v1



# Possible sources of the triplet

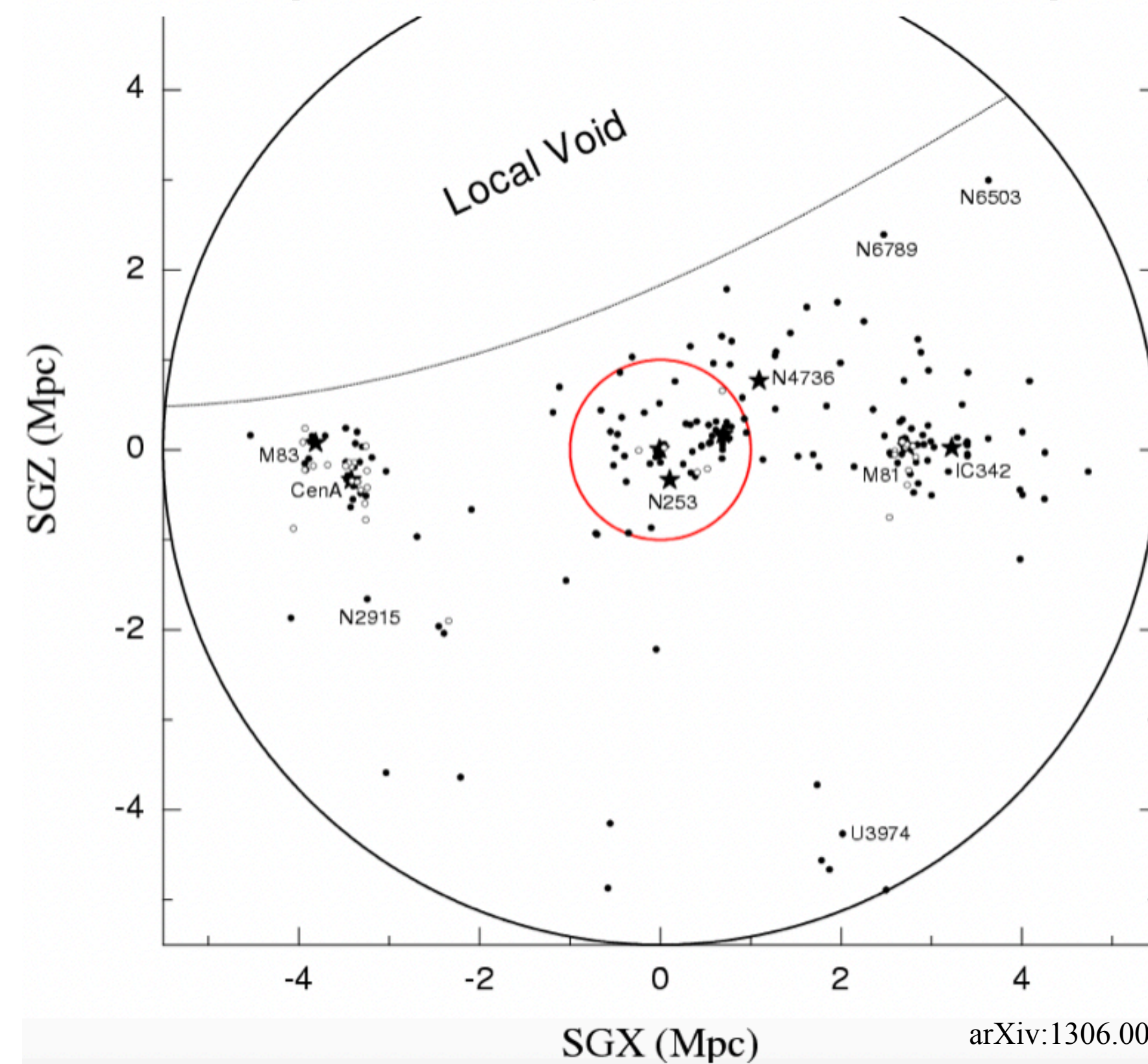


Solid circles - initial positions of CRs in the triplet with 1 sigma errors

Dashed circles - positions of CRs ( $Z=6$ ) at the distance 12.5 kpc from the Earth

No	Name	Type	$l$ , deg	$b$ , deg	$d$ , kpc
1	GRS 1915+105	Microquasar	45.37	-0.22	$8.6 \pm 2.0$
2	SS 433	Microquasar	39.69	-2.24	$5.5 \pm 0.2$
3	NGC 6760	Globular cluster	36.11	-3.9	$7.4 \pm 0.4$
4	<b>SGR 1900+14</b>	<b>Magnetar</b>	<b>43.02</b>	<b>0.77</b>	<b><math>12.5 \pm 1.7</math></b>

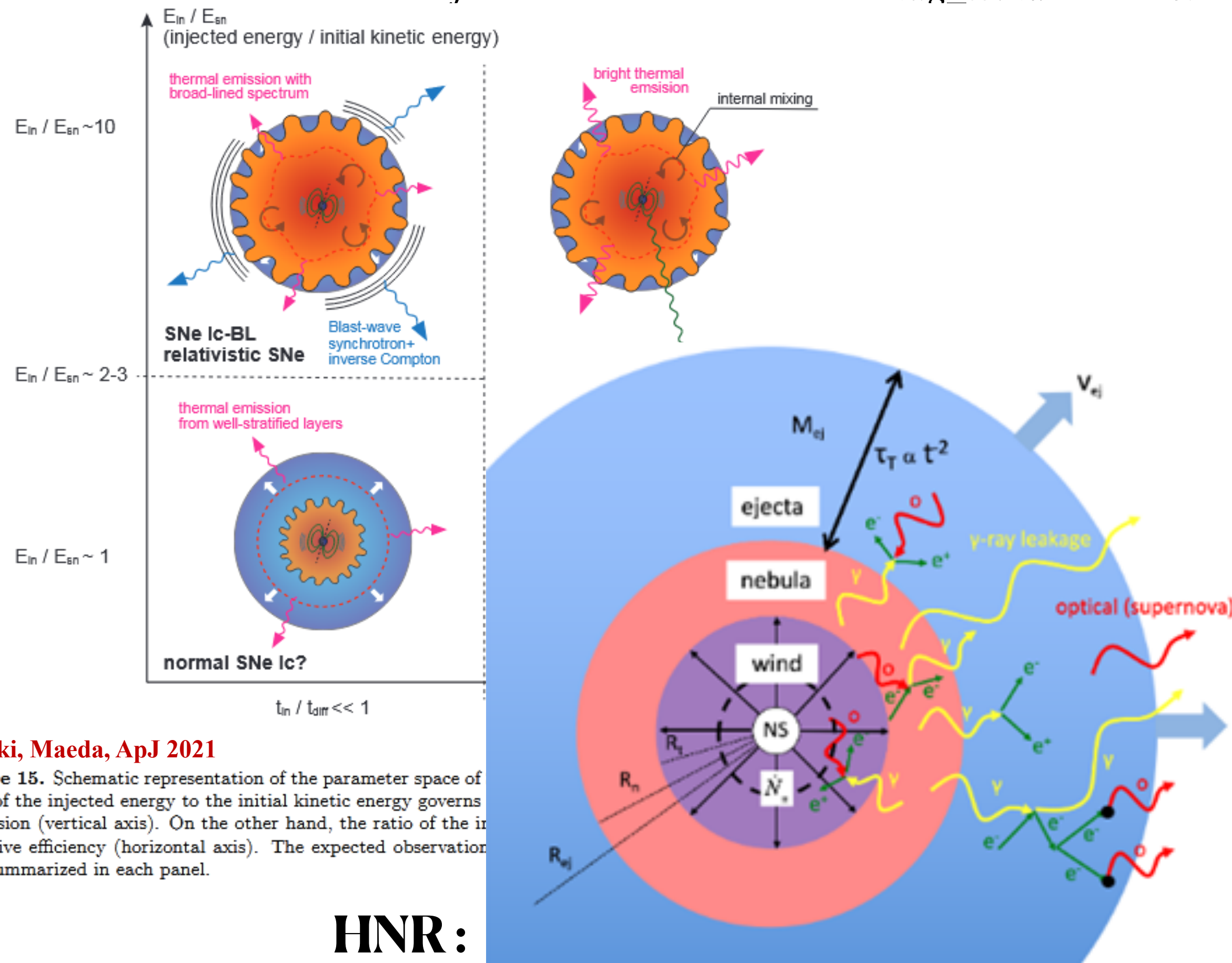
Local void resides at distance 2Mpc from our Galaxy, and extends for 50 Mpc, so considering energy loss length, there are no possible extragalactic sources for triplet



Magnetar SGR1900+14 is the most promising potential source

# Evolution of the magnetar driven Hypernova/MWN

$$E_{ejecta} = 10^{51} \text{ erg}, \quad E_{mag\_wind} = E_{rot} = 10^{52} \text{ erg}$$



Suzuki, Maeda, ApJ 2021

Figure 15. Schematic representation of the parameter space of ratio of the injected energy to the initial kinetic energy governs expansion (vertical axis). On the other hand, the ratio of the radiative efficiency (horizontal axis). The expected observation also summarized in each panel.

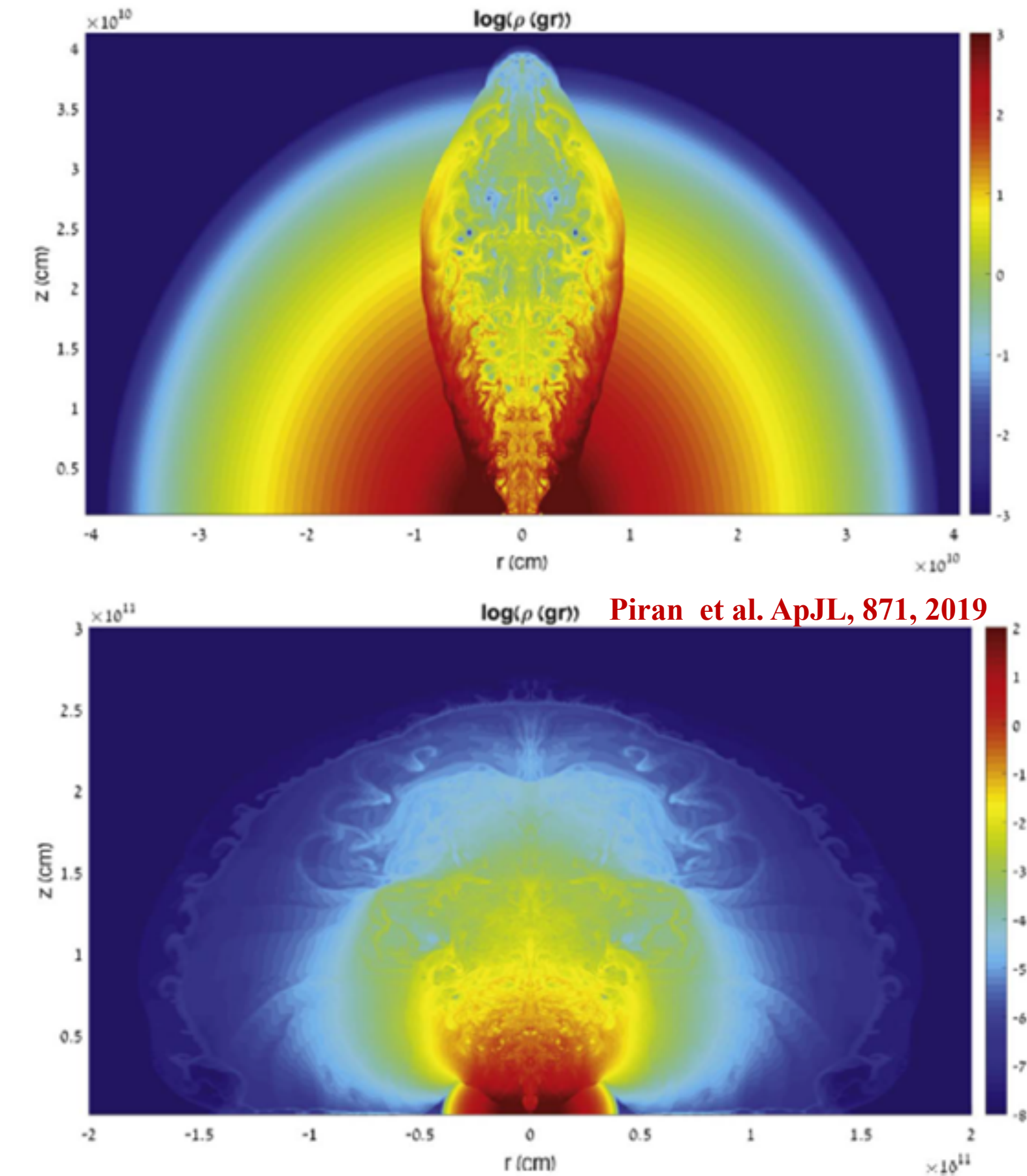
**HNR:**

Magnetar Wind Nebula (MWN) pressure protrudes dense internal part

of ejecta and accelerates its external layers up to  $E_{ejecta} = 10^{52}$  erg

Diffusive Shock Acceleration at HNR shock:

$$E_{cr,p} = (3-5) \cdot 10^{50} \text{ erg}, \quad E_{cr,e} = K_{ep} \times E_{cr,p} \sim 10^{48} \text{ erg}$$



Piran et al. ApJL, 871, 2019

**MWN:**

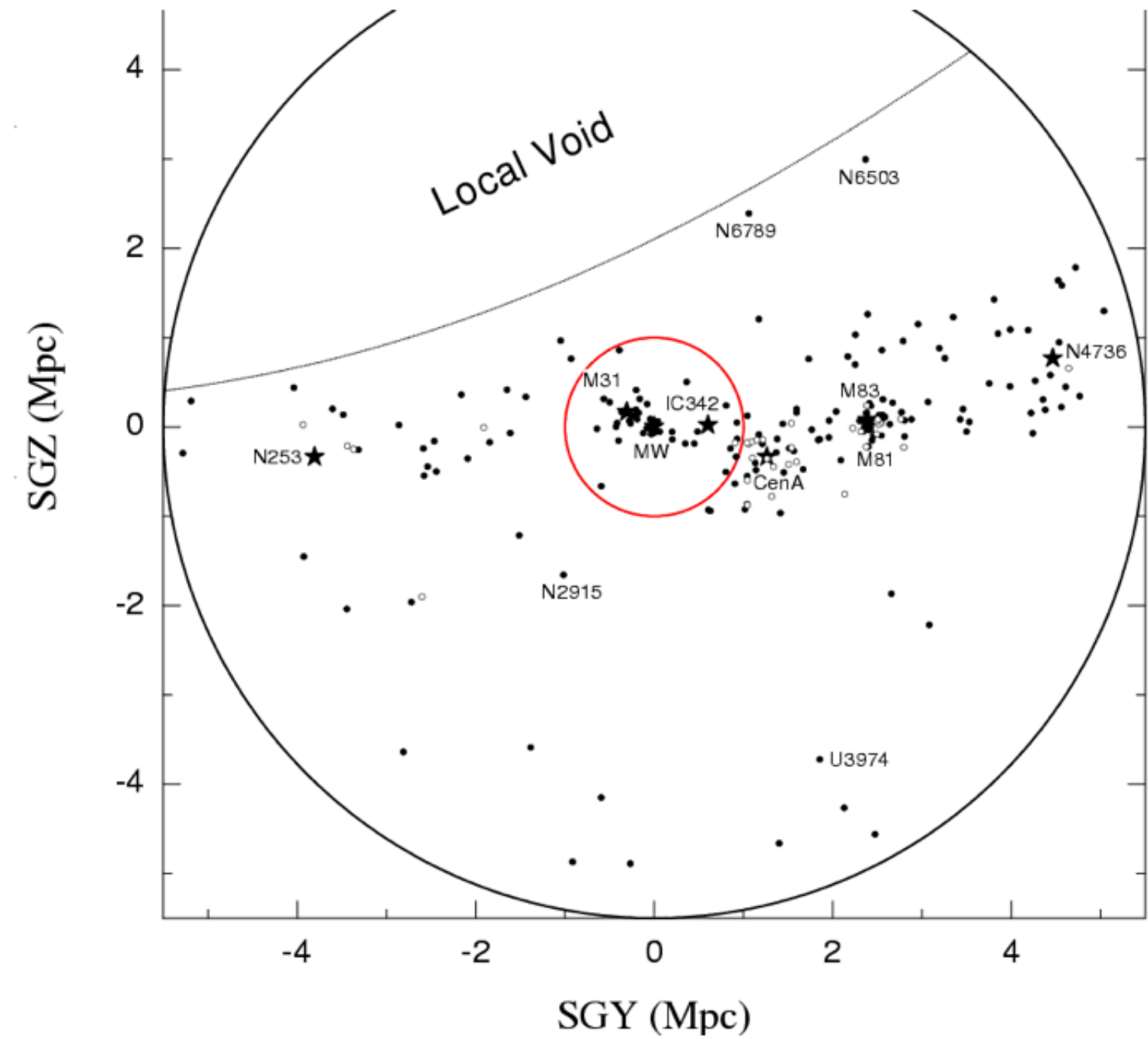
Break out of collimated wind jet creates large-scale MWN ( $r \sim 30$  pc)

with  $E_{MWN} \leq 10^{52}$  erg and  $E_{cr,e+e-} \sim 10^{50}$  erg ahead ejecta

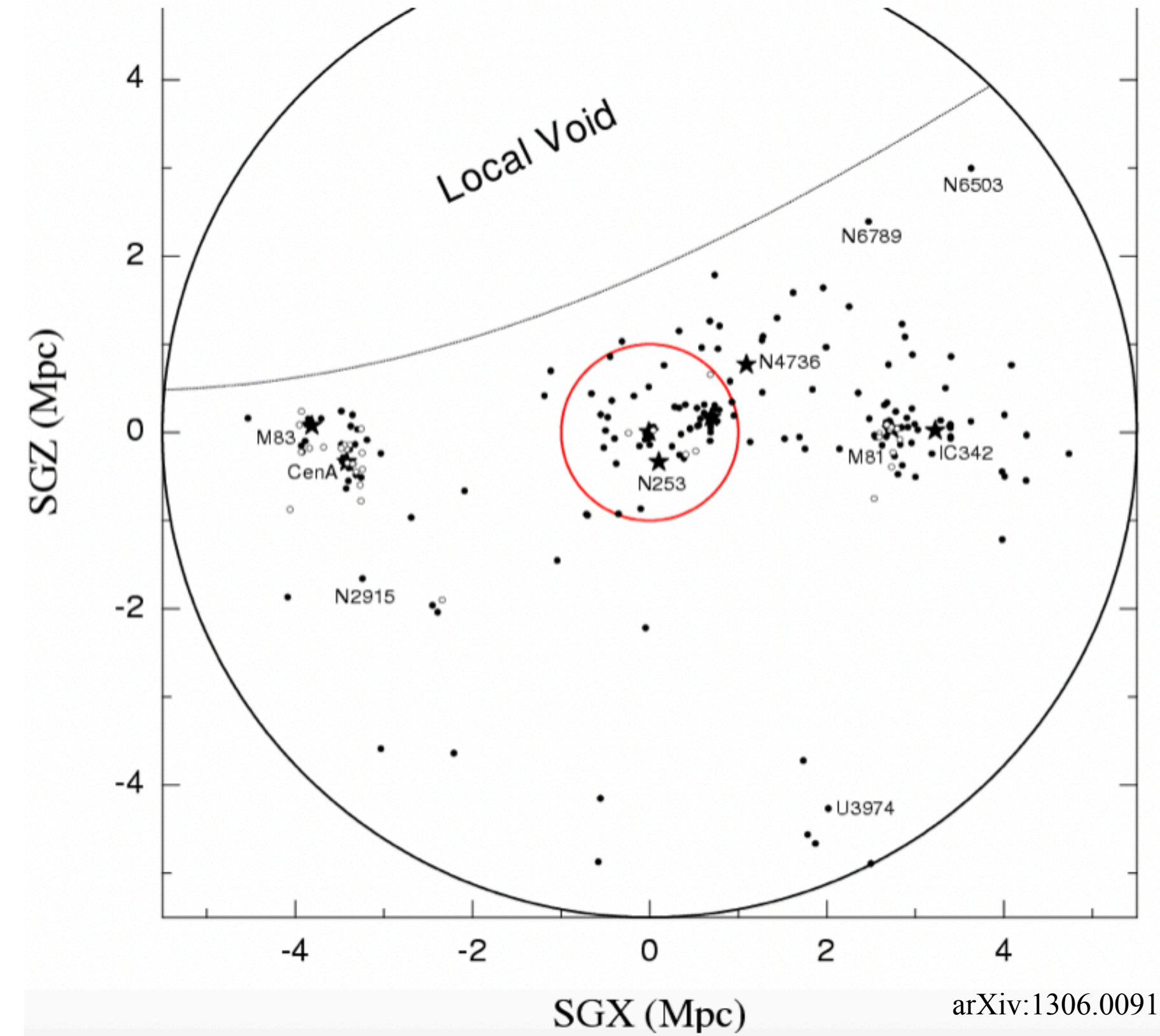
debris

( $R=2-3$  pc IR shell)

# Possible sources of the triplet



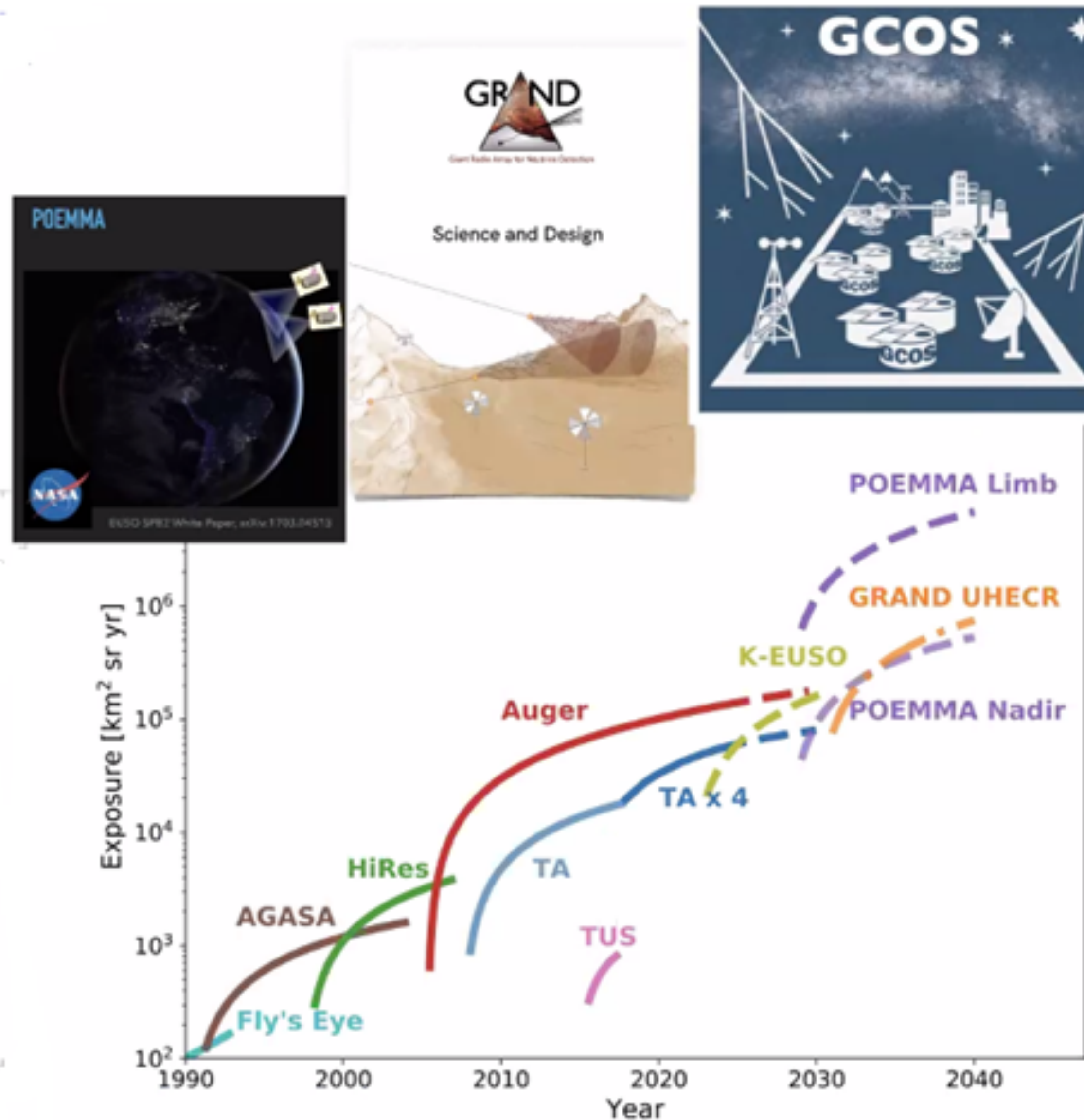
Local void resides at distance 2Mpc from our Galaxy, and extends for 50 Mpc, so considering energy loss length, there are no possible extragalactic sources for triplet



No	Name	Type	$l$ , deg	$b$ , deg	$d$ , kpc
1	GRS 1915+105	Microquasar	45.37	-0.22	$8.6 \pm 2.0$
2	SS 433	Microquasar	39.69	-2.24	$5.5 \pm 0.2$
3	NGC 6760	Globular cluster	36.11	-3.9	$7.4 \pm 0.4$
4	<b>SGR 1900+14</b>	<b>Magnetar</b>	<b>43.02</b>	<b>0.77</b>	<b><math>12.5 \pm 1.7</math></b>

Magnetar SGR1900+14 is the most promising potential source

# Cosmic rays: present and future detectors

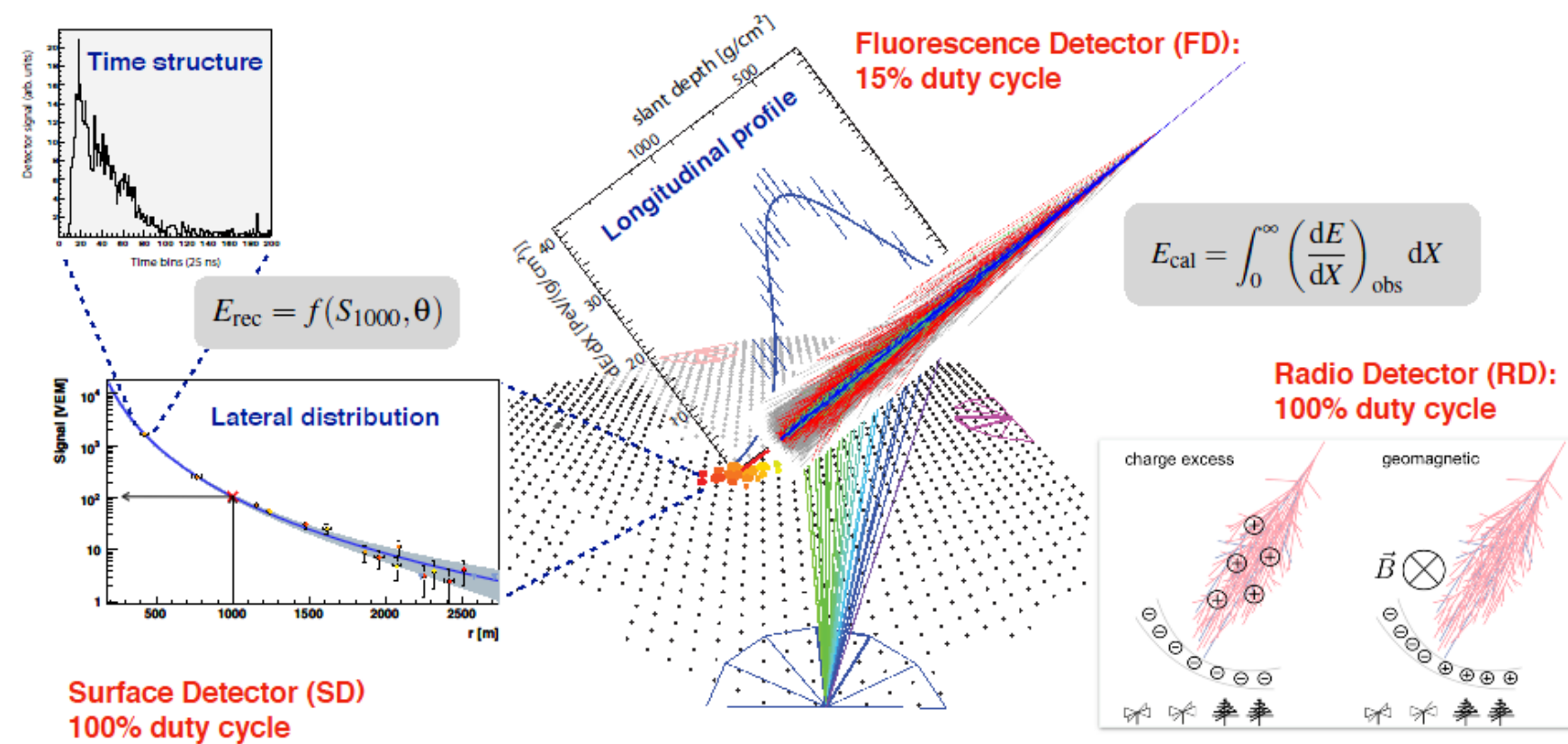


(Alves Batista et al, 1903.06714)

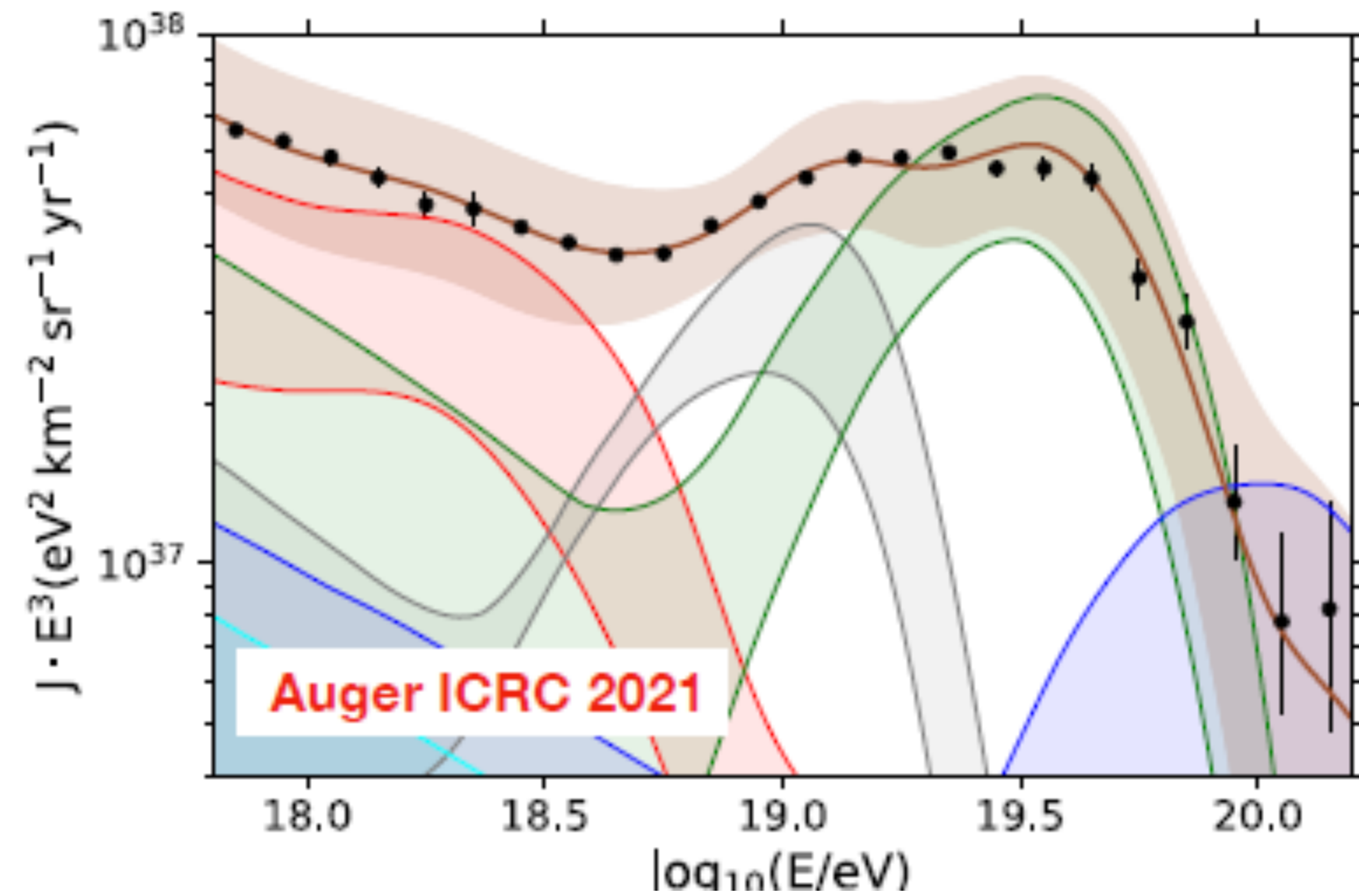
Telescope Array and Pierre Auger Observatory are the main state-of-the-art detectors

# Energy spectrum and chemical composition of UHECR: recent Auger and TA data

Air shower observables (hybrid observation)



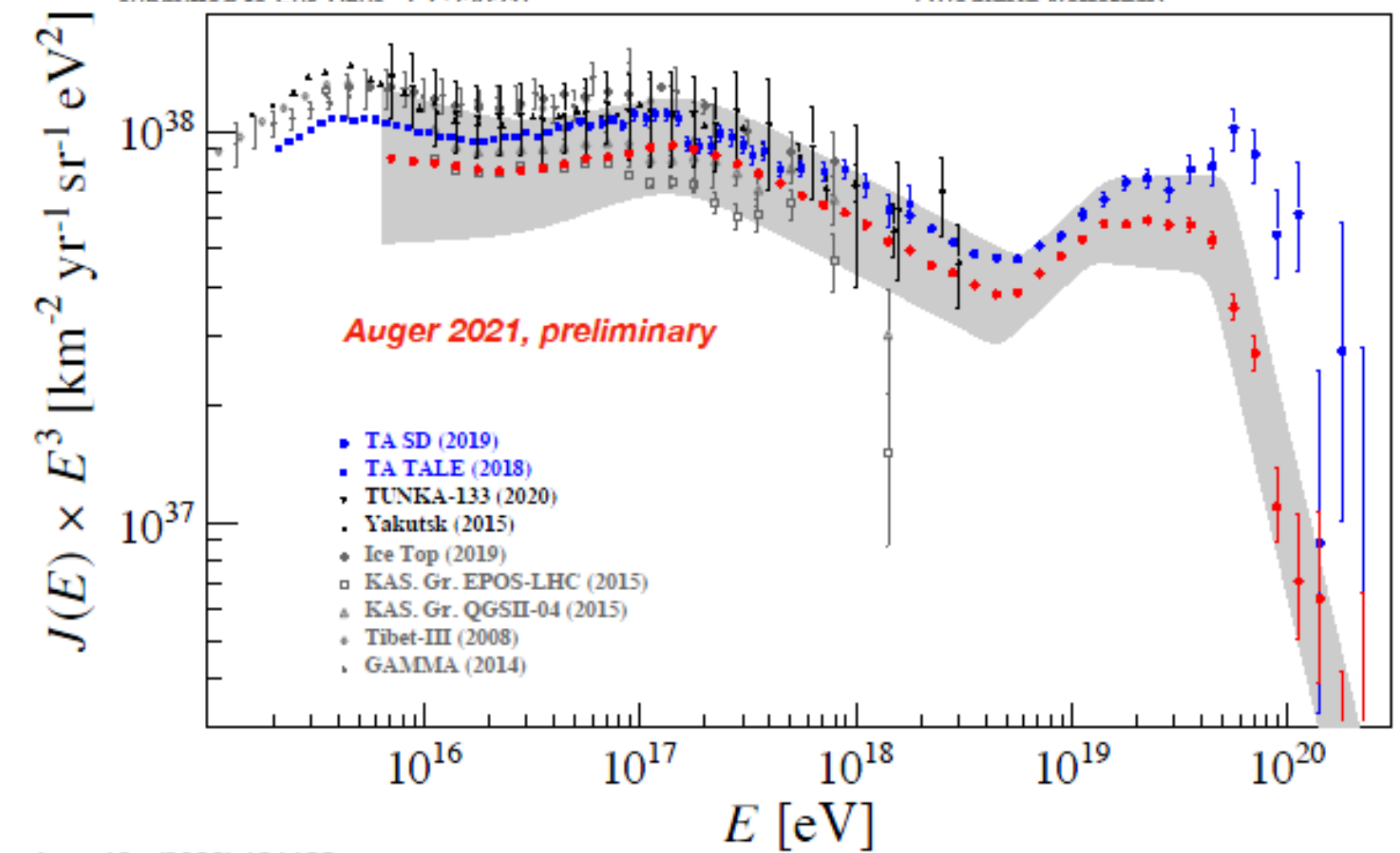
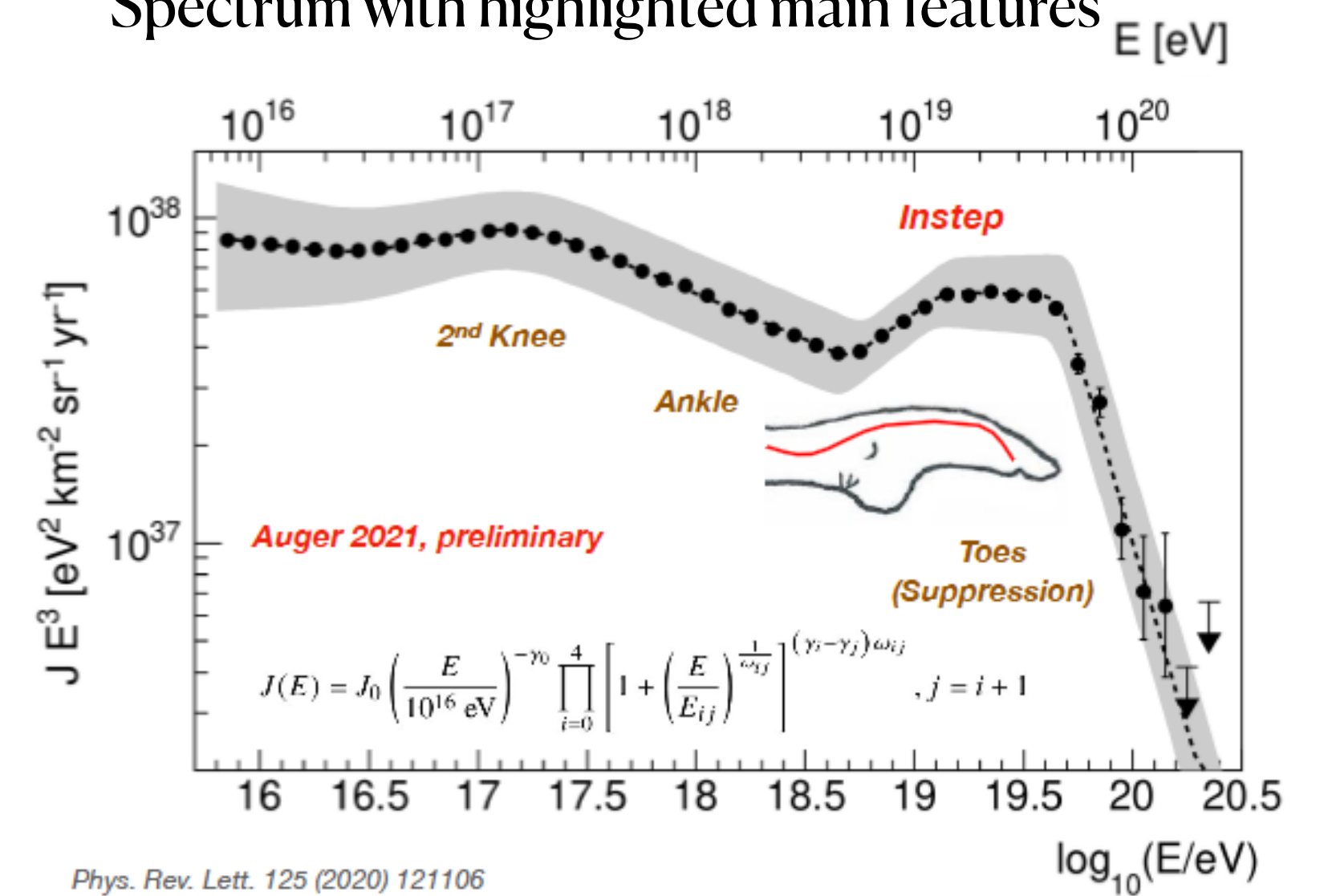
Modern technical principles of CR detection



(Eleonora Guido)

Chemical composition

Spectrum with highlighted main features

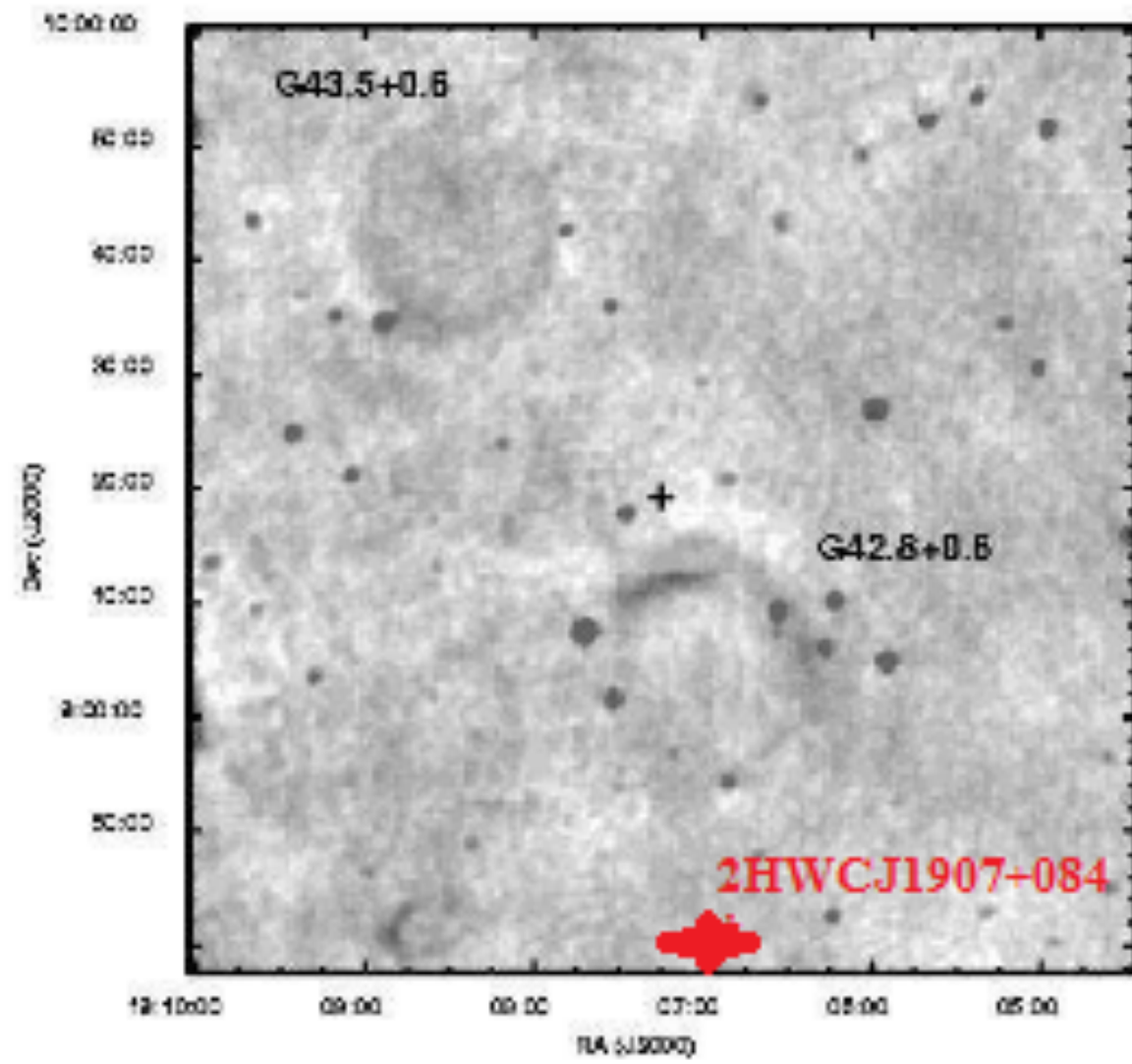


Phys. Rev. Lett. 125 (2020) 121106  
Phys. Rev. D102 (2020) 062005  
submitted to Eur. Phys. J. C (2021)

(Vladimir Novotny)

# Multiwavelength observations of SGR1900+14

Radio



Kaplan et al, ApJ 566(2002)

Optical

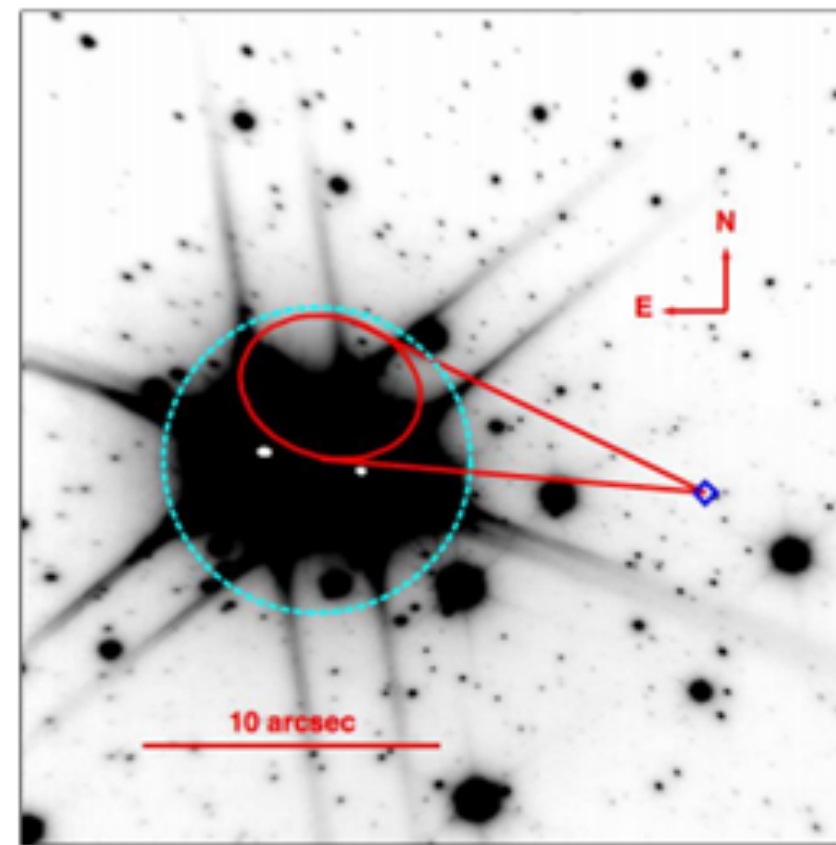
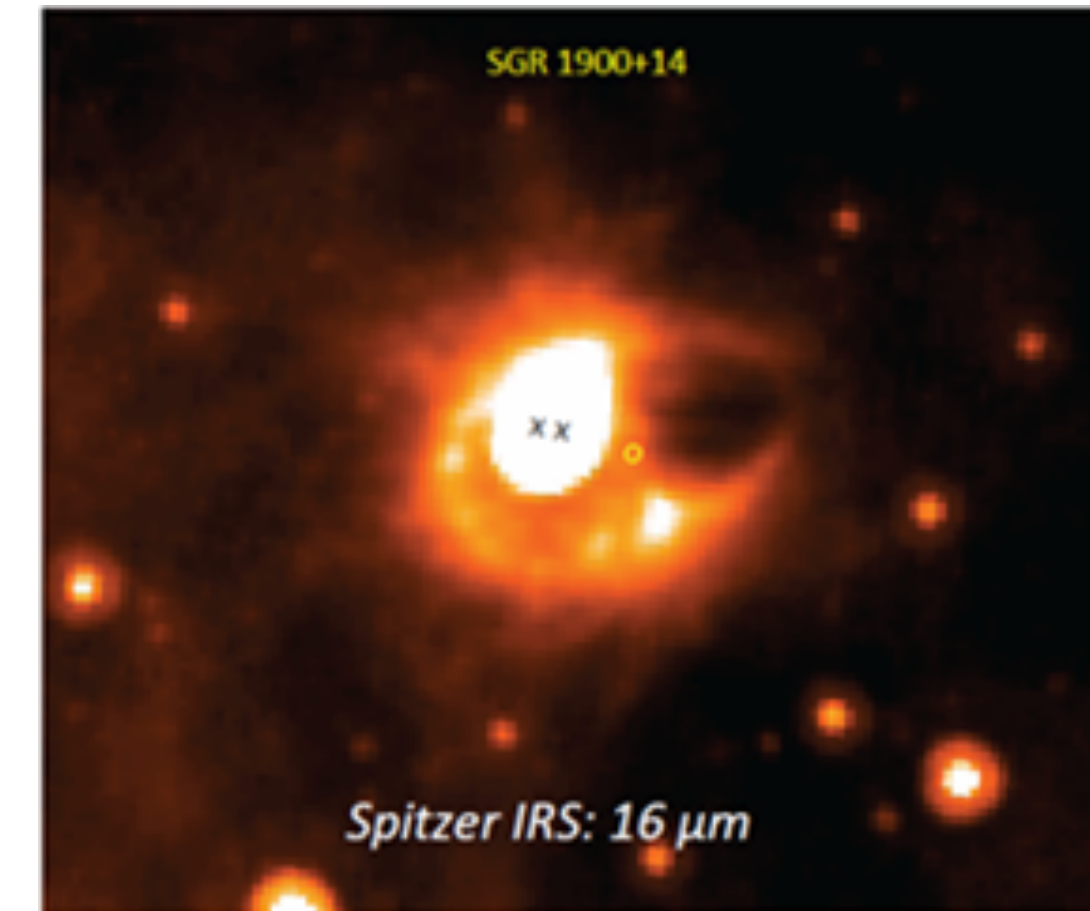


FIG. 9.— The position of the putative counterpart of SGR 1900+14 (blue diamond) traced back by 6kyr is marked by the solid ellipse (red in the online version). The size of the ellipse denotes the positional uncertainty corresponding to the uncertainty in the proper motion measurement. The solid (red) lines represent the  $1-\sigma$  limits on the angle of motion. The dashed circle (cyan in the online version) denotes the cluster of massive stars (Vrba et al. 2000).

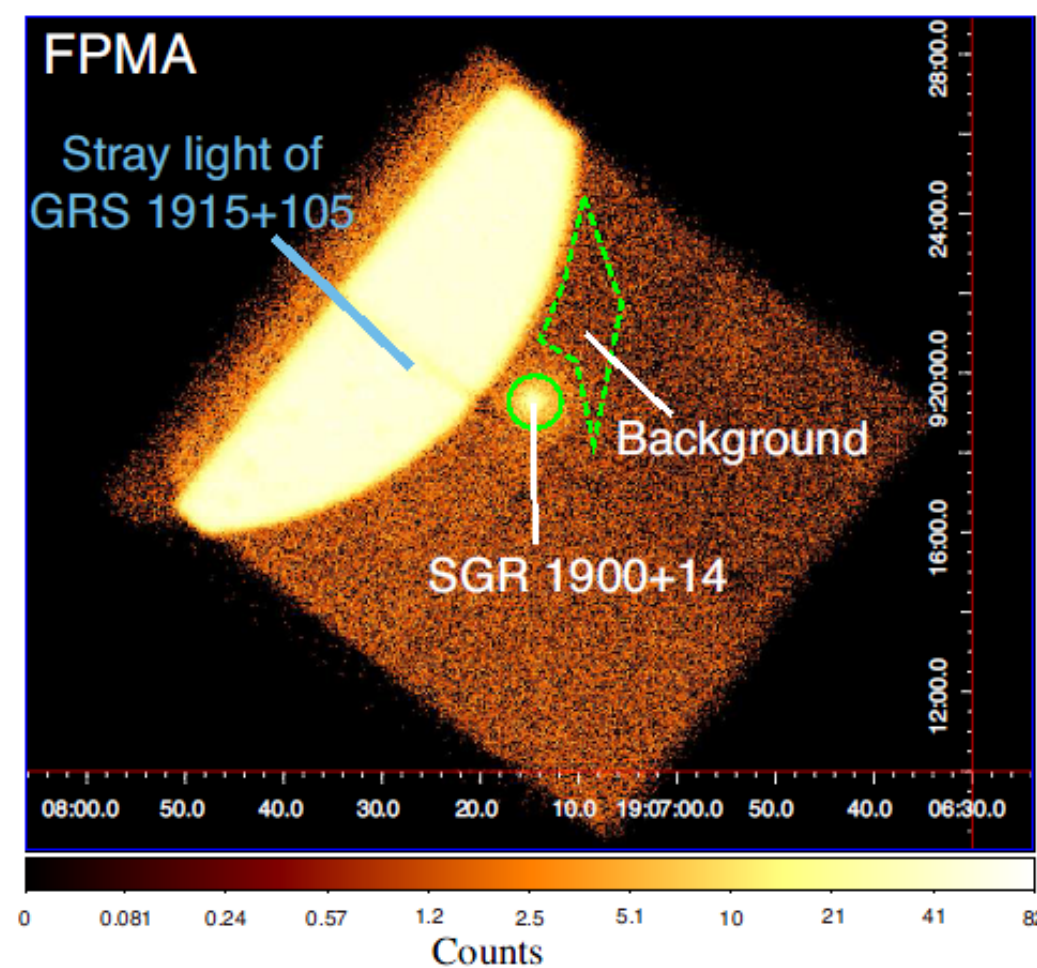
Tendulkar et al, ApJ 761 (2012)

IR



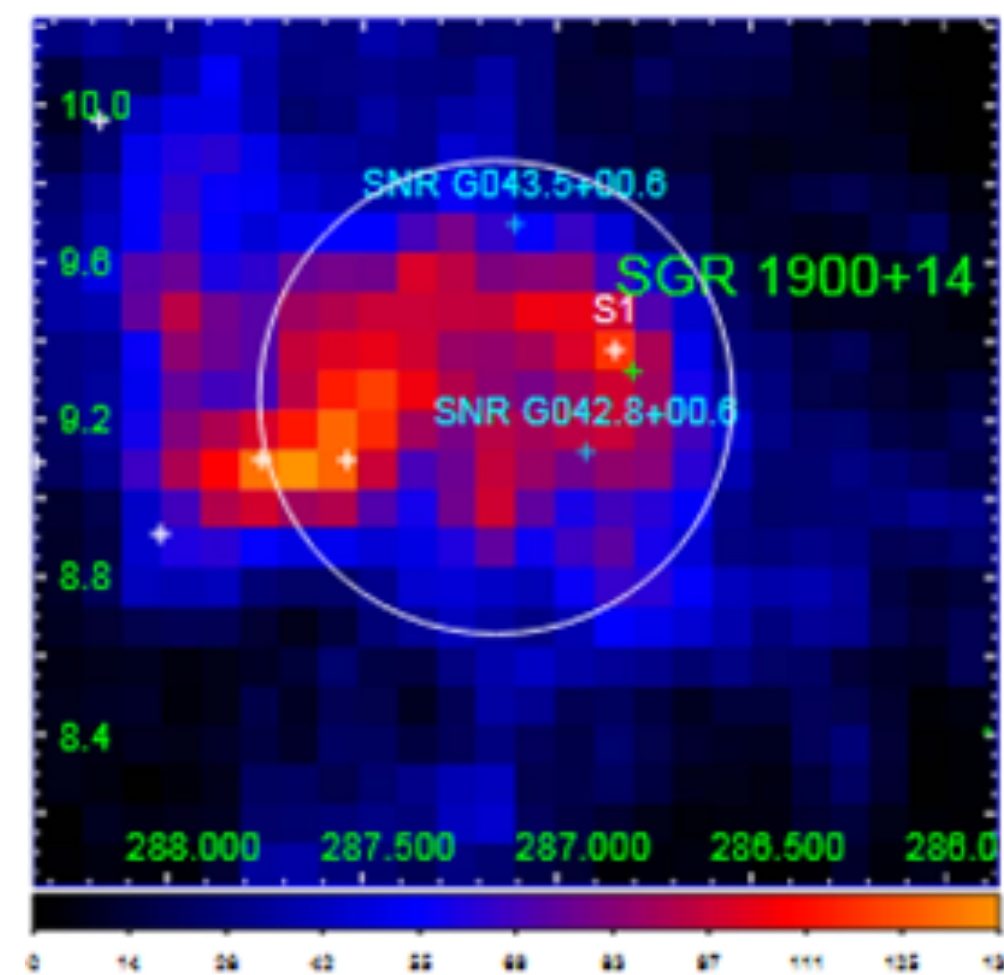
Natale G et al. ApJ837(2017)

X-ray NuSTAR 3-78 keV



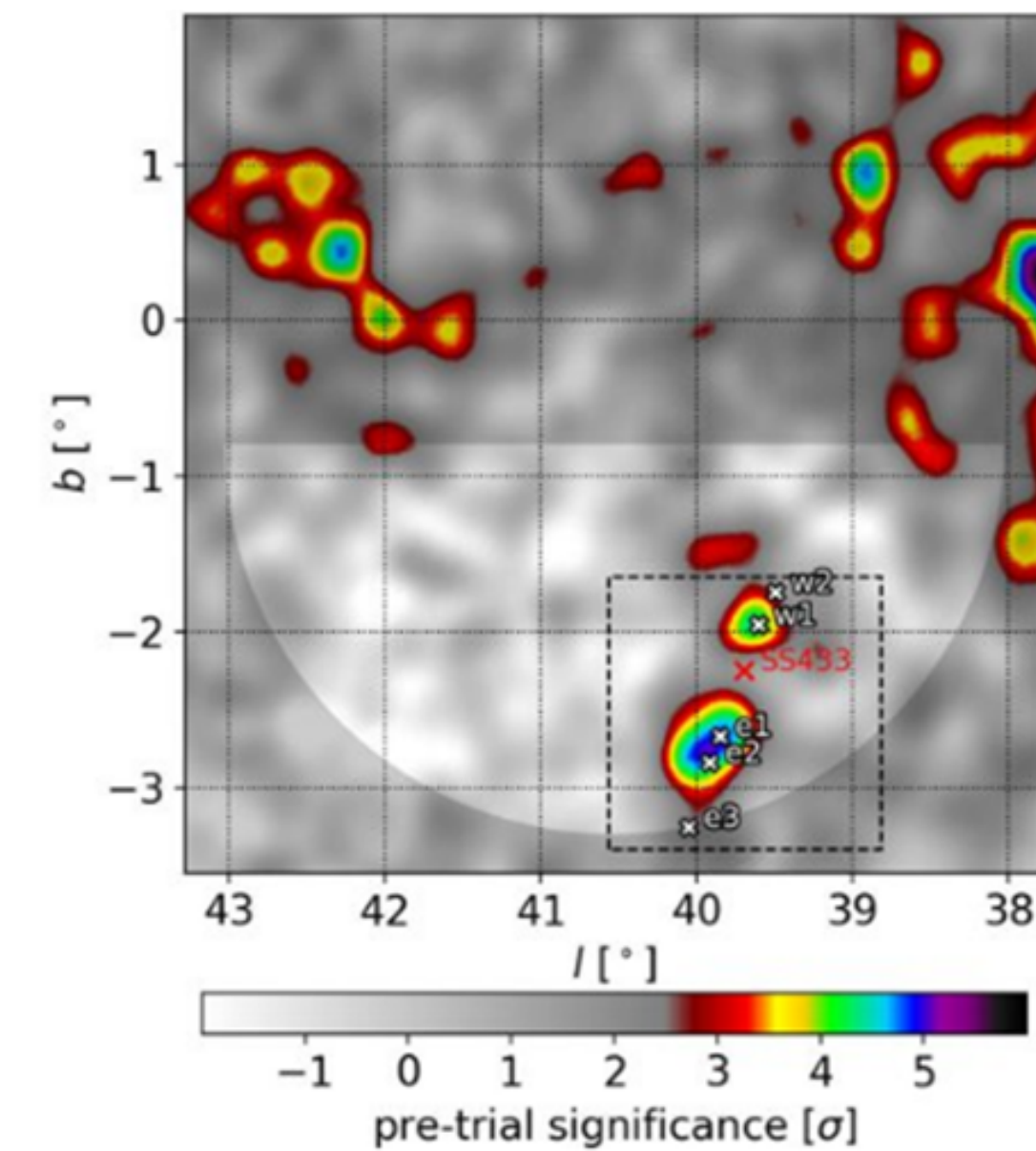
Tamba et al, PASJ 71(2019)

Fermi-LAT (100 MeV - 1 TeV)



Li et al. ApL 835(2017)

HAWC (1-100 TeV)



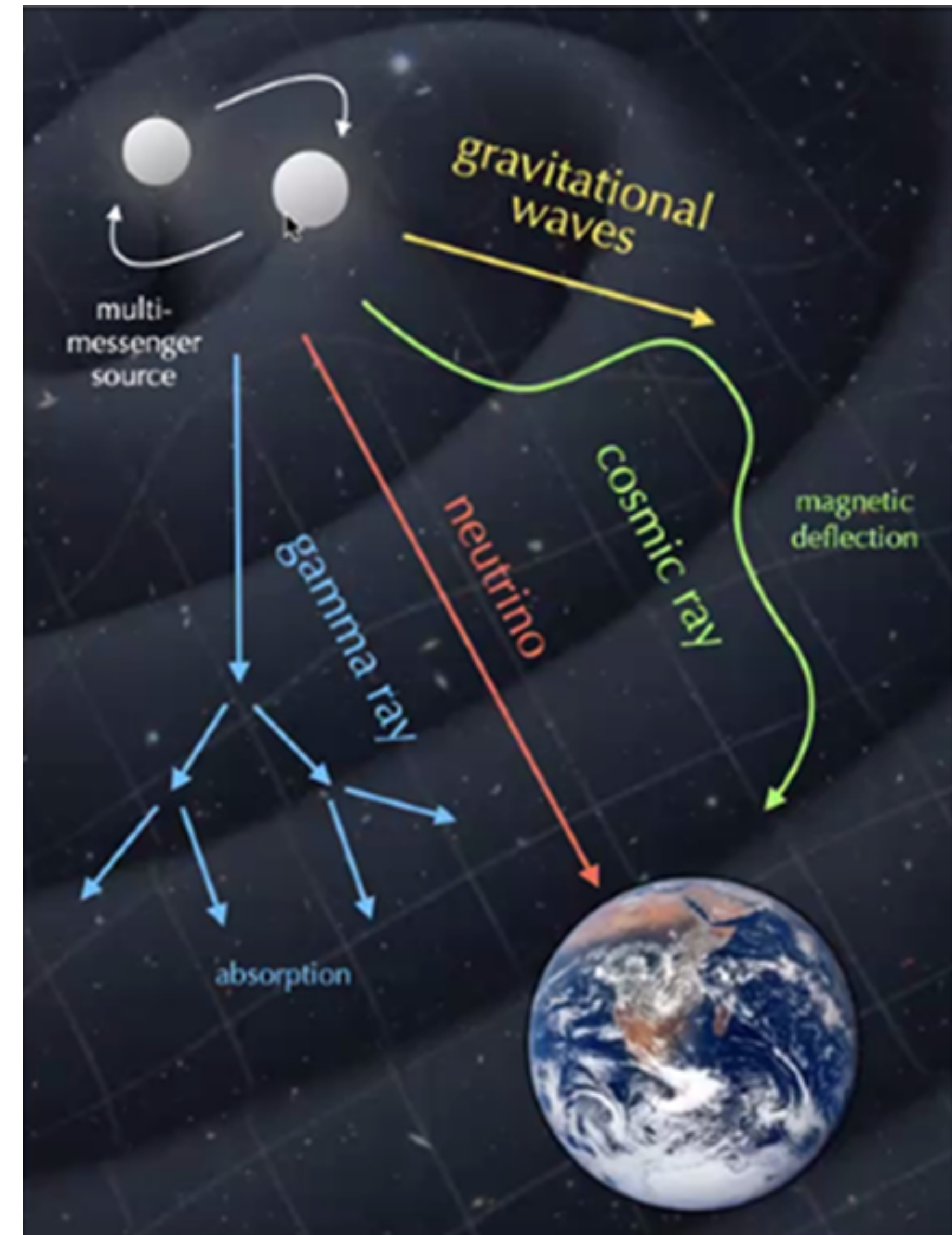
# The era of multi-messenger astronomy

Multi-messenger carriers:

- Cosmic rays (CR, protons, nuclei leptons)
- Neutrinos
- EM radiation (gamma-rays etc.)
- Gravitational waves

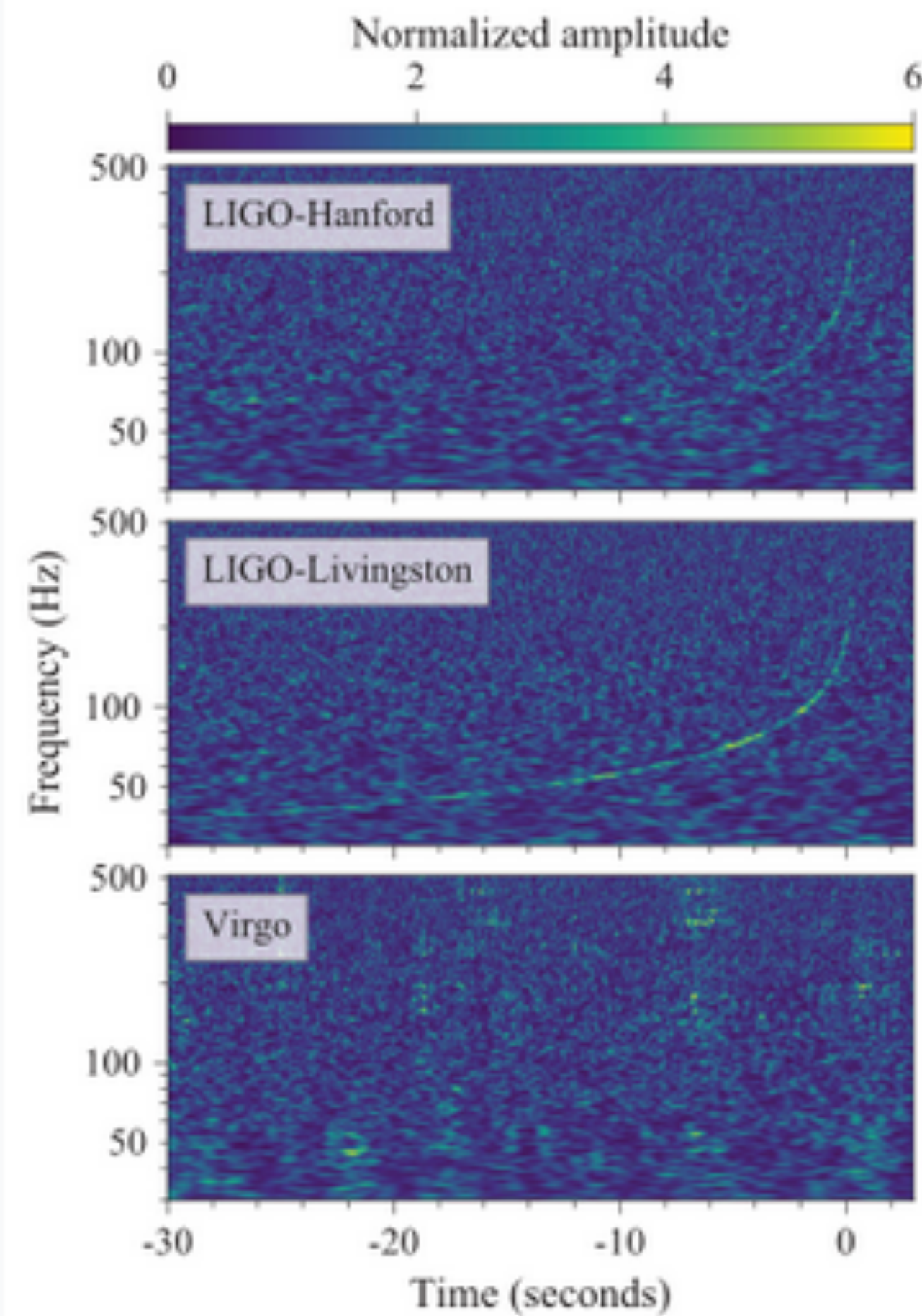
CR are the principal, because:

Interaction of accelerated particles (CR) with magnetic fields and EM background results in generation of nonthermal emission and neutrinos



# First steps in multi-messenger astronomy

Coordinates:   $13^{\text{h}} 09^{\text{m}} 48.08^{\text{s}}$ ,  $-23^{\circ} 22' 53.3''$   
**GW170817**



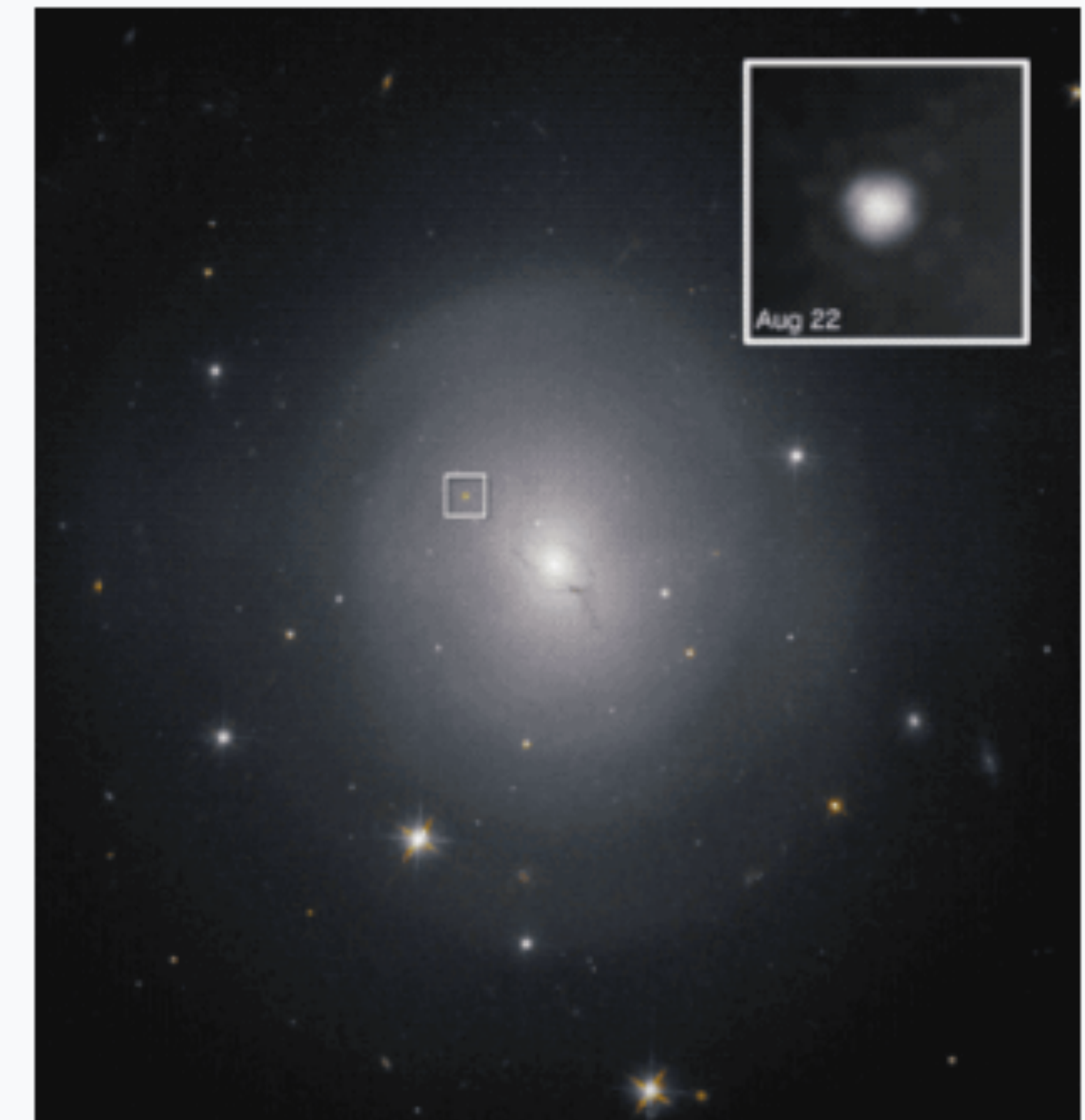
The GW170817 signal as measured by the LIGO and Virgo gravitational wave detectors

Neutron\_star\_collision.ogv



**(1)**  
**NS-NS merger:**  
**kilonova:**  
**gravitational waves + short GRB**

Coordinates:   $13^{\text{h}} 09^{\text{m}} 47.2^{\text{s}}$ ,  $-23^{\circ} 23' 4''$   
**NGC 4993**



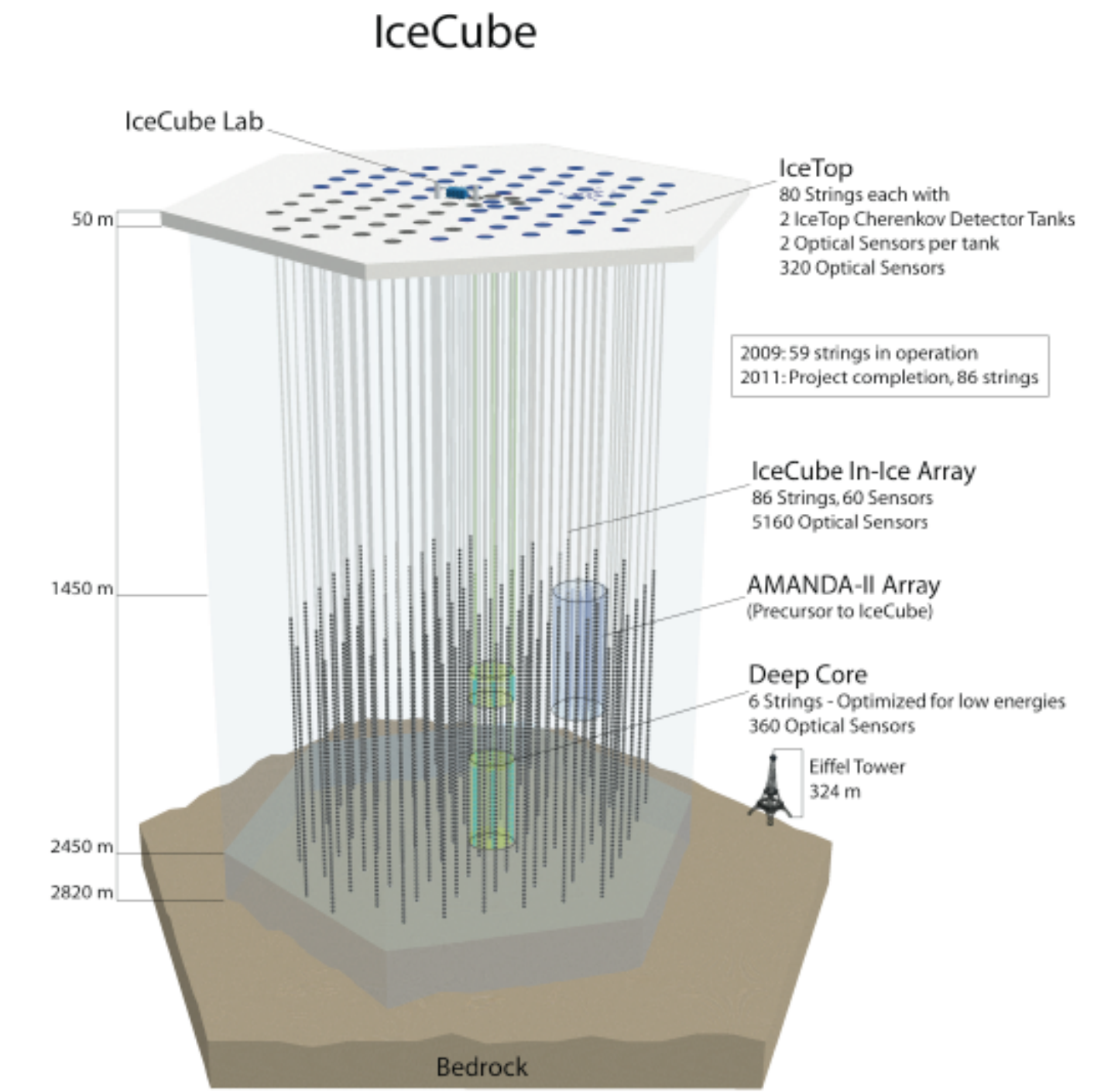
NGC 4993 and GRB 170817A afterglow as taken by [Hubble Space Telescope](#)<sup>[1]</sup>



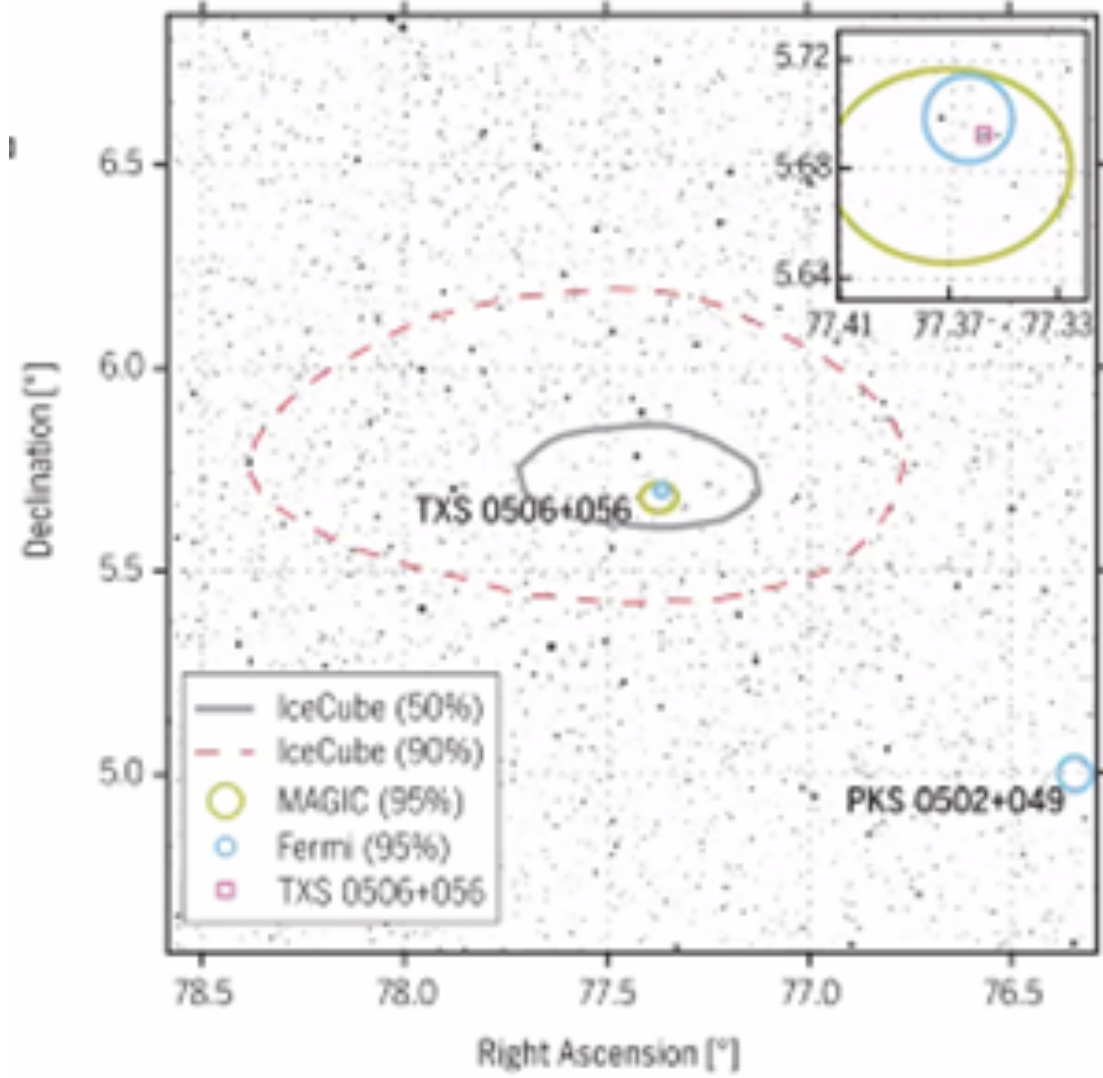
# Multimessenger observations of a flaring blazar coincident with high-energy neutrino IceCube-170922A

The IceCube Collaboration, *Fermi*-LAT, MAGIC, *AGILE*, ASAS-SN, HAWC, H.E.S.S., *INTEGRAL*, Kanata, Kiso, Kapteyn, Liverpool Telescope, Subaru, *Swift*/*NuSTAR*, VERITAS, and VLA/17B-403 teams<sup>†</sup>

## (2) Blazar flare: gamma-rays+neutrino

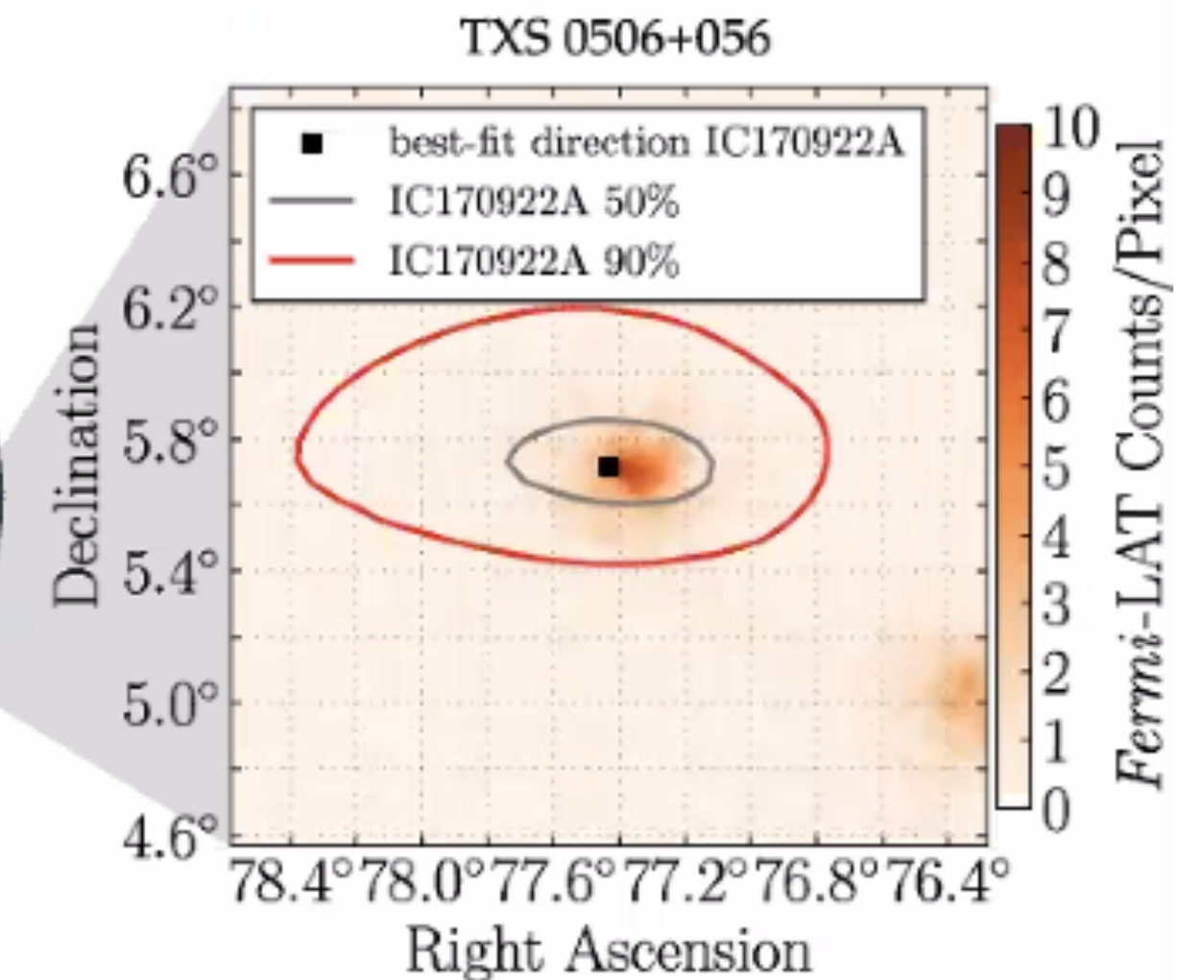
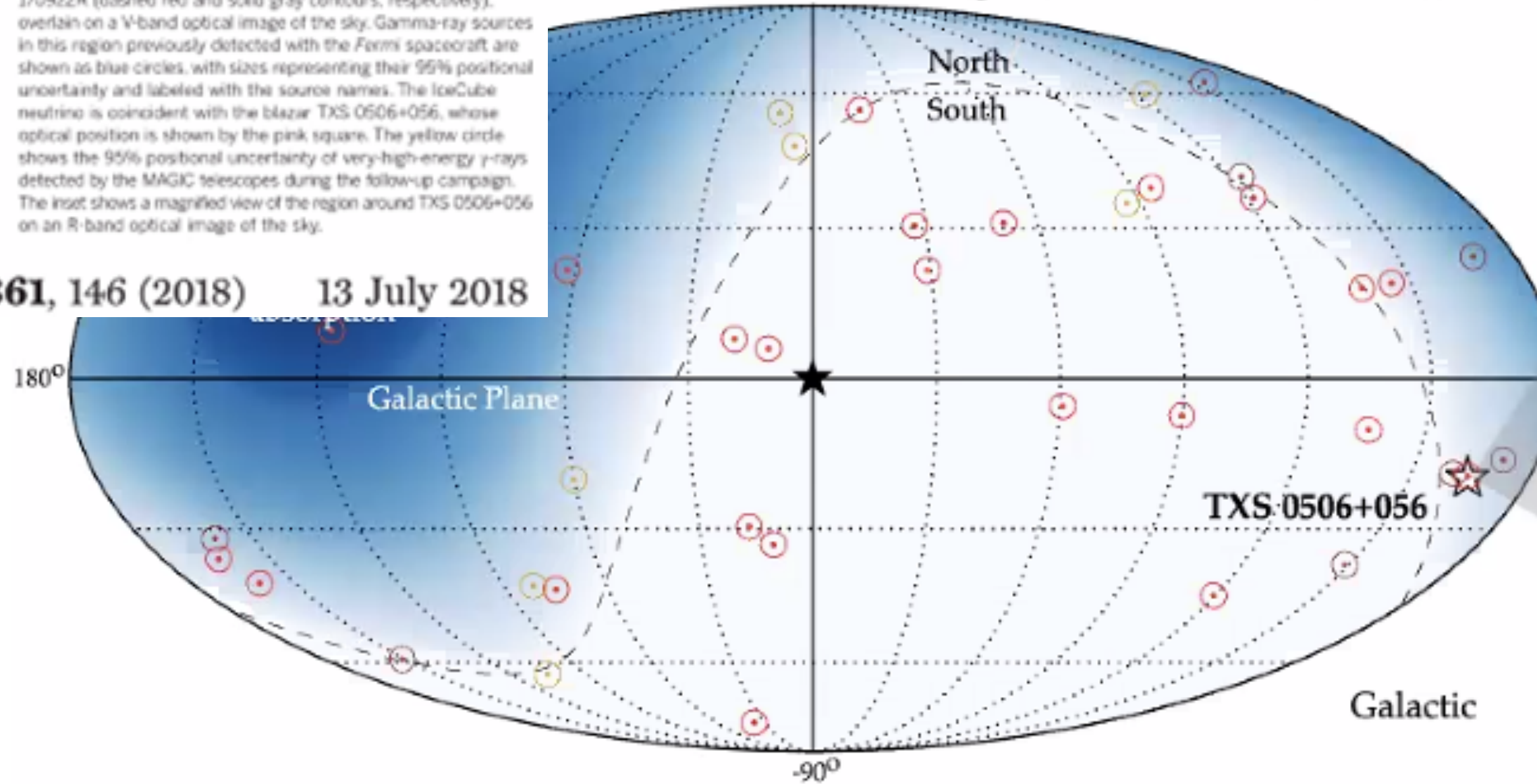


[IceCube, PoS (ICRC2019) 1021]



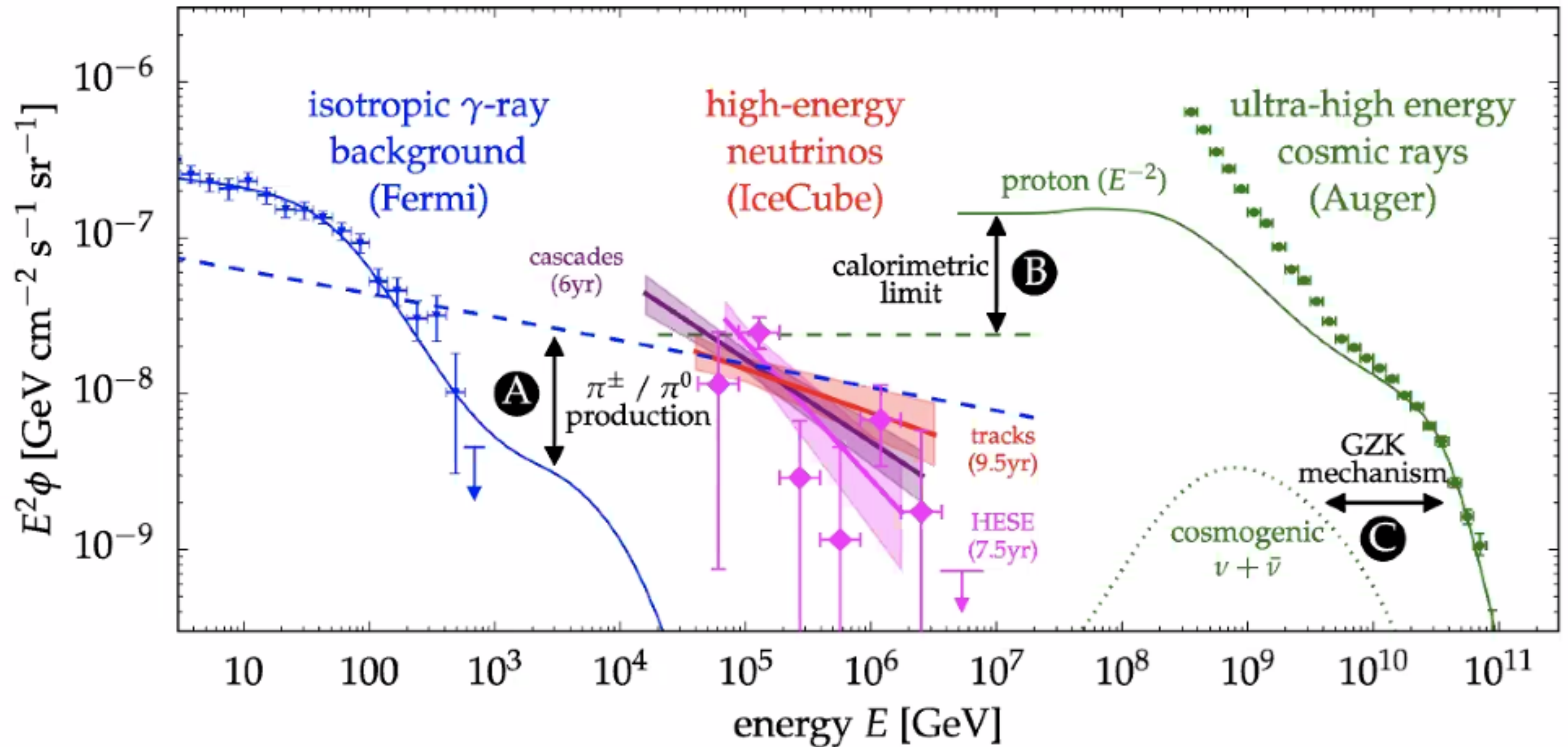
Multimessenger observations of blazar TXS 0506+056. The 50% and 90% containment regions for the neutrino IceCube-170922A (dashed red and solid gray contours, respectively) overlain on a V-band optical image of the sky. Gamma-ray sources in this region previously detected with the *Fermi* spacecraft are shown as blue circles, with sizes representing their 95% positional uncertainty and labeled with the source names. The IceCube neutrino is coincident with the blazar TXS 0506+056, whose optical position is shown by the pink square. The yellow circle shows the 95% positional uncertainty of very-high-energy  $\gamma$ -rays detected by the MAGIC telescopes during the follow-up campaign. The inset shows a magnified view of the region around TXS 0506+056 on an R-band optical image of the sky.

& EHE (red) / GFU-Gold (gold) / GFU-Bronze (brown))



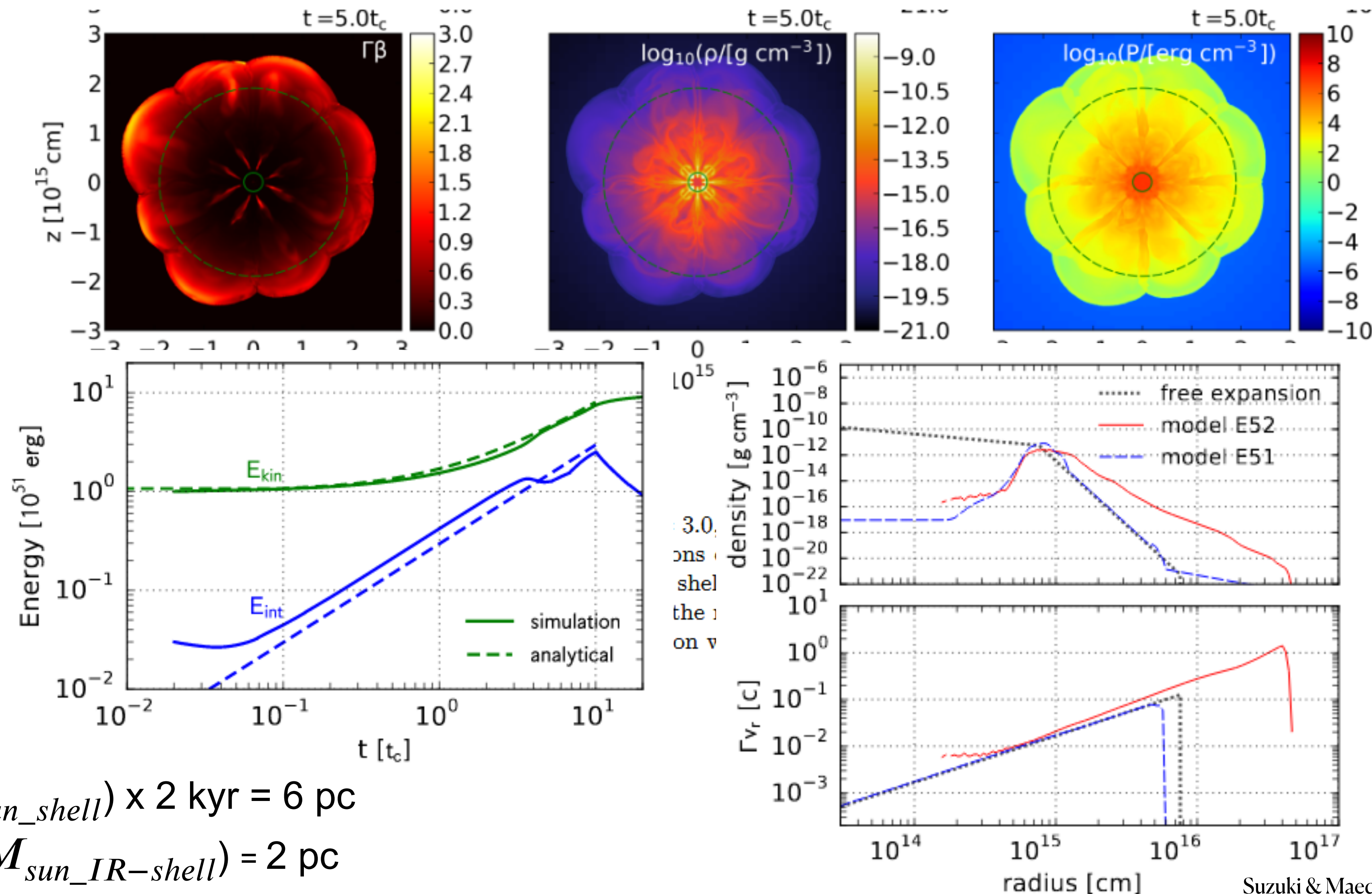
The IceCube Collaboration *et al.*, *Science* **361**, 146 (2018) 13 July 2018

# Multi-messenger carriers: photons, neutrinos, CR + (gravitational waves)



# Variant 2: protrusion of SN ejecta due to CD instability

3D HD simulations of SN ejecta ( $10^{51}$  erg,  $10M_{sun}$ )  
 with a central energy source  $10^{52}$  erg =  $L(10^{46}$  erg/s)  $\cdot t_c$  ( $10^6$  s)



$$t = 20 \cdot t_c = 20 \cdot 10^6 \text{ sec}$$

$V(10M_{sun\_shell}) \times 2 \text{ kyr} = 6 \text{ pc}$   
 cf.  $R_{IR}(5M_{sun\_IR-shell}) = 2 \text{ pc}$

# Variant 1: Evolution of magnetar driven Hypernova

$$(E_{ejecta} = 10^{51} \text{ erg}, E_{mag\_wind} = E_{rot} = 10^{52} \text{ erg})$$

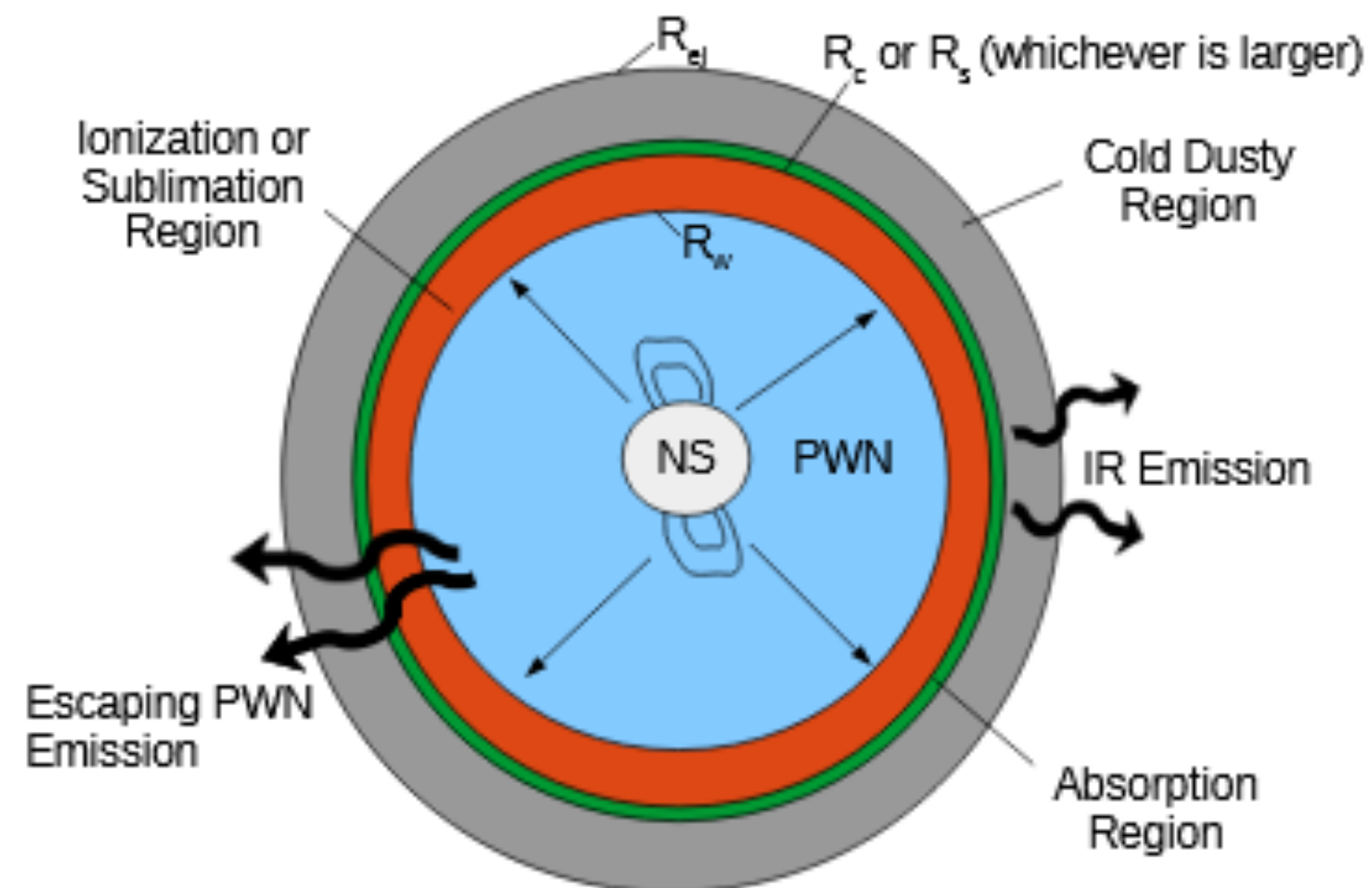
**CLASSICAL SITUATION: HNR**  
Magnetar Wind pressure accelerates ejecta

$$\text{up to } E_{ejecta} = 10^{52} \text{ erg}$$

**Diffusive Shock Acceleration:**

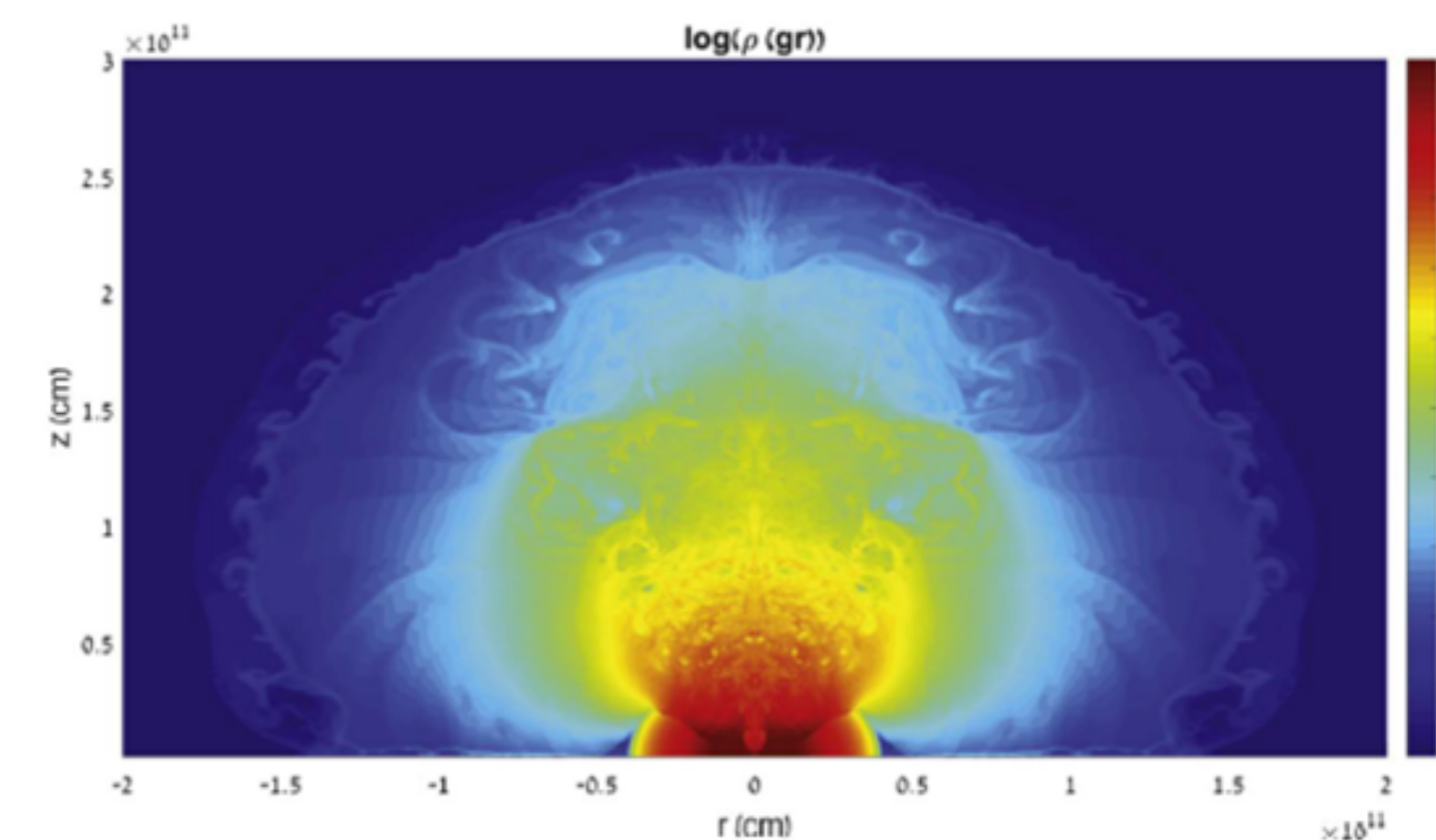
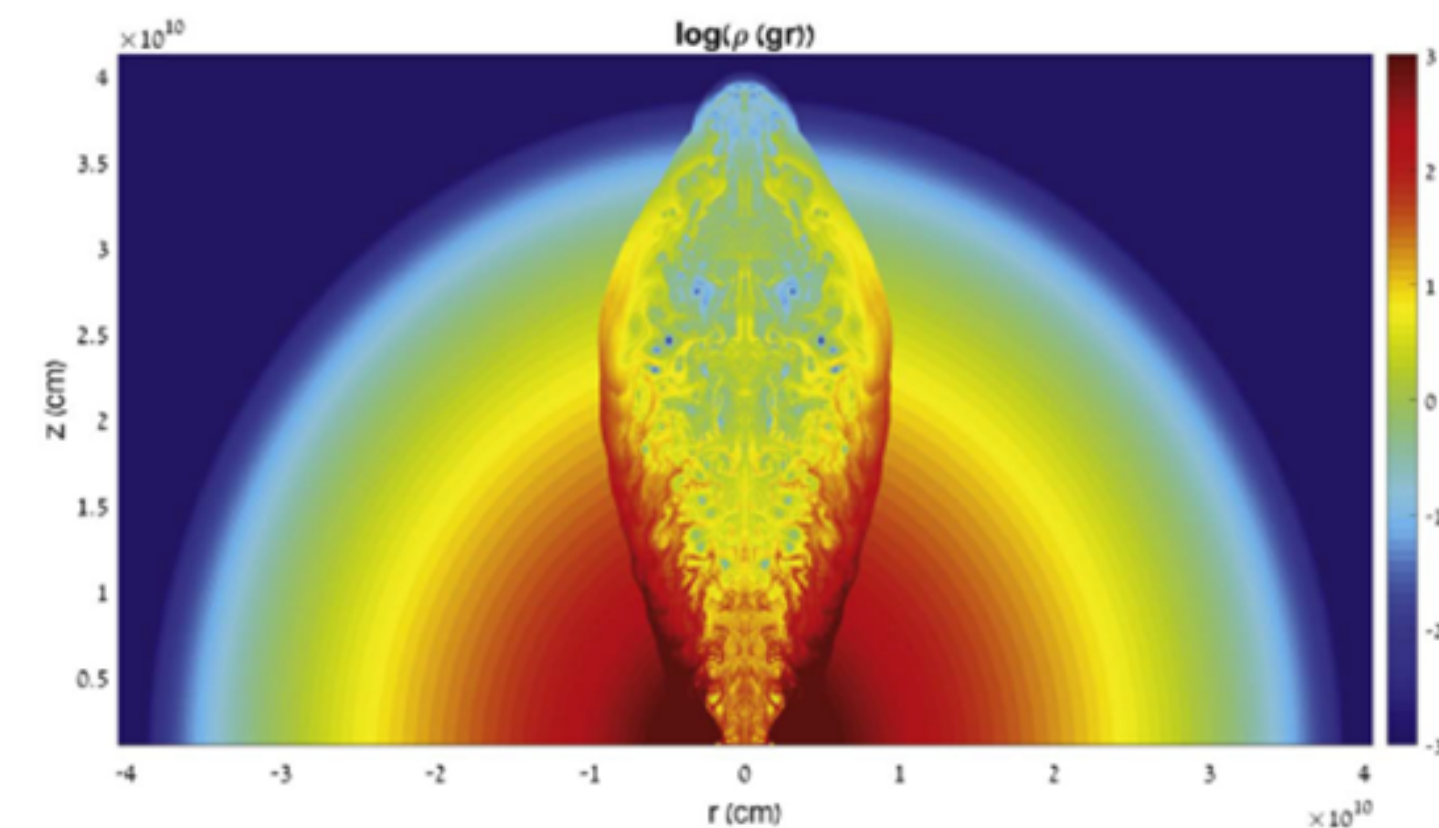
$$E_{cr,p} = (3 - 5) \times 10^{50} \text{ erg}$$

$$E_{cr,e} \sim 10^{48} \text{ erg}$$

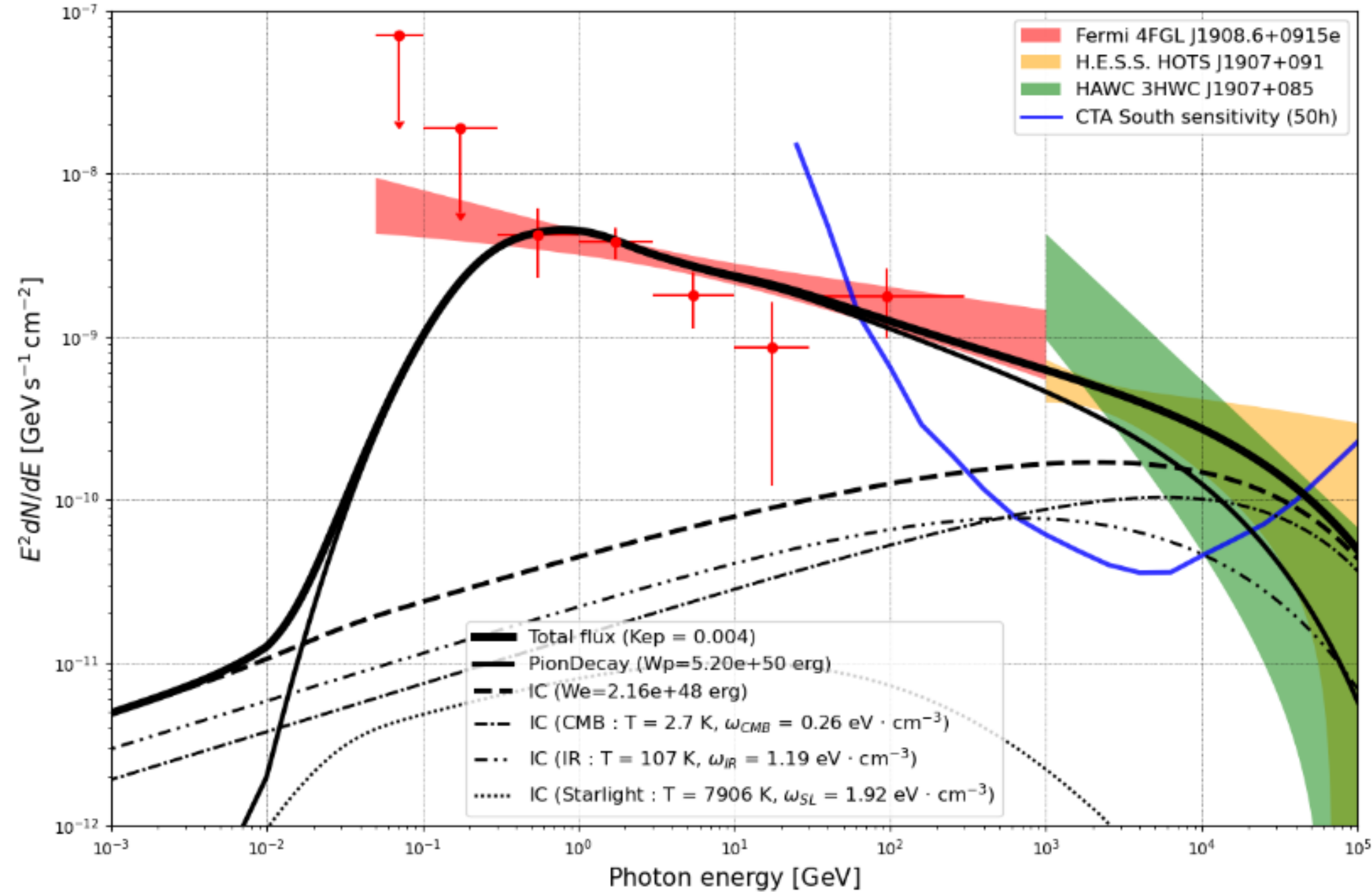


**Energy Dominated MWN SITUATION:**  
large-scale MWN ( $r > 30 \text{ pc}$ ) with  $E_{MWN} \leq 10^{52} \text{ erg}$

**VARIANT 1: BREAK OUT OF COLLIMATED WIND JET**  
(Piran et al. 2020)

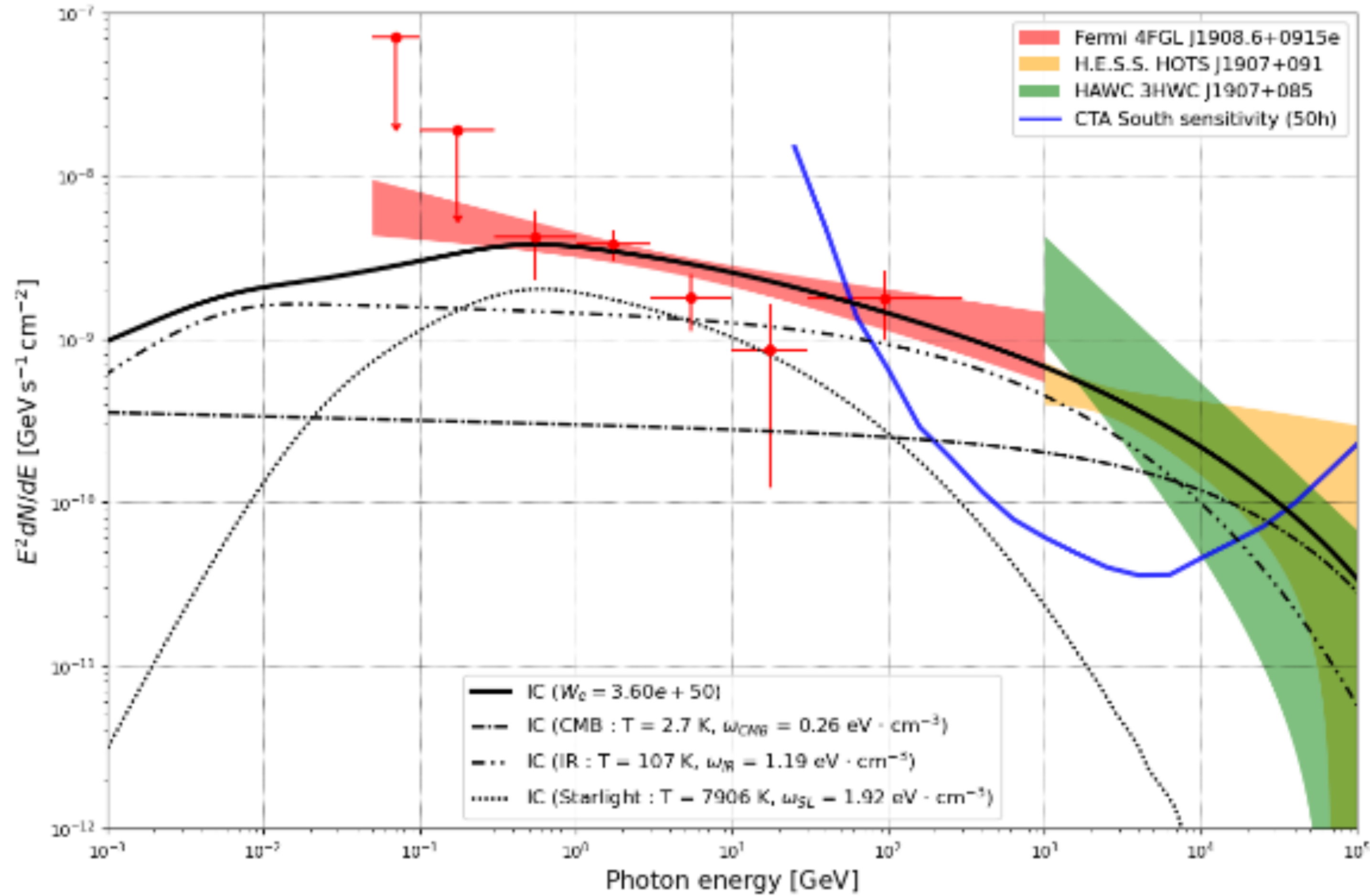


# Spectral energy distribution modeling in case of HNR model



Best-fit spectrum corresponds to  $W_p = 5 \times 10^{50} \text{ erg}$ ,  $K_{ep} = 0.004$

# Spectral energy distribution modelling in case of MWN model with ECBPL lepton spectrum



Best-fit spectrum corresponds to  $W_e = 3.6 \times 10^{50}$  erg

# Summary

The most promising candidates for UHECR accelerators are Hypernovae with millisecond pulsar/magnetar, giant flares of magnetars, Kilonovae (NS-NS mergers), tidal disruption events etc. accompanied by (mildly) relativistic jets with close to the Earth directions.

Galactic magnetar SGR1900+14 may be responsible for the observed EHECR triplet

Promising signature of effective acceleration processes in magnetars' neighbourhoods should be nonthermal high-energy and very high-energy gamma-ray emission

# Naima package

Naima is a Python package for computation of non-thermal radiation from relativistic particle populations. It includes tools to perform MCMC fitting of radiative models to X-ray, GeV, and TeV spectra.

Model:

- 1) Power law spectrum or power law spectrum with exponential cut-off

$$f(E) = A(E/E_0)^{-\alpha}$$

$$f(E) = A(E/E_0)^{-\alpha} \exp(-(E/E_{cut})^\beta)$$

- 2) Pion decay, Inverse Compton, Synchrotron
- 3) Prior parameters for fitting: spectral index, A,  $E_0$ ,  $E_{cut}$ , nh (for pion decay), B (for synchrotron)



# Hadronic mechanism of emission

The main mechanism for the energy loss of protons and nuclei of the TeV-PeV bands in the ISM is the inelastic nucleon-nucleon (mainly proton-proton) collisions, as a result of which charged and neutral pions are born. The decay of the neutral pions into gamma-photon pairs completes the operation of the so-called hadronic mechanism of gamma-ray production.

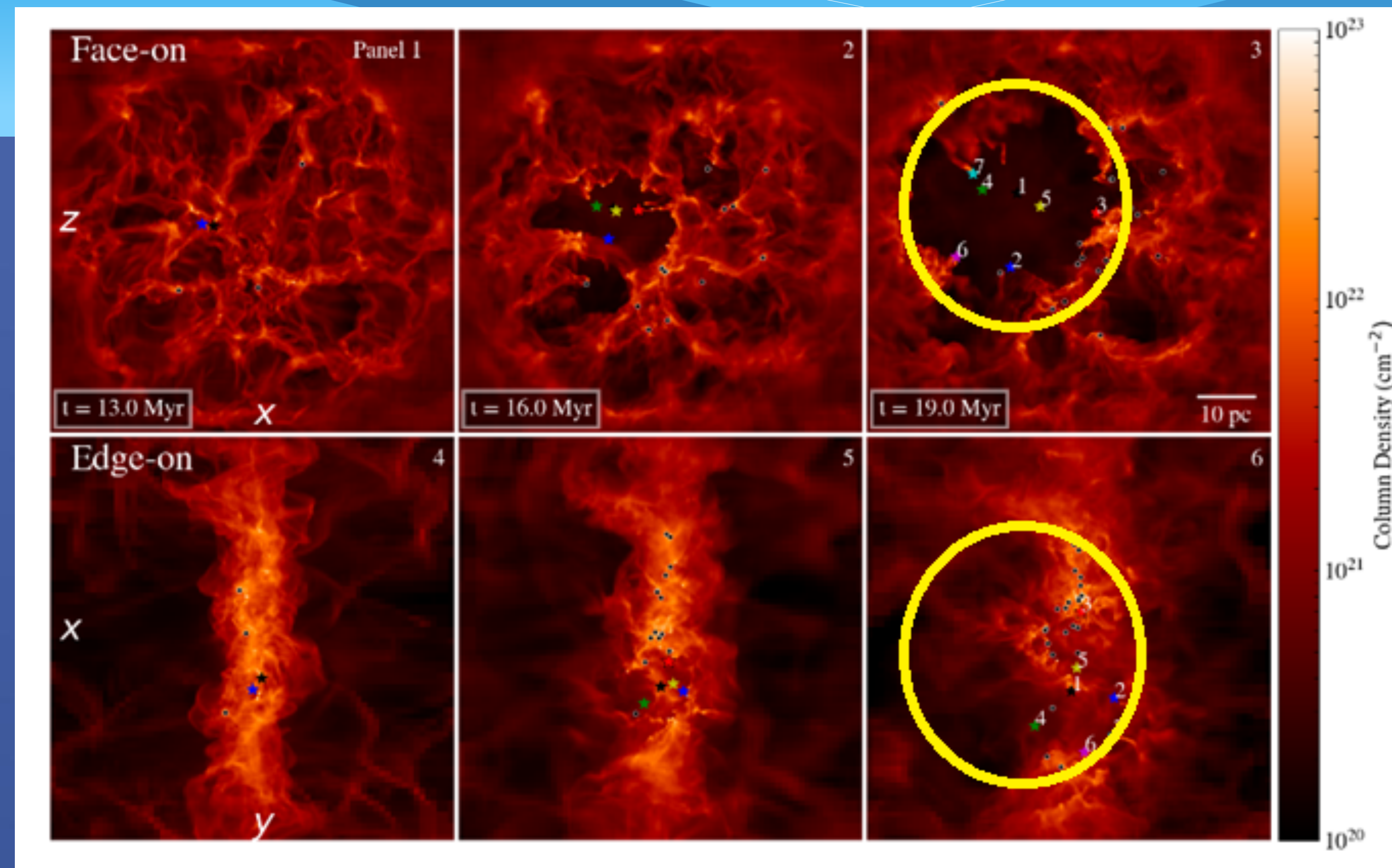
$$p + p/\gamma \rightarrow p/n + \pi^{\pm} + \pi^0 + K^{\pm} + \dots$$

$$\begin{aligned} \pi^+ &\rightarrow \mu^+ + \nu_{\mu}, \\ &\mu^+ \rightarrow e^+ + \nu_e + \bar{\nu}_{\mu} \\ \pi^- &\rightarrow \mu^- + \bar{\nu}_{\mu}, \\ &\mu^- \rightarrow e^- + \bar{\nu}_e + \nu_{\mu}, \\ \pi^0 &\rightarrow \gamma + \gamma \\ K^{\pm} &\rightarrow \mu^{\pm} + \nu_{\mu}/\bar{\nu}_{\mu} \end{aligned}$$

# OUR MODEL: HYPERNOVA EXPLOSION IN CAVITY BLOWN BY THE WINDS OF STELLAR CLUSTER'S STARS

EVOLUTION of  
YOUNG STAR  
CLUSTER  
IN MOLECULAR  
CLOUD UP TO  
FIRST SN  
EXPLOSION  
( $t=17$  Myr in  
SGR1900 CASE)

SNR SHOCK NOW  
INSIDE SWB

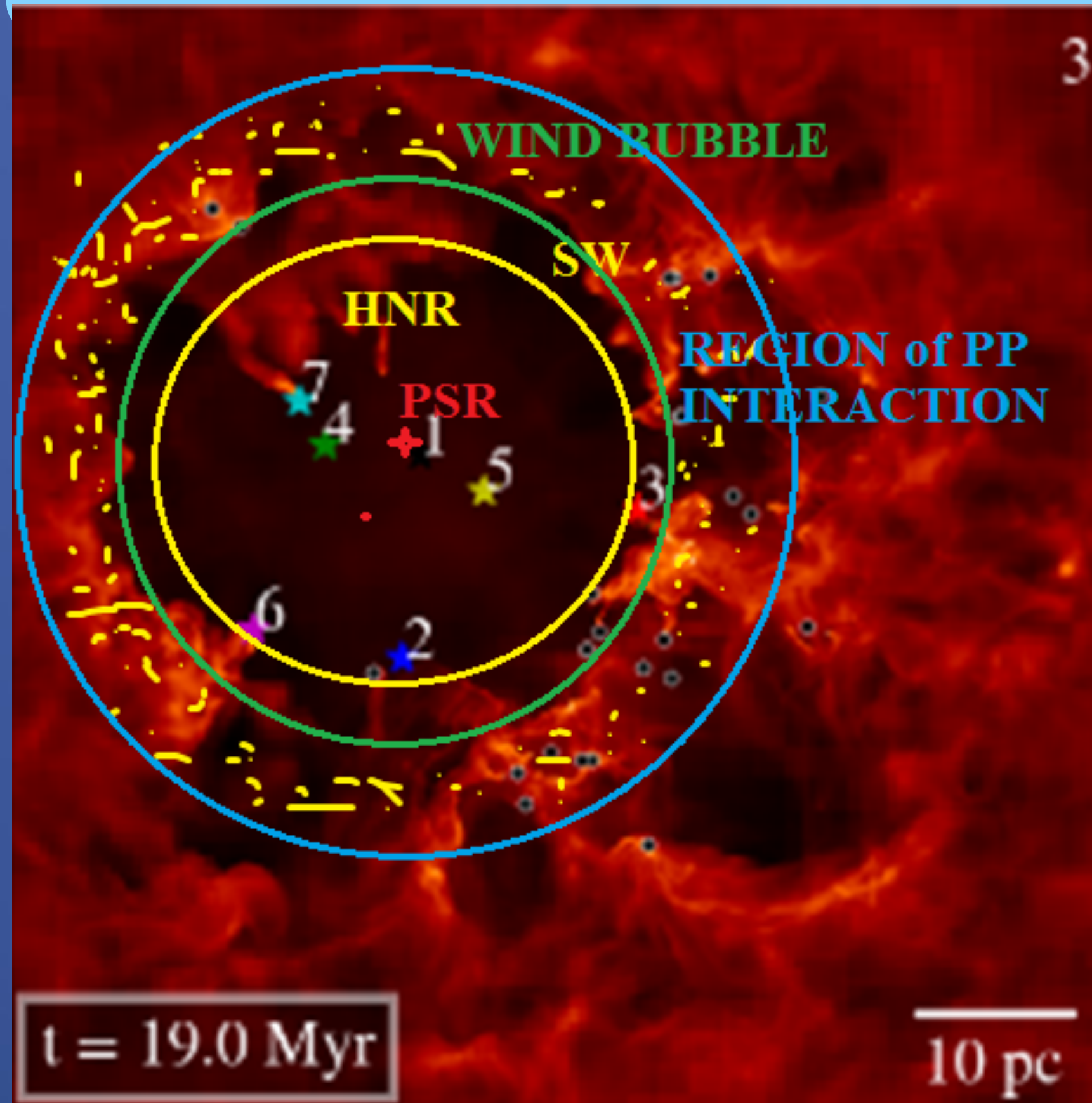


$$n_{in} = 1e(-2)cm(-3)$$

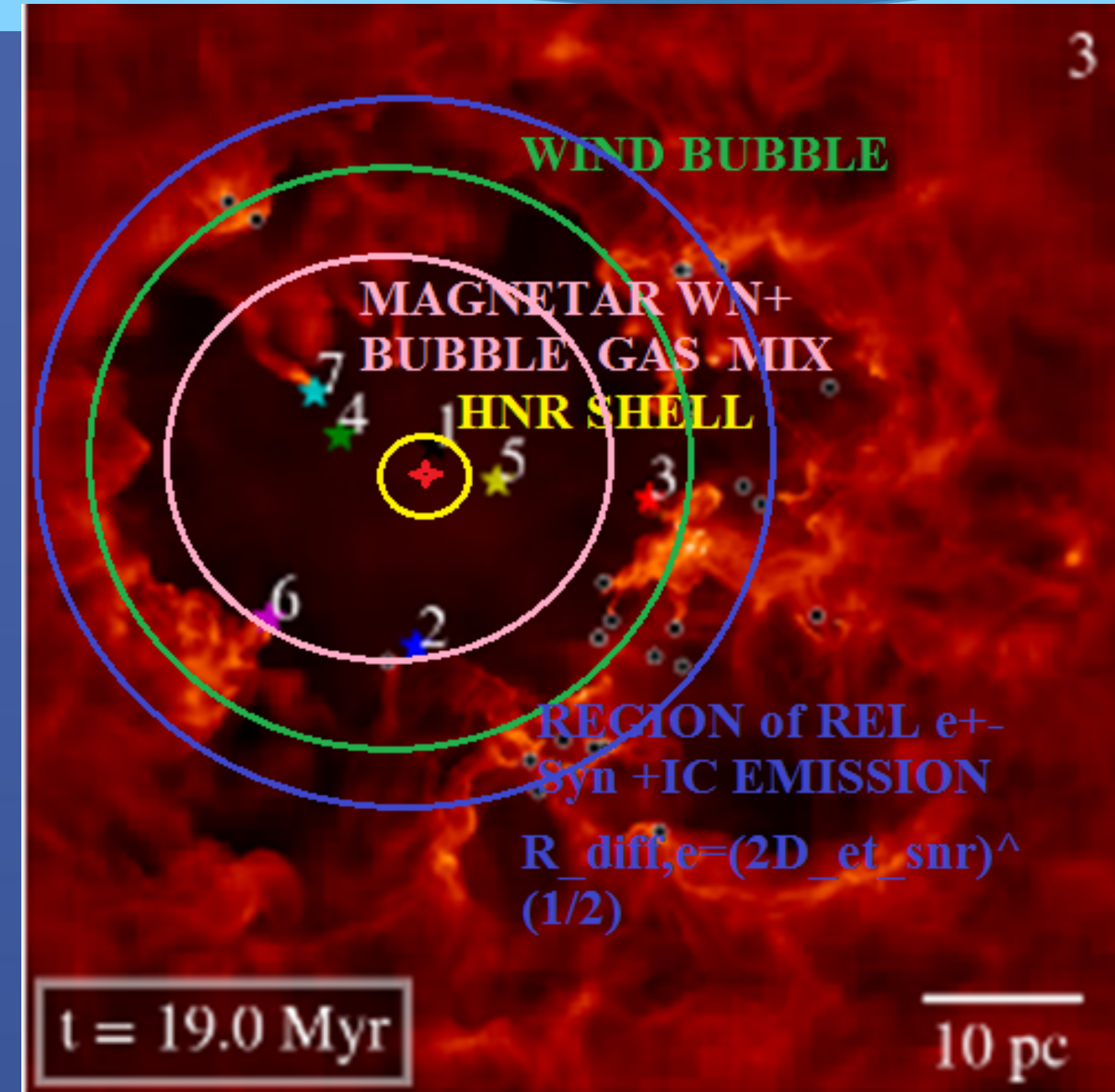
$$n_{swb\_shell} = 50 cm(-3) = 4 \times 12 cm(-3), n_{ism} = 12 cm(-3)$$

# OUR MODELS OF GAMMA-RAY EMISSION

## HADRONIC MECHANISM

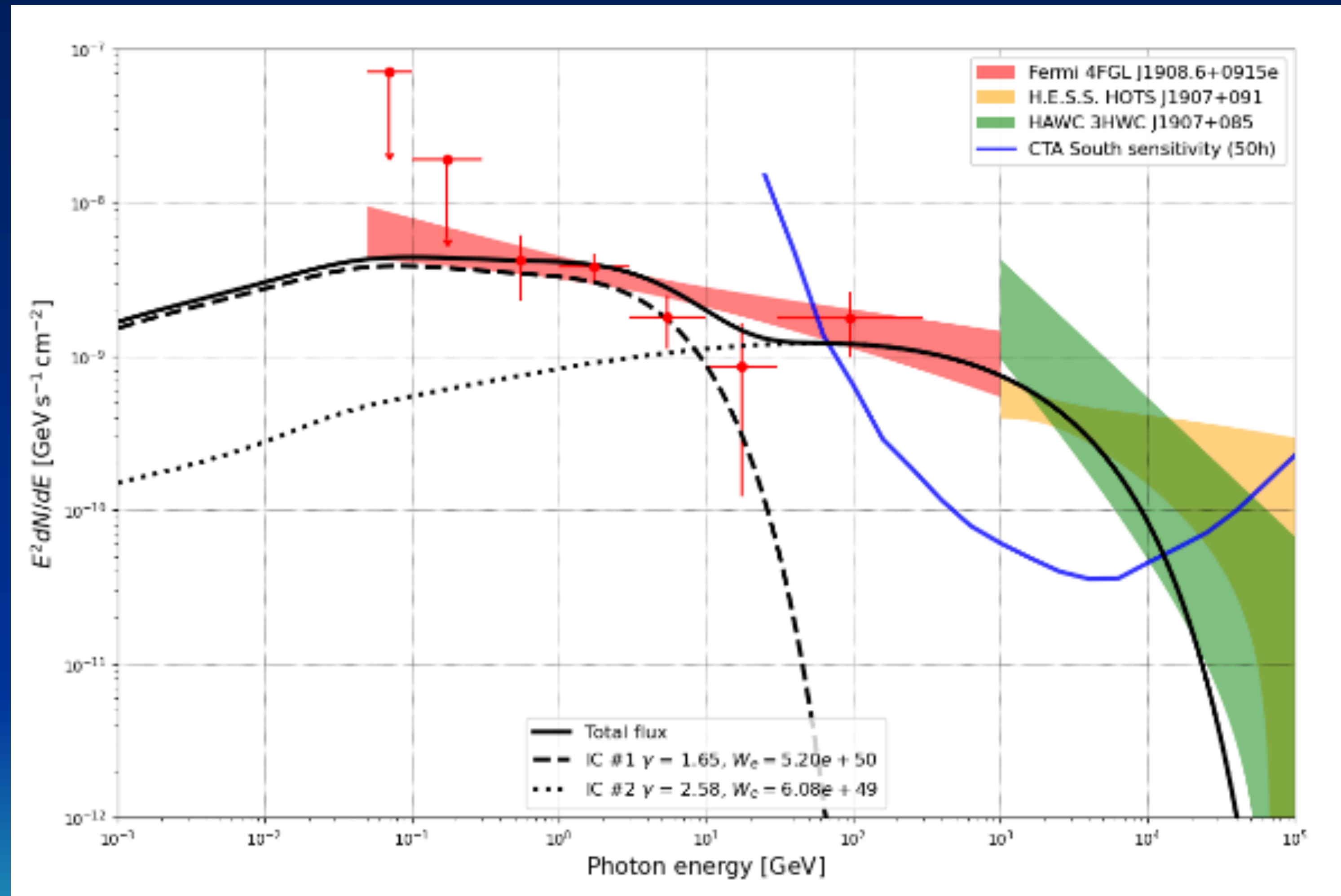


## LEPTONIC MECHANISM



$$R_{diff} = (2D_{pt\_snr})^{1/2} \approx 20-40 \text{ pc}$$

# SED modelling in case of MWN model with 2 component ECPL lepton spectrum



Best-fit spectrum corresponds to  
 $W_{e,1} = 5.2 \times 10^{50} \text{ erg}$ ,  $W_{e,2} = 6.1 \times 10^{49} \text{ erg}$

# **Slide about leptonic mechanism**